Response to associate editor request for major revisions

Low methane concentrations in sediment along the continental slope north of Siberia: Inference from pore water geochemistry; MS No.: bg-2016-308; Clint M. Miller et al.

Specific changes requested by editor:
Referee/Editor Comments (*italic font*) with direct responses (**bold font**).

How your pore-water profiles are effective in ruling out bubble-mediated methane transport.

As expressed in the MS, sites with bubble-mediated CH_4 transport have truly different chemistry that bears no similarity to those observed during SWERUS-C3 Leg 2. Additionally, Section 5.6 describes how, given sufficient permeability and time, CH_4 charged sediments show connectivity of pore water chemistry over hundreds of meters. Thus, CH_4 ebullition near our coring locations is unlikely.

The authors agree that advection between transects should be discussed more completely. Therefore, we have added discussion focusing on the following:

1. **No major physiographic provinces exist between transects. All major sedimentary regions within the field area are included within the transects.**
2. **All observed large-scale gas hydrate accumulations with bubble-mediated CH_4 transport also have significant CH_4 diffusion. This is because sediment sequences with gas hydrate have gas hydrate formation, gas hydrate dissociation, and gas hydrate dissolution all co-occurring. The pore water gradients between the top of the gas hydrate stability zone and the seafloor occur due to steady-state formation and dissolution.**

Therefore, it is unlikely that widespread gas hydrate accumulations exist and are somehow only venting in small localized regions.

Be more precise about your geographical coverage visavi earlier work. Avoid "East Siberian Margin" and instead describe your study area as something like the slope and rise sediments off the Chukchi and East Siberian Sea. When referring to earlier work on the shelf system, describe that as Laptev and East Siberian Sea shelves. These two systems are very different and should not be lumped together.

The study area is now referred to as the, "slope and rise sediments off the Chukchi and East Siberian Sea (CESS)" throughout the MS.

I agree with both reviewers that your paper can be substantially reduced in length (by up to 1/3-1/2).

The MS has been extensively condensed, and several sections (4.2, 4.3, 5.1, and 5.3), figures (4, 5, 11, and 12), and tables (1 and 2) have been removed. Additionally, every section has been reduced especially sections 2.2 and 3.1-3.4.

Specific comments from Referee 2:

Figures 1 and 3: I suggest placing both maps next to each other in one figure (ie.,Fig.1a and 1b). This would make it much easier for the reader to find out where the sampling sites are located relative to predicted gas hydrate occurrence. Figure 4: This is a nice picture but does not convey any important information. Given the total number of figures in this MS, I suggest deleting it.

The authors agree with both points, however combining Figures 1 and 3 so that both are readable is challenging. Therefore, the caption has been imbedded in Figure 1, and the symbol description of Figure 3 (now Figure 2) is in prose. Figure 4 has been deleted from the MS.

Figure 6-9: These figures are hard to read. I suggest plotting each core in a specific figure in a different color rather than all data in one figure in the same color. There is very limited discussion/comparison of the ACEX data; why plot it then?

We regret these figures are difficult to read. Given the extremely large dataset over this vast region, it is difficult to clearly present results concisely. It seemed to us somewhat overwhelming to plot the chemistry at every site independently, or alternatively every species analyzed at multiple sites independently. The authors have tried many different plotting methods including plotting each core in a different color. This style did not improve figure readability, and removes the color distinction carried over into Figure 8 (which is the most important figure in this group). Instead, we have chosen to increase panel, symbol, and line widths while minimizing white space. The ACEX data has been

removed, as suggested, and the legends are imbedded within the panels. Hopefully, this improves readability without lengthening the paper.

Lines 187-242 vs. lines 616-657: The sections are basically saying the same thing with a few additional points in the latter, discussion section. I suggest removing lines 616-657 and taking the few "new points" that are mentioned here and adding them to the background section. I found it tiring to read the same "intro to reading pore-water profiles" twice.

The entire section 5.3 "Reading the Pore Water Profiles" has now been removed.

"Rhizone experiments": These are very helpful experiments that install additional confidence in this comparably novel sampling technique. With that being said the description of these experiments, including the results and discussion of the results take up a lot of space and distract from the main story of the MS. I suggest moving all of this into a supplementary material section. This would include the experiment description (line 310), section 4.3, the discussion sections 5.1 and 5.2 and Figures 5 and 11 (and maybe 12 if the authors think that the porosity-rhizone aspect could also be trimmed), Tables 1 and 2. Basically, all we need to know is what is in the short summary in lines 606-614. The reader can be referred to the supplementary material for the detailed experiments.

Rhizons have been subject to debate leading the some misunderstanding in their applicability to marine settings. The authors believe these experiments provide some much needed clarification to Rhizon sampling fidelity, but agree with the reviewer that this section distracts from the primary purpose to the MS. Therefore, lines 310-315, sections 4.2, 4.3, 5.1, 5.2, Figures 5, 11, 12, Tables 1, and 2 have been edited and moved to supplementary materials.

Dissolved hydrogen sulfide "analysis": It seems like the authors did not actually do any sulfide analyses but just "visually" observed whether white precipitates were forming when zinc acetate was added. To me this is not an appropriate "analysis" to detect hydrogen sulfide. This is especially important since the authors did not do any sulfate analyses but only analyzed total dissolved sulfur and based on their visual "analysis" of the sampling vials- assumed that no hydrogen sulfide was present and the total sulfur *only reflects sulfate. I strongly suggest doing at least a few hydrogen sulfide analyses with the Cline method, for example of the samples from deeper layers especially on the cores from Lomonosov Ridge, to confirm the absence of hydrogen sulfide.*

The term "analysis" may be confusing. This section has been reworded to describe "visual inspection" of ZnS precipitate. Unfortunately, pore water sulfide analyses are not possible.

Lines 176-178- Microbial processes at cold seafloor temperatures: I disagree with the authors here. There are plenty of studies that have shown that organic carbon turnover rates or "bacterial degradation" in high latitude environments are/can be as high as in mid-latitude or tropical environments. For example: Glud et al., 1998: Benthic mineralization and exchange in Arctic sediments (Svalbard, Norway) Arnosti et al., 2005: Anoxic carbon degradation in Arctic sediments: Microbial transformations of complex substrates.

Here, we do not state that bacterial degradation is lower in high latitude than lower latitudes. Rather, line 176 states that burial "might" be enhanced by colder temperatures. This idea is quite logical given our understanding of bacterial processes at different temperatures, and has been discussed in the literature previously (Ex. Darby et al., 1989; Max and Lowrie, 1993). We provide no evidence either way, but simply supply this as a possibility. To make this abundantly clear we have reworded line 168.

Carbon isotope sections: Generally, the sections discussing the carbon isotope system, e.g., processes associated with carbon isotope fractionation, the discussion of the carbon isotope data etc. is very weak and needs more clarification. Also, it is incorrect to present equations (1) and (8) with 12C and state that it indicates "depletion in ^{13}C". As such, the equations written just present the reaction of one organic molecule containing 12C to bicarbonate which of course also has to contain 12C. Please take the notations out.

The subscript notations have been removed from both equations. See the following comment regarding improving the carbon isotope discussion.

Line 227-229: This needs to be expanded and maybe clarified. Both the Holler and the Yoshinaga references are discussing carbon isotope fractionation during AOM. As stated here, the authors only *consider the original ^{13}C-depleted value of the CH_4 in explaining the light DIC formed. Additionally consider: Alperin, M.J., Reeburgh, W.S., Whiticar, M.J., 1988. Carbon and hydrogen isotope fractionation resulting from anaerobic methane oxidation. Glob. Biogeochem. Cycles 2, 278–288. Martens, C.S., Albert, D.B., Alperin, M.J., 1999. Stable isotope tracing of anaerobic methane oxidation in the gassy sediments of Eckernforde Bay, German Baltic Sea. Am. J. Sci. 299, 586–610. And for the first part, asides from Paull et al., a reference such as Whiticar, M.J., 1999. Carbon and hydrogen isotope systematics of bacterial formation and oxidation of methane. Chem. Geol. 161, 291–314.*

We consider DIC ^{13}C depletion at to result from a variety of factors in CH_4 charged sediments including: fractionation during AOM, fractionation during organoclastic sulfate reduction (OSR) and other bacterially mediated reactions, differential diffusion of $^{12}CH_4$ and $^{13}CH_4$ from deep sediments, as well as the light CH^4 input from below. The authors thought this was clear, however this entire section has been reworded to clarify.

Line 681-687: Similar to the previous carbon isotope section, there is some more detail needed here. For example, carbon isotope fractionation during organoclastic sulfate reduction needs to be discussed. The Chatterjee reference (which should be 2011 not 2001) is insufficient here.

Indeed, the authors interpret the observed ^{13}C depletion as fractionation during OSR and other bacterially mediated reactions. This section has been reworded to clarify this point.

Line 706: "almost necessarily implies CH_4 oxidation.. ". This statement needs an explanation and the appropriate literature. . .

The δ^{13}C-DIC values are comparable to a great many published results from CH_4 charged sediments. Additionally, these results imply CH_4 oxidation because no other process can realistically create <-40‰ δ^{13}C-DIC values. This section has been rewritten to make this clear.

Results section: When you list what the concentrations were, they are in past tense, when you describe what the reader sees in the graph, this is in present tense.

Discussion of concentrations are now in present tense.

Lines 508-519, Figure 14: This is a nice exercise but I am wondering why this is included? I could not find any reference to this approach/figure in the discussion section. If it is not relevant to your discussion- delete! Or add a section in the Discussion part that evaluates the plot.

Deviations from the Redfield ratio in marine environments may be caused by different organic matter sources (terrigenous?) than primary productivity. Given this MS's results differ markedly from previously assumptions regarding past organic matter turnover; this exercise seems particularly germane! These results, however, are not enough by themselves to show organic source, but simply imply the terrigenous component may be important. This section has been rewritten, and a short paragraph has been added in the discussion section to explain this figure more completely.

Lines 728-733 and elsewhere: I disagree with this general interpretation. Many of the collected cores also show decreases in sulfur concentration which point to the occurrence of organoclastic sulfate reduction, and you interpret the delta^{13}C-DIC profiles as being imprinted by this process! While the dissolved Mn profiles can be interpreted as reflecting dissimilatory manganese oxide reduction, there has been a lot of recent work discussing the –somewhat intriguing- manganese biogeochemistry of Arctic Ocean sediments, including evidence for dissolved manganese profiles reflecting diagenetic remobilization of Mn and diffusion from deeper sediment intervals. I suggest preparing this section with more caution. For reference: März et al. 2011: Manganese rich brown layers in Arctic Ocean sediments: Composition, formation mechanisms, and diagenetic overprint (and references therein).

The first author was unware of März et al. (2011), and thanks the reviewer for this comment. Indeed, the reviewer is correct the Mn profiles in this MS may be partially affected by diagenetic remobilization of Mn below the sampled intervals. The above section has been altered to discuss this possibility.

Line 735-737: This section is somewhat incorrect as well. What Mn and Fe is consumed? I assume you are now referring to Mn- and Fe-oxides. I suggest: 1) making it clear that dissolved Mn and Fe are produced during dissimilatory Mn- and Feoxide reduction; 2) highlighting that the reason for the decline in concentrations are consumption processes (assuming steady state you would otherwise expect constant pore-water values below the current reaction zone), which likely include the reaction of Fe with hydrogen *sulfide, and interactions of Fe with Mn-oxides. (Again the sedimentary Mn story may be more complicated; see comment above); 3) stepping back from the idea that there is "complete consumption of Fe and Mn". If you are referring to the oxides, then especially in the case of Fe it is the very reactive (towards H2S) iron (oxyhydr)oxide phases that are being reduced (see Canfield et al., 1992: The reactivity of sedimentary iron minerals towards sulfide) but there is without a doubt no "complete Fe consumption"!*

See the above comment response. This section has been reworded to reflect the possible importance of Mn remobilization in these sediments. The portion on "complete" consumption has been removed.

Section 5.7 and Figure 16: In this form, I find the plot misleading and somewhat irrelevant (or not providing any new helpful information). First, as you have discussed, sites with methanogenesis and AOM are characterized by much higher DIC concentrations and much lighter delta^{13}*C-DIC values than sites lacking these processes. If you multiply these two, of course you get more negative values at the AOM sites. Second, I am not sure what you are actually plotting as ˆDIC here ? You state that other authors have used the concentrations at the seafloor and the SMT. What do you do for your data where there is no SMT? Third, in line 760 you state "two basic models help explain the relationships in Figure 16." However, you are in the following section only discussing the C:S ratios, including their relative changes with depth (as you are interpreting them from the mudline downward using the changes in DIC*delta*^{13}*C-DIC as an alternative measure for depth). Why then do such a crossplot? On a side note – why is the ratio for the OSR model increasing past 2:1? Because the DIC reflects additional bicarbonate production by dissimilatory Mn and Fe oxide reduction rather than only from sulfate reduction ? Fourth, in line 747 you are stating that "a flux of HCO3- from below the SMT can augment the DIC produced. . .Thus, changes in alkalinity relative to sulfate often exceed 1:1. . .". Now the conclusion from your model/plot is that -line 768-769-"..*CH_4 *charged locations with migrating DIC must have C:S molar ratios in excess of 1:1. . .". So what have we learned? It would be honest to also mention the studies by Snyder et al., 2007 and Wehrmann et al. 2011 (Coupled organic and inorganic carbon cycling in the deep subseafloor sediment of the northeastern Bering Sea Slope (IODP Exp. 323)) in lines 740-750 who used fluxes instead of concentrations.*

As quoted above, line 748 in the previously submitted MS discusses the upward DIC flux common to sites with high CH_4 concentrations. This flux is often ignored, but has been shown to broadly affect

both solute concentrations and isotopic values in CH_4 charged sediments (Dickens and Snyder, 2009; Chatterjee et al., 2011). An improved section 5.5 clarifies the signatures of AOM and OSR for which this flux is a strong component. Importantly, the x-axis of Figure 16 is NOT simply a result of high DIC concentrations, but rather shows a very large continuum of values in supposedly similar environments which do not follow the 1:1 and 2:1 ratios many authors use. Additionally, plotting the sites from this MS versus locations with high CH_4 flux clearly juxtaposes our results.

Specifically from above: The DIC question is irrelevant because all locations other than results from this MS have SMTs. The two models were intended to expand the above concept, but appear to be confusing. We are therefore, removing them from the MS. The Snyder and Wehrmann references have been added.

Lines 808-816: I suggest expanding this section, and maybe including relevant literature to support the different hypotheses, even if it means speculating. The finding that CH_4 is low in the sediment in this part of the Arctic is the essential message of this study; the major question that arises is why? Do the ACEX studies provide any clues that would support any of your hypotheses? Lines 817-820 need more details and references as well! Discussion section: the Ba and Sr data are not discussed.

This section has been expanded with references.

Technical corrections:
Line 17:. . .methane (CH_4). . .

Fixed

Line 27: replace “nutrient” with “phosphate and ammonium”. . .Also, the “nutrient data” does not provide evidence for the dominance of metal oxide reduction but evidence for very low organic carbon turnover rates. Please re-phrase.

Line 35:. . .substantial amounts of CH_4. (or something similar); Line 44:. . .in the form of gas hydrates,

Fixed

Line 79/80: Please re-phrase. Methane is not "reacting with sulfate". Obviously this is still debated but a term like "sulfate reduction coupled to the anaerobic oxidation of methane" or "sulfate reduction-coupled AOM" is more appropriate or rephrase to "microbes utilize methane. . ." or so.

Line 84: "Where CH_4 *flux to. . .*

Fixed

Line 96-100: I suggest deleting these sentences. First, giving the total number of samples etc. is a little too much detail for the intro. Second, putting a "conclusion" sentence here, seems confusing (this is not the abstract).

Lines 150-157: Change all [] to ()

Fixed

Line 152: Limited information on what?

Geologic

Line 193: I don't think the Schulz, 2000 reference is appropriate here. I suggest Boudreau (1997) and Iversen and Jørgensen (1993) instead.

Changed

Line 241: Delete summary sentence; Line 273: Remove ; at end; Line 314: Table 4? Line 338: Should be Table 3. Line 340: ..dissolved sulfur and metal concentrations. . . Line 342: HNO_3
All Fixed

Lines 353-381: Please shorten these sections. These are very common methods and you can reference the appropriate literature. We don't need to know exactly how much of which chemical you weight in etc.

This section has been significantly shortened

Line 389: Can you find a better title for this section than "Generalities"?

Yes

Line 390: Table 1?; Line 405-412: Move to methods section.

Fixed

Line 422-428, section 4.3: As outlined above, I suggest moving this to an supplementary material section.

This section has been moved.

Line 459: I am not sure a "decrease" can "change"

Changed to "is most pronounced."

Line 477: Replace "faster" (time component) with " displayed a steeper decrease" or so; Line 479: Replace "sulfate" with "sulfur"

Fixed

Line 480: I don't see where the 0.98 comes from.

The ratio to change in alkalinity to sulfate.

Line 482 etc.: I suggest taking the "nutrient" term out. As you discuss, you are considering phosphate and ammonium as mineralization products. Instead of the discussion in Lines 483-485, why not just say "..the mineralization products. . .."

"Nutrients" removed and line 483 reworded.

Line 621: Replace symbol.

Fixed

Line 633: I am not sure this is correct. A concave-down sulfate concentration profile usually implies on-going organoclastic sulfate reduction above the SMT. Otherwise you get a linear profile driven by diffusion of sulfate from the sediment-water interface to the SMT.

Line 633 has been reworded.

Lines 635-637, 637-639, 639-641: These sentences need references.

References added.

Line 650 etc.: Do you actually calculate the methane fluxes somewhere? If so, how were methane fluxes calculated? What was taken into consideration? What if organoclastic sulfate reduction is occurring in close vicinity above the SMT, ie, your upward methane flux would then not be equal to the downward sulfate flux (at a 1:1 ratio). Where is the methane flux data?

We do not understand this comment. We infer little to no CH_4 in the sediments, therefore we cannot calculate CH_4 flux.

Line 671: "...imply a $SO_4$2- flux.."; Line 674: 6.8 mol/m^2

Fixed

Line 687-688: Ok, it has a different ratio. . .and ? I am not sure you mention this here?

Section 5.5 goes into detail explaining the importance of this ratio.

Line 706: 43.54‰

Fixed

Line 708-709: I don't think that this is an "issue" but as you point out earlier it is very common to only observe hydrogen sulfide very close to the SMT. Nonetheless, if "none was detected" what do you conclude from that (ie, here please insert a short discussion on the reaction of hydrogen sulfide with dissolved iron and iron oxides, pyrite formation etc)?

This section has been reworded.
Line 724: manganese oxide reduction, iron oxide reduction; also denitrification and nitrate reduction ???;
Line 742: "The idea. . ." There is a word missing here.

All fixed

Line 779: Can you find a better title than Explanations"?

How about "Possible Explanations for Methane Absence?"

Response to Referee 1:

The authors thank Reviewer 1, and wish to make some general comments before discussing individual criticisms. Unfortunately, this review is difficult to read, and many comments are not germane to the original MS. In order to explain our overall response, we first summarize this review:

1. The MS does not contain additional data, even though it is one of the most comprehensive pore water chemistry data sets within a single effort generated to date in any region, let alone from a previously virtually unexplored section of the Arctic Ocean.

2. The pore water results cannot be used to understand CH_4 abundance, although numerous papers in multiple regions, including the Arctic offshore Alaska, convincingly demonstrate the opposite (eg. Borowski et al., 1996; Jørgensen et al., 2001; Torres and Kastner, 2009; Treude et al., 2014; etc.).

3. The primary interpretation and conclusion conflicts with previous speculations in the region, although no pertinent information to the problem exists beyond the current work.

Additionally, in certain parts, the reviewer appears to be discussing a different MS than ours. Page C4, for example, the reviewer criticizes the authors for "vigorous" referencing of a study (Nauhaus et al., 2002) that we neither cite nor discuss.

Specific Comments from Referee 1:

However, this ms rather demonstrates that the current state of knowledge of pore water biogeochemistry in particular areas of the ocean is very incomplete; a great deal of effort will be required in order to improve our understanding of the relationship between sulfur and carbon cycling in the Arctic.

We do not follow this comment. The community has published volumes of detailed research about pore water chemistry in regions that contain gas hydrate (Borowski et al., 2000; Torres et al., 2004; Treude et al., 2005; Dickens and Snyder, 2009; Coffin et al., 2013). This is stressed throughout the updated MS, and where possible, we have added additional discussion and references.

The authors of the ms come to the following conclusions: 1) Based on interpretation of the pore water profiles, they found no evidence for upwardly diffusing CH_4. 2) Based on these data, they strongly suggested that gas hydrates do not occur on the slopes of the ESM. 3) They claimed that previous investigators who suggested that hydrate deposits exist in the Arctic shelf/slope based on results of their investigations were simply wrong.

This point has been clarified in the updated text. We strongly suggest WIDESPREAD gas hydrates do not occur as previously speculated. It is important to note our results and interpretations DO NOT CONFLICT with any previous data or direct results from the region.

First of all, I do not understand why, when reporting low CH_4 concentrations and the relationship between CH4 and sulfate dynamics in the pore water, the authors did not measure the concentrations of either parameter. Is it not logical to measure CH_4 and sulfate in pore water if one is going to report "low methane concentrations in the sediments"? These are rather routine measurements.

Not all measurements could be generated given the limitations of the expedition and subsequent funding. However, we did measure the S concentrations of pore water, and know these are representative of SO_4^{2-}, because we checked for H_2S as well as measured dissolved Ba^{2+}. Moreover, there are problems with generating quantitative dissolved CH_4 profiles in marine sediment because of degassing associated with changes in pressure and temperature.

Here, it is absolutely crucial to realize that, as stressed in the text and at least to our knowledge, no region with significant CH_4 in moderately shallow sediment (< 500 m) has high dissolved S/dissolved SO_4^{2-} in pore waters near the seafloor, as well as other certain chemistry documented here. This is now stated in the updated MS, including discussion of localized areas of high advection and CH_4 venting.

The authors referred to other researchers in their ms to present supportive arguments, but none of these referenced studies avoided taking measurements.

In fact, a significant fraction of the research referenced was partially generated by one of the authors (Dickens). It should be noted that the measurements were not avoided in some means to hide information, but rather that we know how CH_4 exists and cycles in many regions, and the most prudent means of tackling the problem at a first-order level over an immense area from an ice-breaker is to generate numerous detailed pore water profiles (Borowski et al., 1999; Snyder et al., 2007; Hu et al., 2015).

In addition, the authors of this ms speculate about the particulate organic carbon (POC) and OC content of sediment, but did not measure either parameter. OC content of sediments should be reported as a number of different carbon stocks, not just POC.

This comment is unclear. As numerous studies have shown (Borowski et al., 1996; Dickens, 2000; Hensen et al., 2003; Geprags et al., 2016), the abundance of CH_4 in shallow sediment on continental slopes does not depend on the current supply of POC, but rather on the integrated input of POC over long time intervals (e.g., hundreds of thousands to million year time scales), which cannot be assessed without drilling. This last point has been added to the updated MS.

Second, I do not understand why the presence or absence of CH_4, either in the sediments or in the water column in this area, should be necessarily connected to the existence or non-existence of hydrates. Are hydrates the only possible source of CH_4 in the Arctic shelf/slope? I believe not; hydrates could be only a tiny fraction of the source, because the hydrate stability zone (HSZ) created by P/T conditions could compose only a small fraction of the sedimentary drape (a few hundred meters), while the sedimentary drape could be a few kilometers thick.

The authors do not understand this comment. Gas hydrates are not a source of CH_4, but rather, one phase of CH_4 in open and dynamic systems, where CH_4 carbon can exist as dissolved gas, free gas, and gas hydrate.

This project cannot link shallow water chemistry profiles to CH_4 abundance at truly deep depths, and the MS does not attempt to do so. However, deep CH_4 cannot exist as gas hydrates, for reasons of P/T conditions. On the other hand, the presence of gas hydrate in the upper few hundreds of meters of sediment is absolutely related to total CH_4 concentrations in pore space, which are linked to shallow sediment through diffusion or in some cases advection. This point is clarified in the updated discussion section.

Third, the purpose of this massive MS is not clear to me. This paper is flooded with equations and details devoted to methods, but mathematics, first of all should be applicable; then, the accuracy of mathematics does not aid in interpreting the inconclusive data.

We do not understand this comment. The purpose, as outlined in the MS, is very clear: we know how pore water chemistry profiles look above gas hydrate systems at numerous locations around the world, and we know how to interpret them at a basic level; we generated such profiles in the region

of interest; the pore water profiles do not conform to those at any region where significant CH_4 occurs in shallow sediment nor our understanding as to why such profiles arise.

However, we agree the MS can be shortened significantly. The revised MS has moved essentially all of the Rhizon discussion to supplementary materials, deleted several sections, figures, and tables, and streamlined much of the text including the methods section. In total, almost 200 lines were deleted.

Below are my comments on some aspects of this ms. A more detailed look would be as long as the ms itself, because nearly every page of this ms would benefit from clarification. The methodology chosen by the authors of this ms and their level of understanding of the processes they were trying to investigate are my greatest concern. Biogeochemists working in the marine ecosystems have already gained some understanding of the fact that biogeochemical processes associated with diagenetic transformation of organic matter under anaerobic conditions in marine sediments are very complex microbe-mediated processes. These processes involve microorganisms from various physiological groups: aerobic and anaerobic saprophylic and cellulose degrading bacteria, sulfate reducers, methanogens, denitrifiers, and methylotrophs. Transformation of organic matter is a multi-stage process: primary anaerobes decompose polymeric compounds to monomers, which, in turn, serve as a substrate for fermentation agents and gas-producing bacteria. A general conclusion is that the major fraction of OC preserved in the sediments is oxidized to CO2 by the sulfate-reducing bacteria (SRB) and that 2 moles of OC are oxidized for every mole of sulfate reduced: 4H(CH2)n COO- + (3n + 1)SO42-+ H2O!(4n + 4)HCO3- + (3n + 1)HS- + OH- + nH+. When acetate is oxidized completely, the atomic ratio of OC oxidized to sulfate-S reduced is 2 : 1. However, as 'n' increases, the C: S ratio changes; the ratio between the reactants could be different because it depends on the varying nature of the organic matter (Lerman 1982). This is because most of the photosynthate is not immediately available for oxidation; only the low molecular weight (LMW) fraction of dissolved OC (DOC) is rapidly oxidized by SRB, while the high molecular weight (HMW) fraction of POC, which usually increases with depth, is refractory. There are severe restrictions on microbial activity other than substrate availability, including that SR as a biotic process may be more strongly coupled to mineralogy (Ivanov et al., 1989). The knowledge that has been accumulated by scientists so far is very limited and only applicable to those particular ecosystems which were investigated beyond the Arctic.

The authors are perplexed by this comment, as most of it does not pertain to our MS, and it seems to belie faulty logic. At a basic level the referee appears to think biogeochemical processes are so complex that the community cannot obtain overall net chemical reactions and flux of carbon from pore water chemistry.

If we are interpreting the comment correctly, we then return an obvious question: how and why can the community measure similar pore water chemistry profiles at myriad locations and see basic commonalities (e.g., the absence of SO_4^{2-} above sites with the presence of significant CH_4 below), irrespective of the specifics and microbiology involved? No change has been made to the MS regarding this comment.

The most reliable method to trace the course of sulfate reduction in sediments uses radioactive sulfate (35S). By the use of this method it was shown that most reduced 35S-sulfate was in pyrite and organic sulfur (Lein et al., 1982). The relationship between sulfur and carbon cycling in the Arctic marine systems is even more complicated, because the relationships between the sites of primary production and the sites to which organic matter is translocated and deposited, including organic matter delivered to the shelf/slope from surrounding land, are difficult to establish both qualitatively and quantitatively.

We do not know how to respond to this comment, as it mostly does not pertain to our MS. It begins with a statement for which we disagree, and it does not make sense in its entirety. No change has been made to the MS regarding this comment.

A recently published review of CH_4 emissions from the seafloor in the Arctic Ocean underscored that the role of SRB in the anaerobic oxidation of methane (AOM) is unclear and the ecology of AOM communities, particularly for high-latitude environments, is not well understood. For that reason, predicting CH_4 fluxes, especially those related to hydrate dissociation, remains highly speculative (James et al., 2016). This is because CH4 is transported within the sediments in two different ways: as a dissolved phase (by diffusion or advection) or as free gas (ebullition). Free gas is inaccessible to microbes, which depend on a diffusive transmembrane gas transport. This means that release of free gas through the sediments might not leave any traces in the pore water (see Fig.5 in James et al., 2016).

The authors are unsure how to respond to this comment because it mostly is irrelevant to the topic of our MS. Crucially, we are not concerned how CH_4 would escape the seafloor via ENHANCED gas hydrate dissociation in the future, but whether significant CH_4 exists in shallow sediment on the SLOPE in the now. We hope this point is clear in the MS.

Additionally, the referenced MS (James et al., 2016) does not conflict with our interpretations. These authors clearly indicate that AOM is a dominant process above methane-charged systems at steady-state conditions, and should impact pore water SO_4^{2-} gradients (e.g., the very Fig. 5 that the referee emphasizes).

The comment that passage of free gas through sediment does not leave traces in pore water is simply incorrect. The paper and figures by James et al. (2006) by no means suggest this concept, and rightfully so. Pore waters in areas where CH_4 advects from below at high rates, such as along faults and fractures (Fig. 5), have truly different chemistry than seawater and anything in our results. The updated Figure 12 emphasizes some of these differences.

Moreover, recently published observational data show that in the Arctic environment, for example in the Alaskan Beaufort Sea continental margin sediments, substantial (30-500 µM) concentrations of sulfate can remain below the sulfate-methane transition zone (SMTZ) although mass balance cannot explain the source of sulfate below the SMTZ.

This comment seems to betray a basic misunderstanding of SO_4^{2-}, CH_4 fluxes, and mass balance. SO_4^{2-} concentrations 0.03-0.5 mM are not "substantial" compared to the ~28 mM in typical seawater. Second, there are at least three known reasons for SO_4^{2-} below the SMT: 1. Pore water contamination, 2. H_2S oxidation, and 3. Barite dissolution. Third, mass balance always applies.

Additionally, the Beaufort Sea results we assume the referee is mentioning (Coffin et al., 2013), show the exact type of shallow pore water profiles which this MS argues would occur above gas hydrates – and do not in our results! No changes have been made to the MS regarding this comment.

In addition, sulfate reduction and anaerobic oxidation of CH_4 can occur throughout the methanogenic zone. Experimental data indicated decoupling of sulfate reduction and AOM and competition between *sulfate reducers and methanogens for substrates, suggesting that the classical redox cascade of electron acceptor utilization based on Gibbs energy yields does not always hold even in diffusion-dominated systems (Treude et al., 2014).*

Yes, this may true at a detailed and microscopic level, as pointed out by numerous authors, but not at any macroscopic level, at least that we are aware of, excepting odd environments (e.g., brines). The true beauty of pore water chemistry in the deep-sea marine environment is the remarkable consistency of multiple constituents linked to an array of environments. To restate from above, and in the text, all pore waters in methane-charged systems on continental slopes that we are aware of have certain commonalities – none that are seen in any of the pore waters generated in this study. This point has been emphasized in the updated discussion section.

Although they vigorously referred to Nauhaus et al. (2002) as a proxy-establishing experiment, the authors did not give this work any critical assessment. If they had done so, they would have definitely questioned the claim that methanotrophic communities associated with SRB oxidize CH_4 *anaerobically in a 1:1 ratio to sulfate reduction. How that could be possible if the reported 4-5-fold increase in H2S production (accumulated over 80 days!) was accompanied by an increase in CH4 concentration of 3 orders of magnitude (from 0.01 to 15.8 mM)? Besides, rates of SR were so small (0.5-3.0 µM/d-1) compared to the concentrations of sulfate (103-1.55 µÐIJ) that the question arises: How could this little change be reliably measured (without using the 35S method, which they did not) and related to AOM?*

This is perhaps the most confusing part of this review. We neither cite nor discuss the paper by Nauhaus et al. (2002). Indeed, the first author had not even read this work prior to submittal. We are forced to conjecture the referee is confusing our MS with another. This would explain a number of seemingly inexplicable comments which do not pertain to our text (ex. the referee statement that we "assumed CH_4 **was being released from destabilizing hydrates, most likely via bubbles and the convective flow of geofluids"). No change has been made to the MS regarding this comment.**

Not to mention that this effect has no applicability to the Arctic Ocean.

We are not sure how to address. The referee seems to have a view that physical chemistry and biochemistry in the Arctic Ocean are somehow special, so that basics and inferences gained from elsewhere around the world do not apply.

Here, it is especially important to note the paper by Coffin et al. (2013), as already highlighted in our MS. These authors characterized pore water chemistry in short sediment cores above sequences with known gas hydrates along the shelf and slope of the Beaufort Sea (Arctic), very much as done in our MS. As predicted, they observed shallow SMTs indicative of a strong diffusive methane flux. As obvious in our work, their pore water profiles contrast with those from the slopes off northern Siberia. This point has been emphasized in the updated MS.

Another concern is this: How representative of the area are these data? Only four short transects consisting of 16 stations are presented; each transect is based on data from 2-6 stations. Data from only 2-4 stations represent all core depths. Core lengths vary from 1.95 to 8.43 m (mean length 5.25 m). Eight of the 16 stations are only represented by the very uppermost layers (from 0.16 to 0.39 m) of sediment collected by the multi-corer. These shortest parts are the most valuable as they represent the least disturbed environment, but they are too short to constitute any sort of conclusive data regarding CH_4 *cycling in the sediments. I can only guess at how the authors succeeded in dividing these tiny cores into numerous parts, each 0.2-0.3 m in length, and accumulated enough data to compare these cores with one of two idealistic schemes to characterize the specific dynamics of processes occurring over a sediment depth of 100 m (Fig.1). Data obtained by other types of sampling (piston/gravity coring) should be treated and interpreted very cautiously as the cores are not only severely disturbed during the coring process, but also chemically altered as they are extracted from the sea floor and lifted onto the ship.*

This comment does not make sense. First, the fact that the pore water profiles give nice, detailed gradients in multiple species, demonstrably indicates that the cores have minimal disturbance. We can add core photos to our already long paper, if desired, to further emphasize this point.

Second, the proposition that the uppermost part of a core is the least disturbed and most important to understanding processes is flat out wrong. This is because of the nature of coring, which tends to disturb (or in many cases not recover) the top few cms, and because of bioturbation and reoxidation.

Third, the methodology for how the cores were sampled is detailed at length in the manuscript. Indeed, the reviewer criticized the authors earlier for the length of this section, and now claims to only "guess" at how this was accomplished. No changes have been made to the MS regarding this comment.

Finally, the authors plotted water concentration profiles along each transect collectively (!) using colors and symbol types which make it virtually impossible to distinguish between these symbols, making interpretation of the data sets very difficult.

We agree these figures are difficult to read. Given the extremely large dataset over this vast region, it is difficult to clearly present results concisely. It seemed to us somewhat overwhelming to plot the chemistry at every site independently, or alternatively every species analyzed at multiple sites independently. In order to improve readability, we have increased panel, symbol, and line widths while minimizing white space. The ACEX data has been removed to limit clutter, and the legends are inside the panels. Hopefully, this improves readability without lengthening the paper.

From this, it follows that the authors assumed complete uniformity of processes occurring not only in the observed settings located tens of kilometers apart from each other, but also over the entire slope area! This is despite the fact that CH4 fluxes on the East Siberian Arctic Shelf (ESAS), which could be associated with CH4 releases from decaying hydrates, have been reported to vary by orders of magnitude within much smaller scales (Shakhova et al., 2015).

We did not assume complete uniformity of processes. In fact, the MS goes into great detail explaining the range of processes that relate to the pore water chemistry -- processes that have been well documented along many continental slopes. The authors see no reason to add to this already lengthy section.

I see a clear discrepancy between the basic assumptions made by the authors and the methodology used to test these assumptions. The authors assumed CH4 was being released from destabilizing hydrates, most likely via bubbles and the convective flow of geofluids.

We do not understand this comment. The referee is stating things that cannot be found anywhere in the text. Additionally, this comment has leapt well beyond anything discussed in the MS. As stated above, and clearly in the MS, we discuss the lack of evidence for CH_4 in shallow sediment. Our MS has little bearing on how gas hydrates would be destabilized and how CH_4 would be released. No change has been made to the MS regarding this comment.

Despite that, all equations used for estimates refer to the diffusive transport of CH_4 and other substances in the sediments. This is understandable; they used what was available. The problem is that the mathematics associated with diffusive transport cannot be used to describe the release of free gas from decaying hydrates. When assuming CH4 release from gas hydrates, one should realize that hydrates convert to free gas; the released gas travels upward much faster than diffusion occurs, through very efficient gas migration paths (chimneys etc.). In most cases, ascending CH4 can avoid oxidation in a few ways. 1) Because free gas resulting from hydrate decay is over pressured, it builds up a gas front; this disturbs sediment layering, creating the characteristic marks of gas release (pockmarks etc.). 2) Only CH_4 dissolved in pore water is reachable by microbial communities; CH_4 released as free gas (ebullition) is not consumable by microbes. 3) AOM rates are only remarkable as compared to rates of modern methanogenesis, because all synergetic processes should be energetically efficient for all members of the microbial community, including SRB, methanogens and methanotrophs, etc.

This comment is simply wrong. In most locations with gas hydrate, the vast majority of CH_4 generated in the sediment ultimately (i.e., long time scales) escapes back to the ocean through diffusion. The assumption that methane-carbon above gas hydrates only returns to the ocean as free gas is entirely incorrect. The authors have added this discussion to the updated MS.

Finally, the authors of the ms used three assumptions to explain their findings. Their first assumption is that bottom seawater on the slope north of Siberia is warming, leading to hydrate destabilization. There are no reports of increased bottom water temperatures along the slope of the Arctic during either the last glacial cycle (Cronin et al., 2012) or the Holocene (Biastoch et al., 2011; Dmitrenko et al., 2011; James et al., 2016). All papers published so far project the response of the hydrate inventory to possible future climate change in the Arctic. The paper of Stranne et al., (2016) the authors refer to assumes a linear rise in ocean bottom water temperatures of 3C over the coming 100 years. This speculative warming of the Arctic is intentionally set higher than in other studies (<2C by Biastoch et al., 2011; <1C *by Kretschmer et al., 2015) while modeling assumptions contradict the existing hydrological data (Biastoch et al., 2011; Dmitrenko et al., 2011; James et al., 2016).*

This is another statement that absolutely cannot be found in our MS. Nowhere do we assume bottom seawater is warming, nor are warming temperatures even necessary to have CH_4 in pore waters above gas hydrates. Here, again, we wonder if the referee is thinking of another project. No change has been made to the MS regarding this comment.

Their second assumption is the quintessential statement that "Implicit of this finding is that sediments sequences along the ESM lack gas hydrates" following the authors' speculations about why predictions of hydrates on the ESM are so markedly wrong.

This statement has been reworded to better reflect the conclusion, as stated elsewhere in the MS, of WIDESPREAD gas hydrates. However, this is not an assumption, but rather a direct consequence of our results. The pore water chemistry profiles strongly indicate the lack of significant methane concentrations in the upper few hundred meters of sediment; given P/T conditions for gas hydrate, this absolutely implies an absence of gas hydrate.

Fascinatingly, prior to this expedition, we did expect widespread gas hydrates.

The authors then suggest that: 1) the significant sea-ice concentration on the ESM diminishes net primary production (NPP); 2) the extremely broad continental shelf prevents accumulation of terrestrial organic-rich sediments; and 3) sediment accumulation is highly variable, so organic matter can be consumed during intervals of low deposition. None of these explanations is true. It was recently shown that the total OC (TOC) content in the ESAS/ESM sediments measured along the transect spanning more than 800 km from the Lena River mouth to the shelf (2000–3000 m water depth) varied between 2 % at shallow water depths and 0.8% in deeper water (Bröder et al., 2016). In addition, TOC values and general patterns, which reflect fractions of terrigenous OC reaching the slope (based on biomarkers), were within the same range as those measured for the North American Arctic margin (Stein and Fahl, 2000, 2004; Goni et al., 2013). For comparison, an average value for the continental slope of the Gulf of Mexico, where large storage of CH4 hydrates has been proven to exist, is 0.8% ±0.2 (Gulf of Mexico Hydrate Research Consortium). Moreover, according to Arrigo and van Dijken (2011), the total annual NPP over *the Arctic Ocean exhibited a statistically significant increase by 20% between 1998 and 2009, due mainly to increases in both the extent of open water (+27%) and the duration of the open water season (+45 days). Most importantly, increases in NPP over the 12 year study period were largest in the eastern Arctic Ocean, most notably in the Siberian (+135%) sector.*

While interesting, none of this is relevant. This is because, for high CH_4 concentrations to exist in the upper few hundreds of meters on the slope, it is past carbon burial (i.e., not recent) that matters. This point has been clarified in the updated text.

It is interesting that the authors themselves confirmed that: 1) environmental conditions on the ESM are highly conducive for gas hydrates; 2) hydrate occurrence in the other areas of the Arctic, where hydrates were predicted, was confirmed by hydrate recovery; and 3) all the models developed by generations of geologists to predict hydrates in the Arctic used the same assumptions.

We would agree with this statement, if logical qualifiers were added. The environmental conditions on the ESM are highly conducive for gas hydrates IF AND ONLY IF THERE IS SUFFICENT METHANE; hydrate occurrence in the other areas of the Arctic, where hydrates were predicted, was confirmed by hydrate recovery AND BY PORE WATER CHEMISTRY IN SHALLOW CORES; all the models developed by generations of geologists to predict hydrates in the Arctic used the same assumptions WHICH ENTIRELY INFER A SOURCE OF CARBON TO PRODUCE CH_4.

The referee is ignoring two crucial facts, both discussed at length in the MS: (1) all previous works hinge on an assumption (not evidence) of significant CH_4 in shallow sediment; and (2) NO pertinent data to the problem exists beyond our current work. These point are clarified in the updated text.

If the authors agree that these statements are true, they failed to be critical of their own work, which is based on a handful of inconclusive data obtained on a single expedition, groundless methodology, and a few erroneous assumptions. Instead of casting doubt on the results of others, I would suggest that the authors question their own results and make a greater effort to accumulate clear, interpretable data. I believe I have made it quite clear that there is a huge discrepancy between the results presented by the authors and the far-reaching conclusions they are trying to support with these data. I see no way to support publication of this MS in its current state.

We respectfully disagree with the referee’s conclusions.

Low methane concentrations in sediment along the continental slope north of Siberia: Inference from pore water geochemistry

Clint M. Miller[1], Gerald R. Dickens[1], Martin Jakobsson[2], Carina Johansson[2], Andrey Koshurnikov[3], Matt O'Regan[2], Francesco ~~Muschitiello[2]~~Muschitiello[4], Christian Stranne[2], Carl-Magnus Mörth[2]

A manuscript submitted to:

Biogeosciences

[~~July 23, 2016~~February 20, 2017]

[1]Department of Earth Science, Rice University, Houston, TX, USA

[2]Department of Geological Sciences, Stockholm University, Stockholm, Sweden

[3]V.I. Il'ichev Pacific Oceanological Institute, RAS

[4]Lamont-Doherty Earth Observatory, Columbia University, NY, USA

Correspondence to: Clint M. Miller (clint.m.miller@rice.edu)

Abstract: The Eastern Siberian Margin (ESM), a vast region of the Arctic, potentially holds large amounts of methane (CH_4) in sediments as gas hydrate and free gas. Although this CH_4 has become a topic of discussion, ~~primarily because of rapid regional climate change,~~ the ESM remains sparingly explored. Here we present pore water chemistry results from 32 cores taken during Leg 2 of the 2014 SWERUS-C3 expedition. The cores come from depth transects across the slope and rise sediments off the Chukchi and East Siberian Sea (CESS) of the ESM between Wrangel Island and the New Siberian Islands.~~the continental slope of the ESM between Wrangel Island and the New Siberian Islands~~. Upward CH_4 flux towards the seafloor, as inferred from profiles of dissolved sulfate (SO_4^{2-}), alkalinity, and the $\delta^{13}C$-dissolved inorganic Carbon (DIC), is negligible at all stations east of where the Lomonosov Ridge abuts the ESM at about 143°E. In the upper eight meters of these cores, downward sulfate flux never exceeds ~~9~~6.2 mol/m^2-kyr, the upward alkalinity flux never exceeds 6.8 mol/m^2-kyr, and $\delta^{13}C$-DIC only slowly decreases with depth (-3.6‰/m on average). Moreover, upon addition of Zn acetate to pore water samples, ZnS did not precipitate, indicating a lack of dissolved H_2S. Phosphate, ammonium, and metal profiles reveal that metal oxide reduction by organic carbon dominates the geochemical environment, and supports very low organic carbon turnover rates. ~~Additionally, dissolved H_2S was not detected in these cores, and nutrient and metal profiles reveal that metal oxide reduction by organic carbon dominates the geochemical environment.~~ A single core on Lomonosov Ridge differs, as diffusive fluxes for SO_4^{2-} and alkalinity were 13.9 and 11.3 mol/m^2-kyr, respectively, the $\delta^{13}C$-DIC gradient was 5.6‰/m, and Mn^{2+} reduction terminated within 1.3 m of the seafloor. These are among the first pore water results generated from this vast climatically sensitive region, and they imply that abundant CH_4, including gas hydrates, do not characterize the CESS continental slope.~~and they imply that significant quantities of CH_4, including gas hydrates, do not~~

Formatted: Subscript

~~exist in any of our investigated depth transects spread out along much of the ESM continental slope~~. This contradicts previous modeling and discussion, which generally have assumed the widespread presence of CH_4.~~This contradicts previous assumptions and hypothetical models and discussion, which generally have assumed the presence of substantial CH_4.~~

1. Introduction

The Arctic is especially sensitive to global climate change~~. Already~~, and over the last century~~, the region~~ has experienced ~~some of the fastest rates of warming on Eart~~anomalous warming~~h~~ (Serreze et al., 2000; Peterson et al., 2002; Semiletov et al., 2004). Past and future increases in atmospheric and surface water temperatures should, with time, lead to ~~substantial~~ significant warming of intermediate to deep waters (Dmitrenko et al., 2008; Spielhagen et al., 2011), as well as sediment beneath the seafloor (Reagan and Moridis, 2009; Phrampus et al., 2014). The latter is both fascinating and worrisome, because pore space within the upper few hundreds of meters of sediment along many continental slopes can contain large amounts of temperature-sensitive methane (CH_4) in the form of gas hydrates, free gas, and dissolved gas (Kvenvolden, 1993 and 2001; Beaudoin et al., 2014). Consequently, numerous papers have discussed the potential impact of future warming upon CH_4 within slopes of the Arctic Ocean (Paull et al., 1991; Archer, 2007; Reagan and Moridis, 2008; McGuire et al., 2009; Biastoch et al., 2011; Elliott et al., 2011; Ferré et al., 2012; Giustiniani et al., 2013; Thatcher et al., 2013; Stranne et al., 2016).

Globally, the amount and distribution of ~~the distribution and total amount of~~ CH_4 in sediment along continental slopes remains poorly constrained (Beaudoin et al., 2014). This is particularly true for the Arctic Ocean, because ice cover makes accessibility to many regions difficult. Nonetheless, numerous papers -have inferred enormous quantities of gas hydrate surrounding the Arctic (Kvenvolden and Grantz, 1990; Max and Lowrie, 1993; Buffett and Archer, 2004; Klauda and Sandler, 2005; Max and Johnson, 2012; Wallmann et al., 2012; Piñero et al., 2013; ~~Figure 1~~Fig. 1 and 2). In some sectors, compelling evidence exists for abundant sedimentary CH_4 and gas hydrate. Bottom simulating reflectors (BSRs) on seismic profiles

Formatted: Font: Not Bold

generally mark the transition between overlying gas hydrate and underlying free gas (Holbrook et al., 1996; Pecher et al., 2001), and thereby imply high quantities of CH_4 in pore space (Dickens et al., 1997; Pecher et al., 2001). Such BSRs have been documented along the North Slope of Alaska (Collett, 2002; Collett et al., 2010), within the Beaufort Sea (Grantz et al., 1976; Grantz et al., 1982; Weaver and Stewart, 1982; Hart et al., 2011; Phrampus et al., 2014), around Canadian Arctic Islands (Judge, 1982; Hyndman and Dallimore, 2001; Majorowicz and Osadetz, 2001; Yamamoto and Dallimore, 2008), adjacent to Svalbard (Eiken and Hinz, 1993; Posewang and Mienert, 1999; Vanneste et al., 2005; Hustoft et al., 2009; Petersen et al., 2010), and within the Barents Sea (Andreassen et al. 1990; Løvø et al., 1990; Laberg and Andreassen, 1996; Laberg et al., 1998; Chand et al., 2008; Ostanin et al., 2013). Furthermore, Lorenson and Kvenvolden (1995) observed high CH_4 concentrations in shelf waters of the Beaufort Sea, and Shakhova (2010a, 2010b) have documented ~~ample evidence for methane~~CH_4 escape to the water column on the East Siberian ~~Margin (ESM)~~shelf. It generally has been assumed that sediment on the adjacent ESM slope contains copious CH_4 and gas hydrate (~~Figure 1~~Fig. 1), although there is little data to support or refute this idea.~~although no scientific expedition has investigated the hypothesis.~~

Formatted: Subscript

Formatted: Font: Not Bold

Regional assessments for the presence of abundant CH_4 in marine sediment can be acquired through two general approaches. The first includes geophysical applications, primarily seismic reflection profiling and the recognition of BSRs (MacKay et al., 1994; Carcione and Tinivella, 2000; Haacke et al., 2008), which are a common, but not ubiquitous feature, of hydrate bearing sediments. The second utilizes chemical analyses of pore waters obtained from~~ short~~ sediment cores (Borowski et el., 1996; Borowski et al., 1999; Kastner et al., 2008b; Dickens and Snyder 2009). In marine sediments with abundant CH_4, a general and important process occurs near the seafloor, typically, within the upper 30 m. Microbes utilize upward migrating CH_4 and downward diffusing sulfate (SO_4^{2-}) via anaerobic oxidation of methane (AOM; e.g., Barnes and Goldberg, 1976; Reeburgh, 1976; Devol and Ahmed, 1981; Boetius et al., 2000):~~Upward migrating methane, either through advection or diffusion, reacts with downward diffusing sulfate (SO_4^{2-}):~~

$$\cancel{{}^{12}}CH_4 + SO_4^{2-} \rightarrow HS^- + H^{\cancel{12}}CO_3^- + H_2O \qquad (1)$$

The reaction leads to characteristic pore water chemistry profiles, ones with a clearly recognizable sulfate-methane transition (SMT; Fig. 3). The depth of the SMT inversely relates to the flux of CH_4, which in turns relates to the distribution of CH_4 beneath the seafloor (Borowski et al., 1999; Dickens, 2001; Bhatnagar, 2011). Where CH_4 fluxes toward the seafloor are high, the SMT is located at shallow depth. For example, along the continental shelf and slope of the Beaufort Sea, where seismic profiles indicate gas hydrate. Coffin et al. (2008, 2013) predictably have documented SMTs in shallow sediment (< 10 mbsf). ~~where the superscript ^{12}C denotes that methane is depleted in ^{13}C. This microbially mediated reaction (Barnes and Goldberg, 1976; Reeburgh, 1976; Devol and Ahmed, 1981; Boetius et al., 2000), commonly called anaerobic oxidation of methane (AOM), leads to characteristic pore water chemistry profiles, including a clearly recognizable sulfate methane transition (SMT; **Figure 2**). The depth of the SMT inversely relates to the flux of CH_4 (Dickens, 2001; Bhatnagar, 2011). Where CH_4 to the seafloor is high, the SMT is located at shallow depth. Along the continental shelf and slope of the Beaufort Sea, where seismic profiles indicate gas hydrate, Coffin et al. (2008, 2013) predictably have documented SMTs in shallow sediment.~~

The joint Swedish, Russian, U.S. Arctic Ocean Investigation of Climate-Cryosphere-Carbon interaction (SWERUS-C3) project was initiated to investigate spatial changes in carbon cycling across the ESM. A central theme concerns ~~of this project was to constrain~~ the amount, distribution, and fluxes of CH_4, and the overall project included two expedition legs in the boreal summer of 2014 using the Swedish icebreaker *IB Oden*. ~~included a two-leg expedition in the boreal summer of 2014 using the Swedish icebreaker *IB Oden*.~~ Between August 21 and October 5, Leg 2 sailed between Barrow, Alaska and Tromsø, Norway, focusing on the continental slope of the ESM. SWERUS Leg 2 included geophysical surveying and retrieval of numerous sediment cores, of which 446 pore water samples from eight piston, seven gravity, and 17 multicores (Fig. 2) are studied here to ascertain potential fluxes of CH_4 toward the seafloor ~~Efforts of Leg 2 (8/21-10/3) included retrieval of 60 piston/gravity/multi cores of which six piston, seven gravity, and 17 multicores spanning the continental slope of the ESM are studied here (**Figure 3**). A total of 446 pore water samples were collected from these cores to document changes in chemistry associated with expected SMTs. Here we present and discuss analytical results of these samples. Surprisingly, pore water profiles strongly indicate that, contrary to general inferences, very little CH_4 exists in shallow sediment along the continental slope north of Siberia, which may preclude the presence of gas hydrate.~~

2. Background

2.1 East Siberian ~~Margin~~ margin ~~Geology~~geology

Extensive continental shelves and their associated slopes nearly ~~enclose~~ encircle the ~~central~~ Arctic Ocean (**Figure 1**). Although it represents only 2.6% of the world's ocean by area (Jakobsson, 2002), the ~~central~~ present Arctic Ocean receives approximately 10% of the global freshwater input (Stein, 2008) as well as corresponding massive discharge of terrigenous material (>249 Mt/yr; Holmes et al., 2002). Only Fram Strait allows deep-water flow to and from the Arctic Ocean. This strait, located between Greenland and Svalbard (~~Figure 1~~Fig. 1), has ~~today a~~a modern sill depth of about 2540 m (Jakobsson et al., 2003). It opened during the early to middle Miocene~~from early to middle Miocene times~~ (Jakobsson et al., 2007; Engen et al., 2008; Hustoft et al., 2009). Prior to this, the ~~central~~ Arctic Ocean only ~~connect~~ was connected to the world oceans through shallow seaways (e.g., Turgay Straight),~~ and~~such that deep waters may have been anoxic for long intervals of the Cretaceous and Paleogene (Clark, 1988; O'Regan et al., 2011). ~~Sediments with very high total organic carbon (TOC) accumulated on Lomonosov Ridge during the middle Eocene (Stein et al., 2006), and on Alpha Ridge during the late Cretaceous (Jenkyns et al., 2004).~~

Formatted: Font: Not Bold

The ESM is ~~here~~ defined here to comprise the margin of the East Siberian Sea, which stretches between Wrangel Island to the east and the New Siberian Islands to the west (~~Figure 3~~Fig. 2). We include the adjacent Chukchi and East Siberian Sea (CESS) continental slope in the ESM~~continental slope in the ESM~~. This continental shelf within this region is the widest in the world~~This stretch of continental shelf is the widest in the world~~, extending 1500 km north from the coast. The ~~huge~~ enormous swath laying in water depths less than 100 m (~987 x 10^3 km^2; Jakobsson, 2002) was likely covered in km-thick ice shelf during marine isotope stage 6 (~140 ka), contributing to extensive formation of submarine permafrost ~~was for the most part, aerially exposed during glacial periods, resulting in extensive formation of submarine permafrost~~ (Judge, 1982; Weaver and Stewart, 1982; Løvø et al., 1990;~~;~~ Collett et al., 2010; Jakobsson et al., 2016). The expansive shelf contrasts with the relative narrow continental slope, which intersects two ridge systems, Mendeleev Ridge to the east and Lomonosov Ridge to the west (Jakobsson et al., 2008). Bounded by these two ridge systems, the steep ESM slope leads into the gently sloping Chukchi, Arlis, and Wrangel perched continental rises (Jakobsson et al., 2003).

Formatted: Font: Not Bold

2.2 Regional Oceanography

Bottom waters impinging the slope of the ESM can generally be divided into three masses: the Pacific Halocline (~50-200m), the Atlantic Layer (~200-800m), and Canada Basin Bottom Water (>800m; Timokhov, 1994; Rudels et al., 2000). The Pacific Halocline is a cold (-1.5-0°C), low salinity (32-33.5 psu) water mass that serves as a boundary (and heat sink) between sea ice (above) and Atlantic Layer water (below) (Aagaard, 1981; Aagaard and Carmack, 1989). The underlying Atlantic Layer is warmer (>0°C) but more saline (33.5-34.5 psu; Rudels et al., 2000). The Atlantic Layer water originates from water partly through Fram Strait and partly through St. Anna Trough. Canada Basin Bottom Water is colder (~-0.5°C) and relatively saline (~34.9 psu), with a residence time exceeding 300 years (Stein, 2008). Importantly, inflow from the Atlantic varies over time, which further influences the temperature of the Atlantic Layer along slopes of the central Arctic Ocean (Dmitrenko et al., 2009; Woodgate et al., 2001).~~arriving to the ESM region partly through Fram Strait via the West Spitsbergen Current and partly over the Barents Sea through St. Anna Trough. The inflow from the Atlantic has been observed to vary over time, specifically striking are observations of warm pulses influencing the core temperature of the Atlantic Layer in the central Arctic Ocean on decadal time scales (Dmitrenko et al., 2009; Woodgate et al., 2001). Canada Basin Bottom Water is colder (~-0.5°C) and relatively saline (~34.9 psu), with a residence time exceeding 300 years (Stein, 2008). The upper halocline shields the lower warmer waters, which may promote sea ice formation (Aagaard and Carmack, 1989). The aspect motivating our study is that climate warming could increase bottom water temperatures on the shelf slope, in the sensitive feather edge of hydrate stability (300-450 m,~~

~~Stranne et al., 2016), which would decrease the extent of the gas hydrate stability zone (GHSZ) and possibly release CH$_4$ to the water column and atmosphere.~~

2.3 Current Speculation on Gas Hydrates in the Arctic

Even during summer months over the last decade, 2-3 m of sea ice covers much of the Arctic Ocean adjacent to Siberia (Stroeve et al., 2012). This necessitates the use of large ice breaking vessels to explore the region. Consequently, limited geologic information exists regarding continental slopes of the ESM. Four icebreaker expeditions, the 1995 Polarstern Expedition ARK-XI/1 [Rachor, 1995], the 1996 Arctic Ocean Expedition ARK-XII/1 [Augstein et al., 1997], the 2008 Polarstern Expedition ARK-XXIII/3 [Jokat, 2010], and the 2009 Russian-American RUSALCA Expedition [Bakhmutov et al., 2009] have retrieved geophysical data and sediment on or adjacent to the ESM slope.

So far, no drilling has occurred on the ESM slope. However, the 2004 Arctic Coring Expedition (ACEX; Backman et al., 2009) drilled and cored the central Lomonosov Ridge (~~Figure 1~~Fig. 1). There are also land based studies (Gualtier et al., 2005; Sher et al., 2005; Andreev et al., 2009), and some public ~~Oil~~ oil and ~~Gas~~ gas ~~Exploration~~ exploration material~~s,~~ which provides indirect data on the ~~ESM~~ shelf (Hovland and Svensen, 2006).

Formatted: Font: Not Bold

Despite the paucity of ground-truth data, ~~as shown by maps of conjectured Arctic gas hydrate distribution (**Figure 1**),~~ many researchers have predicted widespread and abundant CH$_4$, the CESS continental slope, as clearly shown by maps of conjectured gas hydrate distribution in the Arctic (Fig. 1).~~including gas hydrate, along the ESM continental slope~~. This ~~is a logical~~ inference ~~that arose~~has arisen for two main reasons. First, the integrated input of particulate organic carbon (POC) over time provides the ultimate source of CH$_4$ in marine sediments

(Kvenvolden and Grantz, 1990).~~, and~~ Arctic slopes may contain high POC contents, which accumulated prior to the opening of the Fram Strait (Jokat and Ickrath, 2015), or along with terrigenous material during interglacial intervals of the Quaternary (Danyushevskaya et al., 1980; Clark, 1988; Darby, 1989; Moran et al., 2006; Archer, 2015). Certainly, organic rich Eocene sediments have been documented on other Arctic margins and in the ACEX cores on Lomonosov Ridge (Moran et al., 2006; Backman and Moran, 2009~~;~~, O'Regan et al., 2011; Alekseev, 1997; Naidu et al., 2000; Niessen et al., 2013). ~~Moreover, during Pleistocene glacial periods, extensive portions of the adjacent continental shelf were subaerially exposed tundra (Gusev et al., 2009; Jakobsson et al., 2014), and the locus of sediment deposition moved toward the slope (Alekseev, 1997; Naidu et al., 2000; Niessen et al., 2013). Organic matter burial might be enhanced further by cold seafloor temperatures, which should reduce bacterial degradation in shallow sediment (Darby et al., 1989; Max and Lowrie, 1993).~~ Second, the thickness of the gas hydrate stability zone GHSZ depends on bottom water temperature and the geothermal gradient (Dickens, 2001).~~,~~ ~~and~~ Because of very low bottom water temperatures along the slope ~~combined with~~and low regional geothermal gradients (O'Regan et al., 2016) ; an extensive volume of sediment can host gas hydrate (Miles, 1995; Makogon, 2010).~~imply a volumetrically extensive GHSZ (Miles, 1995; Makogon, 2010). Few environmental considerations point against the existence of gas hydrates in the ESM slopes although glacial periods dominated by relatively low sea levels might have kept the sensitive shallow part of the present GHSZ depleted of hydrates (Stranne et al., 2016).~~

2.4 Pore Water Chemistry Above Methane-Charged Sediment Sequences

Pore water chemistry profiles provide a powerful means to constrain CH_4 abundance and fluxes in marine sediment sequences (Borowski et al., 1996; Berg et al., 1998; Jørgensen et al., 2001; Torres and Kastner, 2009; Treude et al., 2014). Such profiles are generated by extracting interstitial water samples from sediment cores, and measuring the concentrations of dissolved species. ~~In the absence of significant advection, depth profiles of various analytes relate to Fick's law of diffusion and chemical reactions (e.g., Berner, 1977; Froelich et al., 1979; Klump and Martens 1981; Schulz, 2000).~~

In regions without significant advection of water, pore water profiles of various analytes relate to Fick's law of diffusion and chemical reactions (e.g., Berner, 1977; Froelich et al., 1979; Klump and Martens 1981; Boudreau, 1997; and Iverson and Jorgensen, 1993). The flux (*J*) of a dissolved ~~The flux (*J*) of a dissolved~~ species through porous marine sediment can be calculated from the concentration gradient by (Li & Gregory, 1974; Berner, 1975; Lerman, 1977):

$$J = -\varphi Ds \frac{\partial C}{\partial Z}, \qquad (2)$$

where φ is porosity, D_s is the diffusivity of an ion in sediment at a specified temperature, *C* is concentration, and *Z* is depth. Note that, as generally written, *J* is positive for upward fluxes and negative for downward fluxes relative to the seafloor. In many locations, φ and D_s change only moderately (<20%) in the upper ~~few~~ tens of meters below the seafloor. However, abundant CH_4 in sediment necessarily leads to a large concentration gradient toward the seafloor and a major upward flux of CH_4. The consequent reaction with SO_4^{2-} via AOM (**Equation 1**) leads to a series of flux changes in dissolved components (addition or removal), and predictable variations in corresponding concentration profiles across a SMT (Alperin, 1988; Borowski et al., 1996; Niewohner et al., 1998; Ussler and Paull, 2008; Dickens and Snyder, 2009; Regnier et al., 2011). In such regions, the depth of the SMT directly relates to the flux of CH_4 from below (Jørgensen et al., 1990; Dickens, 2001; D'Hondt et al., 2002; Hensen et al., 2003), largely because SO_4^{2-} concentrations at the seafloor are nearly constant throughout the oceans.

Alternatively, at seafloor locations with significant upward advection of fluids, such as above faults, pore water profiles become more complicated to model (Torres et al., 2002). This is because multiphase fluid flow (free gas and liquid) rarely reaches steady-state. Additionally, both steady and pulsed multiphase flow physically alters sediments creating soupy or mousse-like textures and sometimes gas pockets. However, if the upward advecting fluids contain significant CH_4 (and no SO_4^{2-}), the SMT shoals toward the seafloor with respect to predictions from considerations of CH_4 diffusion alone (Dickens, 2001). This can be observed generally from the very shallow SMTs observed at locations of CH_4 seepage worldwide (e.g., Aharon and Fu, 2000).

Typically, in all regions and at many locations, the SMT is a thin (<2 m) depth horizon with major inflections in both CH_4 and SO_4^{2-} profiles (**Figure 2**). Sulfate concentrations decrease from seawater values at the seafloor to zero at the SMT; by contrast, CH_4 concentrations rise from zero at the SMT to elevated values at depth. ~~In regions dominated by diffusion, the depth of the SMT relates to the flux of CH_4 from below (Jørgensen et al., 1990; Dickens, 2001; D'Hondt et al., 2002; Hensen et al., 2003). In part, this is because SO_4^{2-} concentrations at the seafloor are fixed.~~

Importantly, though, as one can infer from Equations 1 and 2, AOM affects additional species dissolved in pore water (Alperin et al., 1988; Jørgensen et al., 1990; Dickens, 2001; Hensen et al., 2003; Snyder et al., 2007). Dissolved HS^- and HCO_3^- concentrations necessarily increase across the SMT, so an inflection occurs in their concentration profiles. These two

Formatted: Font: Not Bold

species contribute to total alkalinity of marine water (Gieskes and Rogers, 1973; Haraldsson et al., 1997), which can be defined as:

$$Alk_T = [HCO_3^-] + 2[CO_3^{2-}] + [HS^-] + [B(OH)_4^-] + [OH^-] + [HPO_4^{2-}] + [NH_3] + [X]\ , \qquad (3)$$

~~over the pH range 6.3 to 10.3,~~ where X refers to several minor species. However, in shallow sediments found above almost all CH_4 charged systems, this can be expressed as:

$$Alk_T \approx [HCO_3^-] + [HS^-]\ , \qquad (4)$$

Thus, with the production of HS^- and HCO_3^-, an inflection in Alk_T occurs across the SMT (Luff and Wallmann 2003; Dickens and Snyder, 2009; Jørgensen and Parkes, 2010; Chatterjee et al., 2011; Smith and Coffin, 2014; Ye et al., 2016).

Marked changes in pore water profiles of other components also typically occur across the SMT (~~Figure 2~~Fig. 3). Because CH_4 is greatly depleted in ^{13}C due to isotope fractionation during methanogenesis at depth (Whiticar, 1999; Paull et al., 2000), the conversion of CH_4 to HCO_3^- (Eqn. 1) decreases the δ^{13}C of DIC across the SMT (Torres et al., 2007; Holler et al., 2009; Chatterjee et al., 2011; Yoshinaga et al., 2014).~~(Paull et al., 2000), the conversion of CH_4 carbon to HCO_3^- carbon (**Equation 1**) induces a decrease in the δ^{13}C values of dissolved inorganic carbon (DIC) across the SMT (Torres et al., 2007; Holler et al., 2009; Yoshinaga et al., 2014).~~ However, the magnitude of change in δ^{13}C-DIC ~~becomes~~is complicated because of excess HCO_3^- (formed during methanogenesis and subsequent reactions) can also rise from below ~~rising from below~~ (Snyder et al., 2007; Chatterjee et al., 2011). Dissolved Ba^{2+} concentrations generally increase significantly just above the SMT. This is because solid barite ($BaSO_4$), a ubiquitous component of marine sediment on continental slopes (Dehairs et al., 1980; Dymond et al., 1992; Gingele and Dahmke, 1994), dissolves in the SO_4^{2-}-depleted pore water and dissolved

Formatted: Font: Not Bold

Ba^{2+} then diffuses back across the SMT (Dickens, 2001; Riedinger et al., 2006; Nöthen and Kasten, 2011). Dissolved Ca^{2+} concentrations usually decrease across the SMT. This is due to authigenic carbonate precipitation resulting from the production excess HCO_3^- (Greinert et al., 2001; Luff and Wallmann 2003; Snyder et al., 2007). Importantly, though, dissolved NH_4^+ concentrations exhibit no inflection across the SMT. This is because while decomposition of particulate organic matter generates NH_4^+, AOM does not (Borowski et al., 1996). ~~In summary, pore water analyses at numerous locations demonstrate that characteristic pore water profiles delineate sites with significant CH_4, including gas hydrate, at depth~~ ~~(**Figure 2**).~~

Studies at numerous locations demonstrate that characteristic pore water profiles delineate sediment sequences with significant CH_4, including gas hydrate, in the upper few hundred meters below the seafloor (Fig. 3). Good examples include: Baltic Sea (Jørgensen et al, 1990), Black Sea (Jørgensen et al, 2004), Blake Ridge (Paull et al., 2000; Borowski et al., 2001), Cariaco Trench (Reeburgh, 1976), Cascadia Margin (Torres and Kastner, 2009), Gulf of Mexico (Kastner et al., 2008a; Hu et al., 2010; Smith and Coffin, 2014), Hydrate Ridge (Claypool et al., 2006), offshore Namibia (Niewohner et al., 1998), offshore Peru (Donohue et al., 2006), South China Sea (Luo et al., 2013; Hu et al., 2015), and Sea of Japan (Expedition Scientists, 2014). Moreover, in regions dominated by diffusion, fluxes of dissolved CH_4 can be estimated through use of Equation 2 from concentration profiles of multiple constituents (e.g., SO_4^{2-}, HCO_3^-, Ca^{2+}) and knowledge of porosity and sedimentary diffusion constants (e.g., Niewohner et al., 1998; Snyder et al., 2007). At sites with abundant CH_4 in the upper few hundred meters below the seafloor, notably including sites with gas hydrate and sites in the Beaufort Sea, estimated values for JCH_4 and $-JSO_4^{2-}$ are universally high (> ~50 mol/m^2-kyr).

3. Materials and Methods

3.1 The SWERUS-C3 Expedition, Leg 2

Leg 2 of SWERUS-C3 included four transects across the CESS continental slope (Fig. 2). These transects were along Arlis Spur (TR-1), north of central East Siberia (TR-2), from close to Henrietta Island to the Makarov Basin (TR-3), and on the Amerasian side of Lomonosov Ridge (TR-4). Along each transect, scientific operations involved bathymetric mapping as well as sediment coring at a series of stations. An additional coring station was located on Lomonosov Ridge, near where this bathymetric high intersects the ESM. ~~Between August 21 and October 5, 2014, Leg 2 of the SWERUS-C3 expedition sailed between Barrow, Alaska and Tromsø, Norway with *IB Oden*. This leg included four transects that cross the ESM continental slope (**Figure 3**). These transects were along Arlis Spur (TR-1), north of central East Siberia (TR-2), from close to Henrietta Island to the Makarov Basin (TR-3), and on the Amerasian side of Lomonosov Ridge (TR-4). Along each transect, scientific operations involved bathymetric mapping as well as sediment coring a series of stations. One station also was located on Lomonosov Ridge, near where this long bathymetric high intersects the ESM. Additionally, three days were spent at Herald Trough, a canyon on the shelf of eastern Siberia. Data obtained from the northern Lomonosov Ridge and Herald Canyon are not presented in this manuscript.~~

An array of coring techniques were used along each transect. In total, 50 sediment cores were collected at 34 coring stations. These included: multicore sets (22), gravity cores (23), piston cores (11), and kasten cores (2). The multicorer was an 8-tube corer built by Oktopus GmbH weighing 500kg. The polycarbonate liners were 60 cm long with a 10 cm diameter. The piston/gravity coring system was built by Stockholm University with an inner diameter of 10 cm.

Trigger weight cores also were collected during piston coring. The different coring systems enabled sediment and pore water collection from the seafloor to upwards of ~~eight to~~ nine m below the seafloor (mbsf).

3.2 Core material

Sediment physical properties on gravity and piston cores were analyzed on the ship using a Geotek Multi-Sensor Core Logger (MSCL). ~~Sediment physical properties (piston and gravity cores) were analyzed shipboard using a Geotek Multi-Sensor Core Logger (MSCL) from Stockholm University.~~ Measurements of the gamma-ray derived bulk density, compressional wave velocity (p-wave), and magnetic susceptibility were acquired at a down core resolution of one cm. Discrete samples (2-3 per section) also were collected for sediment index property measurements (bulk density, porosity, water content and grain density). Grain density was measured using a helium displacement pycnometer on oven-dried samples. Porosity profiles were generated using the smoothed (3-pt) MSCL-derived bulk density (ρ_B) ~~(ρ_B)~~ and the average grain density (ρ_g) ~~(ρ_g)~~ from each core, where;

$$\varphi = \frac{(\rho_g - \rho_b)}{(\rho_b - \rho_f)}, \tag{5}$$

and an assumed pore fluid density (ρ_f) ~~(ρ_f)~~ of 1.024 g/cm^3 ~~was assumed. In cases where 2 or more distinct lithologic units existed within a core, the average grain density for each unit was used in this calculation.~~

3.3 Interstitial Water Collection

Pore waters were collected using Rhizon samplers (Seeberg-Elverfeldt et al., 2005; Dickens et al., 2007). Cores were cut into ~1.5 m long sections immediately on *Oden*'s deck, brought to the geochemistry laboratory, and placed on precut racks. Laboratory temperature was a near constant 22 °C. Sampling involved drilling holes through the core liner, inserting Rhizons into the sediment core, and obtaining small volumes of pore water via vacuum and "microfiltration" ~~(**Figure 4**). An individual Rhizon consists of a hydrophilic membrane composed of a blend of polyvinylpyrrolidine and polyethersulfone (nominal pore size of 0.12 - 0.18 µm) connected to a tube. These are pushed into the sediment and, with negative pressure, the filament filters water into the syringe.~~ The Rhizons used were 5-~~five~~ cm porous flat tip male luer lock (19.21.23) with 12 cm tubing, purchased from Rhizosphere Research Products (www.rhizosphere.com).

In total, 529 pore water samples were collected ~~in ~10 mL plastic syringes~~ from 32 cores, which ranged from 0.16 to 8.43 m in length (~~Table 1~~Tabl. S2). Rhizons in gravity and piston cores typically were spaced every 20 to 30 cm~~, although occasionally at five cm increments. Of the total, 456 samples obtained ~10 mL or more of pore water.~~ Because the use of rhizon sampling for collecting pore waters of deep-sea sediments remains a relatively novel and engaging topic (Dickens, 2007), we discuss the procedure, as well as several experiments regarding our sampling, in the supplementary information document. ~~Rhizon sampling from multicores took an average of 1.24 hr per sample, and ranged from 0.08 to 4.01 hr; for gravity and piston cores, the average sampling time was 11.28 hr, and ranged from 1.33 to 23.08 hr. Tabulated Rhizon flow rates averaged 12.72 mL/hr for multicores and 1.29 mL/hr for piston and gravity cores (**Table 2**). After considering the time to recover cores from the seafloor, the total time from core retrieval through sample collection averaged 1.95 hr for multicores and 14.65 hr for piston and gravity cores.~~

~~We highlight the above sampling times due to concerns about the fidelity of chemical analyses using Rhizon samplers in recent literature (Schrum et al., 2012; Miller et al., 2014). Since initial implementation of Rhizons in marine sediment cores (Seeberg-Elverfeldt et al.,~~

Formatted: Font: Not Bold

~~2005; Dickens et al., 2007), they increasingly have been used to collect pore waters (e.g., Pohlman et al., 2008; Gao et al., 2010; Riedinger et al., 2014). This is for multiple reasons, including the capability for high-resolution sampling, the ease of sampling, and the minimal destruction of surrounding sediment (Dickens et al., 2007). However, concerns about using Rhizon samplers include CO_2 degassing during extraction (Schrum et al., 2012) or changes to pore water composition between core retrieval and water extraction. In the latter case, alteration of pore water chemistry may occur through reactions induced by elevated temperature, reduced pressure, evaporation, microbial activity or other processes.~~

~~In order to constrain possible changes in pore water chemistry over time, two experiments were performed onboard *IB Oden*. First, the temperature and pH of a piston core from Station 33 were continuously monitored at five discrete intervals over 24 hours. Probes, inserted into the sediment by drilling holes in the core liner, recorded data at five minute intervals (**Figure 5**). Second, for 46 samples (**Table 4**), after collection of the first 10 mL of pore water, the syringe was removed, and additional pore water was collected in a second (or third) syringe.~~

While in the shipboard laboratory, Rhizon samples were divided into six aliquots when sufficient water was available. This sample splitting led to 2465 aliquots of pore water in total, which then could be examined for different species and at different laboratories. Aliquots 1, 3, and 6 (below) were collected for all samples.

3.4 Interstitial Water Analyses

The first aliquot was used to measure total alkalinity using a Mettler Toledo titrator onboard *IB Oden*. Immediately after collection, pore water was diluted~~2 mL of pore water were diluted to 40 mL~~ with milli-Q water and autotitrated~~ with 0.005M HCl from the original pH to a~~

~~pH of 5.4~~. ~~A total of 15~~Fifteen spiked samples and ~~8 ~~eight duplicates were analyzed onboard for quality control. Spiked samples were created by pipetting certified reference material (Batch 135; www.cdiac.ornl.gov/oceans/Dickson_CRM) into milli-Q water. Results for spiked samples and duplicates are reported in Table 1.~~Batch 135; CRM) into milli-Q water. Results for spiked samples and duplicates are reported in **Table 3.**~~

The second aliquot was used to measure the δ^{13}C composition of DIC ($\delta^{13}C_{DIC}$). Septum sealed glass vials prepared with H_3PO_4 ~~100µL of 85% phosphoric acid ~~and flushed with helium were prepared before the expedition. ~~The analysis required approximately 40 µg of DIC in each pore water sample. Onboard alkalinity measurements were used to estimate the correct volume, and this amount was injected into the vials. ~~Samples were sealed in boxes and refrigerated for the remainder of the cruise. Four field duplicates, two seawater standards, and a field blank were collected, stored, and analyzed with the samples. The δ^{13}C-DIC~~$\delta^{13}C_{DIC}$~~ analyses were performed on a Gasbench II coupled to a MAT 253 mass spectrometer (both Thermo Scientific) at Stockholm University. The δ^{13}C-DIC~~carbon isotope composition of DIC~~ is reported in conventional delta notation relative to Vienna PeeDee Belemnite (VPDB). Results for field duplicates and standards are reported in ~~Table 2~~Table 1. Standard deviation for the analyses of δ^{13}C-DIC was less than 0.1 ‰.~~$\delta^{13}C_{DIC}$ was less than 0.1 per mille. The results for seawater standards collected onboard are given in **Table 3**.~~

Formatted: Font: Not Bold

The third aliquot was used to measure dissolved sulfur and metal concentrations. ~~Approximately 3 mL of pore water were placed into acid washed cryovials. ~~Samples were acid preserved with 10 µL ultrapure HNO^3. Additionally, 11 blind field duplicates and 2 field blanks were collected and processed in the same manner. Concentrations of Ba, Ca, Fe, Mg, Mn, S, and Sr were determined on an Agilent Vista Pro Inductively Coupled Atomic Emission Spectrometer

(ICP-AES) housed in the geochemistry facilities at Rice University. Known standard solutions and pore fluid samples were diluted 1:20 with 18-MΩ water. Scandium was added to both standards and samples to correct for instrumental drift (emission line 361.383 nm). Wavelengths used for elemental analysis followed those indicated by Murray et al. (2000). Following initial analysis, an additional dilution, 1:80 with 18-MΩ water, was analyzed for Ca, Mg, and S. After every 10 analyses, an International Association of Physical Sciences (IAPSO) standard seawater spiked sample and a blank were examined for quality control. Relative standard deviations (RSD) from stock solutions are reported in ~~Table 3~~Table 1.

The fourth aliquot was used to measure dissolved ammonia (NH_4^+) via a colorimetric method similar to that presented by Gieskes et al. (1991).~~. This was carried out shipboard via a colorimetric method similar to that presented by Gieskes et al. (1991)~~. Set volumes ~~(100µL)~~ of pore water were pipetted into ~~1 cm^3 plastic~~ cuvettes ~~and diluted with 900 µL of~~with milli-Q water. Two reagents ~~(100 µL of A and 100 µL of B)~~ were then pipetted into the cuvettes. Reagent A was prepared by adding~~-~~ $Na_3C_6H_5O_7$, C_6H_5OH, and $Na_2(Fe(CN)_5NO)$ to ~~35 g of trisodium citrate ($Na_3C_6H_5O_7$), 2.7 g of phenol (C_6H_5OH), and 0.06 g of sodium nitroprusside ($Na_2[Fe(CN)_5NO]$) to 100 mL of~~ milli-Q water. Reagent B was prepared by NaOH in milli-Q water and adding NaClO solution. ~~dissolving 1.36 g of sodium hydroxide in 100 mL of milli-Q water and adding 3 mL sodium hypochlorite (NaClO) solution~~. ~~After the reagents were added, s~~Solutions were mixed~~,~~ and allowed to react for at least six but not more than 24 hours. Solutions turned various shades of blue, which to relate to NH_4^+ concentration, and ~~which~~ were measured by absorbance at 630 nm on a Hitachi U-1100 spectrophotometer. Five point calibration curves ~~(0 to 200 µM)~~ were measured before each sample set and corrected using VKI standard (QC RW1; ~~www.eurofins.dk~~www.eurofins.dk; Table ~~3~~1).

Formatted: Font: Not Bold

Formatted: Default Paragraph Font, Font: Calibri, 11 pt, Pattern: Clear

Formatted: Default Paragraph Font, Font: Calibri, 11 pt, Pattern: Clear

Formatted: Font: Not Bold

The fifth aliquot was used to measure dissolved phosphate (PO_4^{3-}) following the method given by Gieskes et al. (1991)~~. The method of preparation also followed that given by Gieskes et al. (1991)~~. ~~The remainder of the~~ Remaining pore water (generally between 1 and 3mL) was added to milli-Q water to a sum of 10 mL. Two reagents were ~~then~~ added to the solution to react with PO_4^{3-} ~~phosphate (200 µL of A and B)~~. Reagent A was prepared by ~~first~~ making three solutions: $(NH_4)_2MoO_4$, H_2SO_4, and $C_8H_4K_2O_{12}Sb_2 \bullet XH_2O$ were added to milli-Q water, and the solutions were added dropwise.~~eight grams of ammonium molybdate ($(NH_4)_2MoO_4$) were added to 80 mL of milli-Q water, 50 mL of concentrated sulfuric acid were added to 150 mL of milli-Q water, and 0.01 g of potassium antimonyl tartrate hydrate ($C_8H_4K_2O_{12}Sb_2 \bullet XH_2O$) were added to 10 mL of milli-Q water. Then, 30 mL of the ammonium molybdate solution were added to 90 mL of the sulfuric acid solution, and five mL potassium antimonyl tartrate solution was slowly added dropwise.~~ Reagent B was created with $C_6H_8O_6$~~by dissolving 10 g of ascorbic acid in 50 mL of milli-Q water~~. After the samples were prepared, reagent A and B were added, mixed, and allowed to react for 10 but not more than 30 minutes. Solutions turned various shades of blue, ~~which to relate~~realting to PO_4^{3-} concentration, and ~~which~~ were ~~then~~ measured at an absorbance of 880 nm~~ on the above spectrophotometer~~. Five point calibration curves ~~(0 to 50 µM)~~ were measured before each sample set and corrected using VKI standard (QC RW1; ~~www.eurofins.dk~~www.eurofins.dk; Table ~~3~~1).

For 352 pore water samples, a sixth aliquot of approximately 2 mL could be collected to mix with 200 µL of a 2.5% Zn-acetate ($Zn(C_2H_3O_2)_2$) solution. Given the extremely low solubility of ZnS, when such a solution is added to pore water samples, a white precipitate should form in the presence of even very low H_2S concentrations (Cline, 1969; Goldhaber, 1974).

Formatted: Default Paragraph Font, Font: Calibri, 11 pt, Pattern: Clear

Formatted: Default Paragraph Font, Font: Calibri, 11 pt, Pattern: Clear

Formatted: Font: Not Bold

A method detection limit (MDL) for each species can be determined by the following equation:

$$MDL = \left(\frac{C_{High} - C_{Low}}{I_{High} - I_{Low}}\right) 3\sigma \ , \qquad (6)$$

where C = concentration and I = intensity (counts per second on the ICP-AES). The MDLs were as follows: Ba = 0.01 µM, Ca = 0.08 µM, Fe = 5.9 µM, Mg = 0.22 µM, Mn = 0.24 µM, S = 1.2 µM, Sr = 0.01 µM. On all plots, for reference, we place dashed lines for values of IAPSO seawater standard (Alkalinity = 2.33 mM, Ba = 0.00 mM, Ca = 10.28 mM, Fe = 0.00 mM, Mg = 53.06 mM, Mn = 0.00 mM, S = 28.19 mM, Sr = 0.09 mM, NH_4 = 0.00 mM, HPO_4 = 0.00 mM). ~~In cases of excess sample, an additional aliquot was collected to test for dissolved hydrogen sulfide. Approximately 2 mL of pore water was placed into a cryovial, and 200 µL of a 2.5% Zn-acetate ($Zn(C_2H_3O_2)_2$) solution was added. Given the extremely low solubility of ZnS, a white precipitate should form in the presence of even very low H_2S concentrations (Cline, 1969; Goldhaber, 1974).~~

4. Results

4.1 ~~Generalities~~Broad conclusions

With the large number of pore water measurements (~~Table 1~~Tbl. S1) we begin with some generalities regarding~~ the~~ results. We plot pore water concentration profiles along each transect collectively (Fig. 4-8~~**Figures 6 - 10**~~), irrespective of coring device or water depth, although clear variance in pore water chemistry exists between stations for some dissolved species (e.g., Fe).

Most species display “smooth” concentration profiles with respect to sediment depth (Fig. 4-8~~**Figures 6 - 10**~~). That is, concentrations of successive samples do not display a high degree of scatter. This is expected for pore water profiles in sediment where diffusion dominates (Froelich

Formatted: Font: Not Bold

et al., 1979; Klump and Martens 1981; Schulz, 2000). However, for some~~as best seen for~~ dissolved species whose concentrations do not appreciably change over depth (e.g., Ba^{2+} and Ca^{2+}), scatter exists beyond that predicted from analytical precision. We discuss this in detail in the supplementary information.~~concentrations do not appreciably change over depth (e.g., Ba^{2+} and Ca^{2+}) scatter exists beyond that predicted from analytical precision. This scatter has a weak positive correlation with increased sampling time, which can be shown by comparing time to a deviation in concentration (**Figure 11**). The latter is defined by:~~

~~$\Delta X = X_{Measured} - X_{Predicted}$,(6)~~

~~where *X* is the species of interest, and $X_{Predicted}$ is the concentration of *X* determined from the linear best fit line of a concentration profile.~~

~~A method detection limit (MDL) for each species can be determined by the following equation:~~

~~$MDL = \left(\frac{C_{High} - C_{Low}}{I_{High} - I_{Low}}\right) 3\sigma$, (7)~~

~~where C = concentration and I = intensity (counts per second on the ICP-AES). The MDLs were as follows: Ba^{-} = 0.01 µM, Ca^{-} = 0.08 µM, Fe^{-} = 5.9 µM, Mg^{-} = 0.22 µM, Mn^{-} = 0.24 µM, S = 1.2 µM, Sr^{-} = 0.01 µM. On all plots, for reference, we place dashed lines for values of IAPSO seawater standard (Alkalinity = 2.33 mM, Ba = 0.00 mM, Ca = 10.28 mM, Fe = 0.00 mM, Mg = 53.06 mM, Mn = 0.00 mM, S = 28.19 mM, Sr = 0.09 mM, NH_4 = 0.00 mM, HPO_4 = 0.00 mM). Pore water profiles generated from ACEX cores (Backman et al., 2009) also are shown for comparison.~~

~~*4.2 Porosity and Sampling Time*~~

~~Measured porosity values of piston and gravity cores generally decrease with depth from 80% or greater at the mudline to around 60% at eight mbsf (**Figure 12a**). Over the first 0.1 m, porosity decreases steeply, by an average of 6.8%. From 0.2 to 8.0 m, porosity decreases much more gradually, by an average of 1.3% every meter. The 1σ deviation in porosity between all stations typically ranges between 6 and 10% at any given depth.~~

~~Sampling time inversely relates to porosity (**Table 2**). Multicore rhizon extraction rates (**Table 2**) averaged 12.72 mL/hr while gravity and piston cores averaged 1.29 mL/hr. This flow rate generally decreased with depth. Across all data from all cores, a first-order relationship between depth (z) and extraction rate (ER) can be expressed as~~ $ER = 4.4911z^{-1.512}$ ~~(~~$R^2 = 0.789$~~; **Figure 12b**). The extraction rate correlated with depth more closely than with porosity (**Figure 12c**). The porosity (ϕ)-extraction rate relationship, expressed as~~ $ER = 21.718(\phi)^{8.161}$ ~~had an~~ $R^2 = 0.631$~~.~~

~~*4.3 Physiochemical Conditions During Rhizon Sampling*~~

~~For the five sections from Station 33 examined for changes in physiochemical conditions, temperature rose from ~2°C upon initial measurement to between 16.9 and 18.4 °C within 24 hours (**Figure 5**). In general, the shallow sections increased faster than the deeper sections. Initial pH decreased with depth (0.05 mbsf = 7.79 units, 1.86 mbsf = 7.71 units, 4.80 mbsf = 7.39 units, and 6.30 mbsf = 7.19 units). Over the same time interval, pH decreased significantly in all core sections, by an average of 0.25 units, with a range between 0.18 and 0.38 units (**Figure 5**). Note, however, that pH dropped by 0.3 units at ~20 hrs in one of the pH profiles (Section 2, 1.86 mbsf). This may be due to a temporary crack in the sediment core created by removing pore water through rhizon sampling, although no crack was observed when the core section was split.~~

~~In total, 46 of the 68 Rhizon sampling depths at Station 28 enabled collection of multiple water samples (**Table 4**). This included "second generation" samples, where beyond the first ~10 mL, another 1 to 10 mL were obtained, as well as three "third generation" samples, where beyond the first ~20 mL, another 1 to 10 mL were obtained. The sample depths which did not yield enough pore water for a "second generation" tended to be deeper (16 of 22 were in the deepest section). Relative to the initial 10mL of pore water, alkalinity increased in 43 of the second generation samples, and in all three of the third generation samples by an average 0.15 mM (4.1% increase). Interestingly, no statistically significant changes in concentrations of phosphate, ammonia or any dissolved metal were observed.~~

4.2 Alkalinity and δ^{13}C of DIC~~*4.4 Alkalinity and δ^{13}C*~~

Alkalinity concentrations increase with depth in all cores (Fig. 4-8~~**Figures 6 - 10**~~). Moreover, in most cases, the rise is roughly~~nearly~~ linear. Across all stations on the four transects, alkalinity increases by an average of 0.51 mM/m, although variance exists between mean gradients for each transect (Tr1 = 0.46 mM/m, Tr2 = 0.34 mM/m, Tr3 = 0.91 mM/m, and Tr4 = 0.44 mM/m) and by station along each transect. Overall, the rise in alkalinity at these 15 stations ranges from 0.30 to 0.98 mM/m. The Lomonosov Ridge station differs (Fig. 8~~**Figure 10**~~), as alkalinity increases much greater with depth ~~faster with depth~~ (1.86 mM/m).

Concave-down δ^{13}C-DIC profiles characterize pore waters at all stations (Fig. 4-8~~**Figures 6 - 10**~~). The decrease in δ^{13}C-DIC changes is most pronounced ~~most rapidly~~ near the seafloor. Across all stations along the four transects, pore water δ^{13}C-DIC values decrease from near zero close to the mudline at an average of -3.6 ‰/m. Again, variance in mean gradients occurs according to stations and transects ~~significant variance in mean gradients occurs according to~~

~~transect~~ (Tr1 = -3.3 ‰/m, Tr2 = -3.0 ‰/m, and Tr3 = -4.7 ‰/m) ~~and according to station on each transect~~. As with alkalinity, the δ^{13}C-DIC profile at the Lomonosov Ridge station differs, with values decreasing by 5.6 ‰/m, such that by eight mbsf, δ^{13}C-DIC approaches -45 ‰. In summary, a basic relationship exists between higher alkalinity and lower δ^{13}C-DIC across all stations.~~The range in average δ^{13}C-DIC value gradients across all stations is -2.7 to -4.9 ‰/m. As with alkalinity, the δ^{13}C-DIC profile at the Lomonosov Ridge station differs, with values decreasing by 5.6 ‰/m, such that 8 mbsf, δ^{13}C-DIC approaches -45 ‰. In summary, a basic relationship exists between higher alkalinity and lower δ^{13}C-DIC across all stations.~~

4.5 Sulfur and sulfate

No sulfide was detected by smell smell and no ZnS precipitated ~~or with addition of Zn-acetate~~ in any pore water sample upon addition of Zn-acetate solution. Molar concentrations of total dissolved sulfur should, therefore, represent those of dissolved SO_4^{2-}. Along the four transects, dissolved S concentrations decrease with depth at all stations (Fig. 4-7~~**Figures 6 – 9**~~). The total dissolved S concentrations ~~sulfur concentration~~ in the shallowest samples varied from 27.~~29~~ 3 to 30.~~58~~ 6 mM and averaged 28.7~~0~~ mM. From these “seafloor” values, concentrations decrease by an average 0.69 mM/m, again with variance according to stations and transect (Tr1 = -0.58 mM/m, Tr2 = -0.57 mM/m, Tr3 = -1.09 mM/m; and Tr4 = -0.60 mM/m) ~~and station along each transect~~. The dissolved S gradients across all stations along the ~~ESM~~ CESS slope range from -0.41 to -1.13 mM/m. Total dissolved S at the Lomonosov Ridge station displays a significantly steeper decrease ~~decreased faster~~ than ~~at~~ any of the other stations (-1.92 mM/m). Importantly, decreases in dissolved S are similar in magnitude to increases in alkalinity at each station examined. Indeed, the molar ratio of alkalinity change with depth to sulfur change with depth (-ΔAlkalinity/ΔS) is 0.98 (Fig. 9a).~~increase to sulfate decrease (-ΔAlkalinity/ΔS) is 0.98 (**Figure 13a**).~~

4.4 Ammonia and phosphate~~*4.6 “Nutrients”: Phosphate and Ammonia*~~

The C:N:P molar ratio of typical marine organic matter is approximately 106:16:1 (Redfield, 1958; Takahashi, 1985). Although this ratio differs for terrestrial organic carbon (perhaps closer to 134:9:1, Tian et al., 2010), dissolved HPO_4^{2-} and NH_4^+ concentrations in pore water can be used in a general sense to assess consumption of particulate organic carbon. This is because organic matter degradation releases these species to pore water (Froelich et al., 1979). Notably, concentrations of NH_4^+ and HPO_4^{2-} are near or below detection in samples immediately below the seafloor (Fig. 4-8).~~Often, in discussions of pore water chemistry, dissolved phosphate (HPO_4^{2-}) and ammonia (NH_4^+) are classified as “nutrients”, although the connotation derives from the fact that these two species arise through the oxidation of POM in the sediment (Berner, 1977). The C:N:P molar ratio, known as the “Redfield Ratio”, of initial POM is approximately 106:16:1 (Redfield, 1958; Takahashi, 1985). Therefore, assuming mass balance, dissolved “nutrients” are used as reference for the amount of POC consumed through microbial oxidation. Importantly, concentrations of HPO_4^{2-} and NH_4^+ are near or below detection in samples immediately below the seafloor (**Figures 6 -10**).~~

Dissolved NH_4^+ profiles increase almost linearly with depth, although with slight concave-down curvature. Similar to alkalinity profiles, NH_4^+ concentrations rise with depth below the seafloor more at stations with shallower water depth (although we note an exception for Tr2). Across stations along the four transects, pore water NH_4^+ concentrations increase with depth on average by 38.69 µM/m, with a range from 11.3 to 76.1 µM/m. Along each transect, the average

NH_4^+ gradients are as follows: Tr1 = 43.0 µM/m, Tr2 = 17.4 µM/m, Tr3 = 69.0 µM/m, and Tr4 = 29.0 µM/m.

By contrast, concentrations of dissolved HPO_4^{2-} in our cores typically increase, reach a subsurface maximum, and then decrease (Fig. 4-8). With available data, a more pronounced maximum generally occurs at stations with relatively shallow water depth. For example, consider the peak in HPO_4^{2-} concentrations at four stations. At the two shallow stations, S12 (384 m) and S22 (367 m) the HPO_4^{2-} maxima are, 73 µM (1.91 m) and 18 µM (0.66 m), respectively, but at the two deeper stations, S17 (977 m) and S14 (733 m), the HPO_4^{2-} maxima are only 6.7 µM (1.76 m) and 7.1 µM (2.33 m) respectively. The station on Lomonosov Ridge (S31) has a high in HPO_4^{2-} concentration of 76 µM at 1.02 m below the mudline. In general, stations with more pronounced HPO_4^{2-} maxima also have greater increases in alkalinity with depth.

The NH_4^+, HPO_4^{2-}, and alkalinity profiles relate to one another statistically, although with distinction. All stations have a C:N ratio in pore waters much higher than the canonical Redfield Ratio of 6.625 (Fig. 10). Rather, the concentration relationship of alkalinity and ammonium ion can be expressed by a second order polynomial ($[NH_4^+] = -0.003[Alk]^2 + 0.105\,[Alk] – 0.253$; Fig. 9b) with an average molar ratio ($\Delta Alk/\Delta NH_4^+$) of 14.7, close to what might be expected for degradation of terrestrial organic carbon. Interestingly, this ratio deviates somewhat across transects, increasing at sites from Tr1, Tr3, Tr2, to the Lomonosov Ridge station. The molar ratio of alkalinity to phosphate ion ($\Delta Alk/\Delta HPO_4^{2-}$) averages 55.7 for all stations. This ratio also generally increases in cores from east to west.~~With depth, concentrations of dissolved~~ ~~HPO_4^{2-}~~ ~~typically increase, reach a subsurface maximum, and then decrease (**Figure 6 – 10**). With available data, a more pronounced maximum generally occurs at stations with relatively shallow water depth. For example, and within the spatial resolution of samples, consider the peak in~~

~~HPO_4^{2-} concentrations at four stations. At the two shallow stations, S12 (384 m) and S22 (367 m) the HPO_4^{2-} maxima are, 73 µM (1.91 m) and 18 µM (0.66 m), respectively at the two deeper stations, S17 (977 m) and S14 (733 m), the HPO_4^{2-} maxima are only 6.7 µM (1.76 m) and 7.1 µM (2.33 m) respectively. The station on Lomonosov Ridge (S31) has a high in HPO_4^{2-} concentration of 76 µM at 1.02 m below the mudline. In general, stations with more pronounced HPO_4^{2-} maxima also have greater increases in alkalinity with depth.~~

~~By contrast, dissolved NH_4^+ profiles rise almost linearly with depth, but with slight concave-down curvature. Similar to dissolved HPO_4^{2-} profiles, NH_4^+ concentrations increase with depth fastest at stations with shallower water depth (although we note an exception for Tr2). Across stations along the four transects, pore water NH_4^+ concentrations increase with depth on average by 38.69 µM/m, with a range from 11.28 to 76.08 µM/m. Along each transect, the average NH_4^+ gradients are as follows: Tr1 = 43.02 µM/m, Tr2 = 17.38 µM/m, Tr3 = 68.97 µM/m, and Tr4 = 29.04 µM/m.~~

~~The HPO_4^{2-}, NH_4^+, and alkalinity profiles relate to one another statistically, although with distinction. The concentration relationship of alkalinity and ammonium ion can be expressed by a second order polynomial ($[NH_4^+] = -0.003[Alk]^2 + 0.105 [Alk] - 0.253$; **Figure 13b**) with an average molar ratio ($\Delta Alk/\Delta NH_4^+$) of 14.69. All stations have a C:N ratio in pore waters more than the Redfield Ratio of 6.625 (**Figure 14**). The molar ratio of alkalinity and phosphate ion ($\Delta Alk/\Delta HPO_4^{2-}$) averages 55.72 for all stations. This means that all stations have an average C:P ratio less than 106. Overall, a consistent pattern emerges between changes in NH_4^+, and alkalinity, but one that deviates significantly from Redfield ratio. Interestingly, the C:N ratio appears to vary significantly across transects. This ratio increases from Tr1 (8.61-11.22), Tr3 (12.5-18.14), Tr2 (17.53-18.55), to the Lomonosov Ridge station (22.62). The C:P ratio followed~~

~~a similar pattern, generally increasing from east to west: Tr1 (16.57-74.70), Tr2 (26.32-92.04), Tr3 (26.29-86.34), and Tr4 (52.18-124.35).~~

4.~~7~~ 5 Metals

At most stations, dissolved Ba^{2+} concentrations increase nonlinearly from values at or below detection limit (0.01 µM) near the seafloor to generally constant values (0.6 – 0.7 µM) within 0.8 m below the seafloor. However, at several stations, dissolved Ba concentrations remained at or below the detection limit for all samples.

Overall, dissolved Ca, Mg, and Sr concentrations decrease slightly with depth (Fig. 4-8~~**Figures 6 – 10**~~). Across stations along the four transects, Ca^{2+} concentrations drop on average between -0.094 and -0.12~~2~~ mM/m (Tr1), between -0.09~~2~~ and -0.09~~3~~ mM/m (Tr2), between -0.09~~2~~ and -0.10~~1~~ (Tr3), and -0.~~075~~ 08 mM/m (Tr4). Magnesium concentrations also drop, the average change being between -0.43~~0~~ and -0.48~~1~~ mM/m (Tr1), between -0.274 and -1.~~319~~ 32 (Tr2), between -0.86~~3~~ and -0.94~~2~~ mM/m (Tr3), and -0.~~467~~ 47 mM/m (Tr4). Strontium concentrations decrease by an average amount of 0.3 µM/m, considering all stations along the four transect stations (Tr1 = 0.5 µM/m, Tr2 = 0.3 µM/m, Tr3 = 0.1 µM/m, and Tr4 = 0.1 µM/m). The station on Lomonosov Ridge again stands apart. At this location, the decreases in dissolved Ca, Mg, and Sr are 0.27 mM/m, 1.24 mM/m, and 0.50 µM/m, respectively.

The profiles of dissolved Mn and Fe are complicated in terms of location~~spatially complicated~~. Generally, profiles show a broad rise in concentrations and subsequent ~~fall~~ drop in concentrations at deeper depth ~~at deeper depth~~. Some stations have a maxima in dissolved Mn (Stations S12 (135 µM at 5 m), S28 (66 µM at 3.1 m), and Lomonosov Ridge (86 µM at 1.3 m), where concentrations decrease below. At other stations, Mn concentrations still appear to be increasing at the lowest depth~~are still increasing at the lowest depth~~. Iron concentrations are generally below the detection limit at or near the mudline, and begin increasing around 2.5 – 3.5 m reaching concentrations upward of 20 µM.

5. Discussion

~~*5.1 Flow Rates from Rhizons*~~

~~Pore water flow rate drops quasi-exponentially with depth (**Figure 12b**), similar to what was documented on ACEX (Dickens, 2007). This probably results from the decrease in porosity (and presumably permeability) with depth (**Figure 12c**). Given that individual Rhizons have similar vacuum to pull the water, a decrease in porosity and permeability means a slower flow (Domenico and Schwartz, 1998).~~

5.~~2~~ 1 Fidelity of ~~Rhizon~~ rhizon ~~Pore~~ pore ~~Water~~ water ~~Measurements~~measurements

~~Researchers have employed multiple methods to extract pore waters from marine sediments over the last few decades (Seeberg-Elverfeldt et al., 2005). As the rhizon technique remains relatively novel, the accuracy and precision of analyses obtained through this approach warrant consideration before discussing the results. This issue arises particularly because of the two aforementioned papers questioning the fidelity of pore water records generated through rhizon sampling.~~

~~Schrum et al. (2012) compared dissolved species collected by whole round squeezing and rhizons. They observed very subtle but consistent (0.06 to 0.8 mM) offsets to lower alkalinity in Rhizon samples, and hypothesized that this reflected~~ ~~CO_2~~ ~~degassing during extraction. For example, the release of gas during filtering under vacuum conditions might increase, leading to~~

~~precipitation of $CaCO_3$, and ultimately a drop in alkalinity. They noted, though, that rhizons seemed to provide accurate measurements for nutrients and metals.~~

~~Miller at al. (2014) compared chloride concentrations, oxygen isotopes, and hydrogen isotopes in pore waters collected from whole round squeezing and rhizons. The rhizon samples appeared to have higher [Cl^-] and greater enrichments in heavier isotopes (^{18}O and D). The authors suggested some combination of water absorption onto the hydrophilic membrane, ion exclusion and isotope fractionation due to clay ultrafiltration, and water evaporation during degassing as possible sources for these offsets.~~

~~Rather than an issue with Rhizon sampling per se, an alternative explanation for analytical discrepancies lies with collection time. A lengthy time between core retrieval and final pore water collection could allow for changes in physiochemical conditions, which might relate to evaporation and carbonate precipitation. Our experiments show that significant differences in the chemical environment of cores occur during rhizon sampling. Consider the temperature (**Figure 5a**) and pH (**Figure 5b**) evolution over 24 hours for the five core sections from station S33 that were analyzed. Note that the time to recover, to cut, and to transport these sections from the ship deck to the geochemistry laboratory (total 1.71 hrs) was similar to that involved for other samples (**Table 1**). Thus, we consider results from these cores representative.~~

~~Many authors have observed variations in pore water pH, DIC, alkalinity, and Ca^{2+} values over time (e.g., Gieskes, 1974; Paull et al., 1996; Wang et al., 2010; Sauvage, 2013). The changes in sections from S33 clearly indicate that physiochemical conditions within the core change significantly within 24 hours. The ~15 °C increase will alter inorganic solid-liquid equilibrium conditions (de Lange et al., 1992), and should increase microbial respiration (Sander and Kalff, 1993). The nominal ~0.25 drop in pH implies a reduction in alkalinity. Interestingly,~~

~~though, this appears opposite of results from sequential sampling, where each progressive “generation” of pore water had greater alkalinity.~~

~~One issue is location. The pH sondes were always more than 10 cm from the nearest rhizon. Although it is possible that the Rhizon’s negative pressure in the sediment is compensated by O_2/air increasing respiration, previous experiments on rhizon flow (Seeberg-Elverfeldt et al., 2005; Dickens et al., 2007) indicate that rhizons generally pull water from <3 cm along the core. Thus, water masses adjacent to pH meters were likely “out-of communication” with those being sampled by the rhizons. We suggest that at least two factors effect chemistry: (1) temperature and pH (and pressure) of pore waters change with time after core retrieval; and, (2) pore water chemistry evolves during water removal.~~

~~The observed evolution of pore water chemistry may be related to increasing temperature and possible introduction of atmospheric air via the Rhizon drill hole each time the syringe was removed. As temperature increases, greater microbial activity may drive pH down by increasing CO_2 concentration. Additionally, removing the syringe may have provided opportunity for atmospheric air to enter the sediment through the filament. As the pH decreased, carbonate dissolved, increasing HCO_3^- concentration in the pore water. The Rhizons continually applied additional negative pressure. However, as stated previously, the pH sondes were sufficiently far from the Rhizons to be affected by pore water extraction.~~

~~As clearly documented here and in other works (Seeberg-Elverfeldt et al., 2005; Dickens et al., 2007; Pohlman et al., 2008), rhizon sampling can lead to “smooth” concentration profiles for multiple dissolved species, including alkalinity (**Figures 6 – 10**). The concerns raised about rhizon sampling may be valid for dissolved components when concentration gradients are low. For example, Schrum et al. stressed alkalinity differences of 0.06 to 0.8 mM, but the total~~

~~alkalinity range in this study was 1.80 and 14.58 mM. A similar finding occurs in the dissolved Ca^{2+} and Ba^{2+} profiles of this study, where adjacent samples deviate by amount greater than analytical precision (**Table 3, Figure 11**). However, when the signal to noise ratio become high, as true with most dissolved components at most stations (**Figures 6 – 10**), the rhizon sampling renders pore water profiles with well defined concentration gradients that can be interpreted in terms of chemical reactions and fluxes.~~

~~*5.3 Reading the Pore Water Profiles*~~

~~Pore water profiles in most marine sediment express solute fluxes resulting from chemical reactions, sediment properties, and diffusion (Berner, 1980; Berg et al., 1998). Within 10 m of the seafloor, where temperature and the diffusion coefficient change minimally, depth intervals having inflections in the concentration gradient (dC/dz) generally represent zones where production or consumption of dissolved components occur (ΔJ), or where porosity (ϕ) changes significantly (**Equation 2**). Importantly, excepting areas of the seafloor with strong fluid flow (e.g., mud volcanoes, cold seeps), methane charged sediments along continental margins have very predictable pore water profiles.~~

Formatted: Tab stops: 0.38", Left

~~As previously emphasized, numerous studies demonstrate that a prominent SMT characterizes shallow sediment in locations with high methane concentrations in underlying strata. Moreover, inflections in pore water SO_4^{2-}, alkalinity, $\delta^{13}C$-DIC values, and hydrogen sulfide consistently occur across this geochemical horizon (**Figure 2**). This is because AOM consumes SO_4^{2-} and produces ^{13}C-depleted HCO_3^- and HS^- (**Equation 1**). The overall geochemistry is best understood by considering fluxes (Borowski et al., 1996; Berg et al., 1998; Chatterjee et al., 2011). Across the SMT, upward migrating methane of some flux (JCH_4) reacts with downward diffusing SO_4^{2-}~~

Formatted: Indent: First line: 0", Tab stops: 0.38", Left

~~of equal flux but opposite sign (-JSO_4^{2-}). This leads to a sharp concave-down inflection in SO_4^{2-} concentrations (i.e. the SMT), with the depth driven by JCH_4. Fluxes of HCO_3^- ($JHCO_3^-$) and HS^- (JHS^-) of similar magnitude enter pore water, but are expressed differently in pore water profiles. In general, the input of ^{13}C-depleted HCO_3^- contributes to already ^{13}C-enriched HCO_3^- concentrations, produced during methanogenesis deeper in the sediment column. The consequence is a steep rise in HCO_3^- concentrations with depth, but having a positive kink across the SMT, where a coincident drop in the $\delta^{13}C$-DIC values occur. The input of HS^- diffuses upward and downward, where it reacts with dissolved Fe or sedimentary phases. The consequence is a "bell shaped" HS^- pore water profile with the maxima at the SMT.~~

Formatted: Indent: First line: 0", Pattern: Clear, Tab stops: 0.38", Left

~~Good examples of where such pore water chemistry is documented include: Baltic Sea (Jørgensen et al, 1990), Black Sea (Jørgensen et al, 2004), Blake Ridge (Paull et al., 2000; Borowski et al., 2001), Cariaco Trench (Reeburgh, 1976), Cascadia Margin (Torres and Kastner, 2009), Gulf of Mexico (Kastner et al., 2008a; Hu et al., 2010; Smith and Coffin, 2014), Hydrate Ridge (Claypool et al., 2006), offshore Namibia (Niewohner et al., 1998), offshore Peru (Donohue et al., 2006), South China Sea (Luo et al., 2013; Hu et al., 2015), and Sea of Japan (Expedition Scientists, 2014). In any case, through use of **Equation 2**, fluxes of dissolved ions, and by inference dissolved CH_4, can be calculated from measured pore water concentration profiles with knowledge of porosity and sedimentary diffusion constants (e.g., Niewohner et al., 1998). At sites with abundant methane in the upper few hundred meters, notably including sites with gas hydrate, estimated values for JCH_4 and -JSO_4^{2-} are universally high (**Table 4**).This includes sites in the Beaufort Sea, 154.8 mol/m^2-kyr (Coffin et al., 2013), 102 mol/m^2-kyr (Umitaka Spur; Snyder et al., 2007), 86.2 mol/m^2-kyr (Hikurangi Margin; Coffin et al., 2007), 362.0 mol/m^2-kyr (Chilean Margin; Coffin et al., 2006), 162.5 mol/m^2-kyr (Argentine Basin;~~

~~Hensen et al., 2003;~~ ~~**Figure 15**~~). ~~Methane above gas hydrates can migrate upward even faster through advective bubble ebullition at cold seeps (Joye et al., 2004).~~

Researchers have employed multiple methods to extract pore waters from marine sediments over the last few decades, but the rhizon technique remains relatively novel (e.g., Seeberg-Elverfeldt et al., 2005; Dickens et al., 2007; Pohlman et al., 2008). Several studies have questioned the accuracy and precision of analyses obtained through this approach (e.g., Schrum et al., 2012; Miller et al., 2014). Two experiments conducted during the SWERUS-C3 Leg 2 Expedition using the Rhizons suggest that part of the problem concerns the timing and location of sampling (Supplementary Materials). Notably, however, as clearly documented in previous works (Seeberg-Elverfeldt et al., 2005; Dickens et al., 2007; Pohlman et al., 2008), rhizon sampling can lead to "smooth" concentration profiles for multiple dissolved species, including alkalinity (Fig. 4-8).

Concerns about rhizon sampling may be valid for dissolved components when concentration gradients are very low. For example, Schrum et al. (2012) stressed alkalinity differences between samples collected at similar depth using rhizon sampling and conventional squeezing. However, the total alkalinity range in this study was between 1.6 and 2.6 mM, and typical differences were 0.06 mM. A similar finding occurs in the dissolved Ca^{2+} and Ba^{2+} profiles of this study, where the range in values is small and adjacent samples deviate by more than analytical precision (Tbl. 1, Fig. S3). However, when the signal to noise ratio becomes high, as true with most dissolved components at most stations (Fig. 4-8), the rhizon sampling renders pore water profiles with well-defined concentration gradients that can be interpreted in terms of chemical reactions and fluxes.

5.~~4~~2 General a~~A~~bsence of m~~M~~ethane

Direct measurements of dissolved CH_4 in deep-sea sediment are complicated (Claypool and Kvenvolden 1983). During core retrieval and depressurization, significant CH_4 loss can occur from pore space (Dickens et al., 1997)~~gas ebullition occurs, which leads to significant CH_4 loss from pore space~~. ~~Interestingly, however~~Moreover, in sediments containing high CH_4 concentrations and recovered through piston coring, gas release typically generates obvious sub-horizontal cracks that span the core between the liner. No such cracks were documented in any of the cores.

Excluding Station St31 on the southern Lomonosov Ridge (discussed below), there is no indication of a shallow SMT. Interstitial water sulfur concentrations do not drop below 22.78 mM within the upper 8 m. In fact, calculated downward SO_4^{2-} fluxes, as inferred from sulfur concentration gradients (Tbl. 2~~**Table 4**~~) range from -1.8 to -~~9~~6.2 mol/m^2-kyr for all stations except Station S31. For comparison, a site with a near seafloor temperature of 2 °C (Fig. S2) and porosities similar to those measured (Fig. S1), an SMT at 6.0 mbsf would imply a SO_4^{2-} flux of -40 mol/m^2-kyr.~~with a temperature of 2 °C (**Figure 5a**) and measured porosities (**Figure 12a**), even an SMT at six mbsf would imply SO_4^{2-} flux of -40 mol/m^2-kyr.~~

Given the lack of HS$^-$ and the measured pH at Station S33 (Fig. S2~~**Figure 5**~~), alkalinity should closely approximate HCO_3^- concentrations (Equation 4). Estimated HCO_3^- fluxes ($JHCO_3^-$) do not exceed 6.8 mol/m2-kyr at any station east of the Lomonosov Ridge (Tbl. 2~~**Table 4**~~). For comparison, at sites with abundant CH_4 at depth, $JHCO_3^-$ generally exceeds 30 mol/m^2-kyr above the SMT (Tbl. 2). These extreme fluxes arise because methanogenesis in deeper sediment drives an upward flux of HCO_3^- (Fig. 3), and because AOM contributes additional HCO_3^- and HS$^-$ to pore water at the SMT (Eqn. 1).~~when alkalinity gradients are used~~

Formatted: Indent: First line: 0.38"

Formatted: Font: Not Bold

~~to estimate $J\mathrm{HCO_3^-}$ at sites with abundant $\mathrm{CH_4}$ at depth, values generally exceed 30 mol/m^2 kyr above the SMT (**Table 4**). These extreme fluxes arise because methanogenesis in deeper sediment drives an upward flux of $\mathrm{HCO_3^-}$ (**Figure 2**), and because AOM also contributes $\mathrm{HS^-}$ to pore water at the SMT (**Equation 1**).~~

The δ^{13}C-DIC values of pore water decrease with depth at all stations, almost in concert with the rise in alkalinity, implying no $\mathrm{CH_4}$ production because methanogenesis would increase δ^{13}C-DIC values (Fig. 9c; Whiticar, 1999). O~~However, o~~ther than Station S31, the lowest value of δ^{13}C-DIC is -25.23 ‰ at 5.5 m at Station S22 (Fig. 6~~**Figure 8**~~). This is interesting because a series of microbial reactions utilizing particulate organic matter (POM) can lead to higher alkalinity and lower δ^{13}C-DIC values in pore water~~ (Chatterjee et al., 2001)~~. The most important of these reactions is organoclastic sulfate reduction (OSR), which can be expressed as (Berner, 1980; Boudreau and Westrich, 1984):

$$2\cancel{^{12}}\mathrm{CH_2O} + \mathrm{SO_4^{2-}} \rightarrow \mathrm{H_2S} + 2\mathrm{H}\cancel{^{12}}\mathrm{CO_3^-}\,, \qquad (\cancel{8}7)$$

Formatted: Font: Not Bold

Notably, this reaction has a 2:1 relationship between C and S fluxes, rather than the 1:1 ratio of AOM (Eqn. 1).~~where again the ^{12}C superscript indicates depletion in ^{13}C. Notably, this reaction has a 2:1 relationship between C and S fluxes, rather than the 1:1 ratio of AOM (**Equation 1**).~~

As emphasized previously, methane-charged sediment sequences do occur on continental slopes in the Arctic. Of particular interest to this study are locations in the Beaufort Sea, where indications for gas hydrate manifest on seismic profiles (Grantz et al., 1976; Grantz et al., 1982; Weaver and Stewart, 1982; Hart et al., 2011; Phrampus et al., 2014), and pore water profiles have been generated using shallow piston cores (Coffin et al., 2013). Striking contrasts exist between pore water profiles of the Beaufort Sea and those of the CESS~~ESM~~ (Tbl. 2~~**Table 4; Figure 15**~~). In the Beaufort Sea, there are moderate to high downward $\mathrm{SO_4^{2-}}$ and upward

CH_4~~sulfate and upward methane ~~fluxes (1.9 to 154.8 mol/m^2-kyr), shallow SMTs (6.29 to 1.06 mbsf), high DIC fluxes between the SMT and the mudline (46.3 to 242.6), and negative δ^{13}C-DIC values at SMT's (≈ -20‰).

5.~~5 ~~3 Special c~~C~~ase “Lomonosov Ridge Station”

Station 31 on the Lomonosov Ridge (Fig. 8~~**Figure 10**~~) differs from all other stations examined in this study. Here, pore water chemistry profiles hint at CH_4 in pore space within shallow sediment. Extrapolation of the dissolved sulfur profile suggests an SMT at approximately 1~~3.9~~4 m. Such a depth lies within the range common for locations with AOM (D’Hondt et al., 2002), notably including well studied sites on Blake Ridge (Borowski et al., 1999). Similar to some sites with CH_4, the δ^{13}C-DIC values become very “light”; indeed, the value at the base of the core, -43.54, almost necessarily implies CH_4 oxidation within shallow sediment~~and a shallow SMT~~. Comparably steep alkalinity (1.6 mM/m) and NH_4 gradients (60.4 µM/m) also characterize most~~other~~ sites with CH_4 near the seafloor. However, there is an issue concerning reduced sulfur, which is a product of AOM (Eqn. 1). If AOM was occurring at ~13.9 mbsf, one might expect evidence for HS$^-$ migrating from below (Fig. 3). No ZnS precipitated in pore waters of this core upon addition of ZnAc. ~~However, an issue concerns reduced sulfur produced via AOM (**Equation 1**). One might expect evidence of HS$^-$ migrating from below (**Figure 2**), but none was detected.~~

A comparison of published DIC fluxes, SO_4^{2-} fluxes, and SMT depths (Tbl. 2~~**Table 4**~~) reveals fluxes decrease exponentially with SMT depth (Fig. 11~~**Figure 15**~~). ~~A ~~In fact, a fundamental relationship exists when one considers that upward CH_4 flux controls SMT depth (Eqn. 1; Fig. 3~~**Equation 1; Figure 2**~~). estimated for the Lomonosov Ridge station conform to those expected for an SMT at about 14 mbsf~~The modest SO$_4^{2-}$ flux (-13.9 mol/m^2-kyr) and alkalinity flux (11.3 mol/m^2-kyr) of the Lomonosov Ridge station fits quite well with literature values of similar SMT depth~~. For example, Hensen et al. (2003) calculated a -14.~~69~~ 7 mol/m^2-kyr SO$_4^{2-}$ flux for a site with an SMT at 14 m in the Argentine Basin. Berg (2008) calculated a SO$_4^{2-}$ flux of -8.05 mol/m^2-kyr for a site with an SMT at 16 m at the Costa Rican Margin.

5.~~6~~ 4 Other Chemistry

Microbial communities preferentially utilize the most energetically favorable oxidant available, which leads to a characteristic sequence of reactions in marine sediment (Froelich et al., 1979; Berner, 1980; D'Hondt et al., 2004; Miller et al., 2012). ~~A well-documented sequence of reactions characterize shallow marine sediment (Froelich et al., 1979; Berner, 1980). Microbial communities preferentially utilize the most energetically favorable oxidant available (Froelich et al., 1979; D'Hondt et al., 2002).~~ W~~Thus, w~~ith increasing depth below the seafloor, these reactions are: aerobic respiration, denitrification, manganese oxide reduction, iron oxide reduction, SO$_4^{2-}$ reduction, and finally methanogenesis~~, a near universal order of oxidation/reduction reactions arise: aerobic respiration, denitrification, manganese reduction, nitrate reduction, iron reduction, sulfate reduction, and finally methanogenesis~~. Importantly, depths dominated by these reactions generally depend on the supply of POM to the seafloor, and these reactions impact pore water chemistry.~~these reactions impact pore water chemistry and the depths of zones dominated by these reactions generally depend on the supply of POM to the seafloor.~~

Many of the cores collected along the CESS slope ~~slope of the ESM~~ appear to terminate in the zone of metal oxide reduction. This is because, at most stations, Mn and Fe profiles are still increasing at the bottom of the sampled interval (Fig. 4-8~~Figure 6-10~~) which may be due to dissimilatory Mn- and Fe-oxide reduction. However, Mn in particular may be more complicated. März et al., (2011) find evidence from Mn profiles along the southern Mendeleev Ridge which may reflect diagenetic remobilization and diffusion from deeper sediments. The relatively deep depths of metal oxide reduction nevertheless, are consistent with a relatively low input of POM to the seafloor, and ~~moreover~~ generally contrast with sites of high CH_4 concentrations in shallow sediment. From a simple perspective, there may be insufficient POC to drive methanogenesis near the seafloor.

The station on the Lomonosov Ridge again stands apart. Here, Mn and Fe concentrations reach maxima at 1.3 mbsf and 0.5 mbsf, respectively, and decrease below. This is likely due to Mn and Fe produced during dissimilatory oxide reduction occurring below consumption. Thus, the Lomonosov Ridge site appears to have higher organic turnover and possibly more organic burial than all the other locations.~~Thus, complete consumption of Mn and Fe occurs in the upper few meters, and methanogenesis could be occurring below 13.9 mbsf.~~

5.~~7~~ 5 Signatures of AOM and Organoclastic Sulfate Reduction

Some authors have used changes in DIC and SO_4^{2-} concentrations between the seafloor and the SMT to infer the relative importance of AOM and ~~organoclastic sulfate reduction (~~OSR~~)~~ in marine sediments (Kastner et al. 2008b; Luo et al. 2013; Hu et al. 2015). ~~The idea is~~This idea can be expressed by comparing $\Delta(DIC+Ca^{2+}+Mg^{2+})$ and ΔSO_4^{2-}, where Ca^{2+} and Mg^{2+} are included to account for loss of DIC via carbonate precipitation (other authors, such as Snyder et al., 2007 and Wehrmann et al., (2011) use fluxes instead of concentrations). The rationale lies in the fact that the C:S ratio for AOM is 1:1 (Eqn. 1~~Equation 1~~), whereas the C:S ratio for OSR is

2:1 (Eqn. 8~~**Equation 8**~~). However, this approach neglects two considerations: (1) changes in concentration do not directly relate to fluxes, because of differences in diffusivities of various ionic species, and, (2) a flux of HCO_3^- from below the SMT can augment the DIC produced from AOM or OSR at or above the SMT (Dickens and Snyder, 2009). Thus, changes in alkalinity relative to SO_4^{2-} often exceed 1:1, even at locations completely dominated by AOM (Chatterjee et al., 2011).

Rather than just comparing changes in C:S molar ratios, to interrogate the importance of the two reactions, one might also incorporate δ^{13}C-DIC value. This is because δ^{13}C-DIC values and the depth of DIC production differ considerably for AOM, OSR and methanogenesis at many locations. We generate a figure expressing these relationships at multiple sites (Fig. 12~~**Figure 16**~~), where the y-axis is:

$$\frac{\Delta(DIC + Ca^{2+} + Mg^{2+})}{\Delta(SO_4^{2-})}, \qquad (9)$$

and the x-axis is: DIC*δ^{13}C-DIC. The C:S ratios of dissolved species lie above 1:1 at most locations, regardless of whether CH_4 exists in shallow sediment However, sites with CH_4 have considerably more negative DIC*δ^{13}C-DIC values. Notably, all CESS stations~~ from the ESM~~, except S31 on the Lomonosov Ridge, have modest DIC*δ^{13}C-DIC values.

~~Two basic models help to explain the relationships in **Figure 16**. The first model assumes all SO_4^{2-} consumption occurs through OSR; whereas the second model assumes that SO_4^{2-} consumption occurs via AOM and OSR, but DIC from methanogenesis also migrates upward from below the SMT. The details of both models are included in **Appendix 1**. For the "OSR only" model a C:S ratio of 2:1 at the mudline slowly increases as ^{13}C-depleted carbon is produced. The ESM stations plot near to this model. In the AOM model a C:S ratio of 2.5:1 at the mudline decreases rapidly to an asymptotic value of 1.6:1. The additional flux of DIC from~~

~~below the SMT prevents the second model from approaching 1:1. Although the height and slope of this model can be changed by altering the fluxes, it shows that CH_4-charged locations with upward migrating DIC must have C:S molar ratios in excess of 1:1. It is possible that this upward flux is a necessary characteristic of all sites with methanogenesis.~~

In summary, from general pore water considerations as well as from comparisons to pore water profiles at other locations, sediments along the ESM continental slope do not contain significant CH_4 in shallow sediment. Implicit in this finding is that sediment sequences along the ~~ESM~~ CESS lack large-scale gas hydrate. As models for gas hydrate occurrence in the Arctic (Fig. 1~~**Figure 1**~~) correctly predict gas hydrate in several regions (e.g., Kvenvolden and Grantz, 1990; Max and Lowrie, 1993; Max and Johnson, 2012), our findings prompt an interesting question: why are predictions so markedly wrong for the ~~ESM~~CESS?

5.6 Possible explanations for methane absence~~*5.7 Explanations*~~

To understand the absence of gas hydrates on the ESM, one needs to consider the generalities of gas hydrate occurrence in marine sediment. There are two basic conditions for gas hydrate on continental slopes (Kvenvolden, 1993; Dickens, 2001). The first is the "potential volume", or the pore space where physiochemical conditions (e.g., temperature, pressure, salinity, sediment porosity) are amenable to gas hydrate formation. As stressed in previous works, the ESM, with cold bottom water and a low geothermal gradient, has a relatively large volume of sediment with appropriate gas hydrate stability conditions (Stranne et al., 2016). The second is the "occupancy", or the fraction of sediment pore space with sufficient CH_4 to precipitate gas hydrate. The short answer is that environmental conditions on the ~~ESM~~ CESS are highly conducive for gas hydrate, but there is little CH_4.

It is also important to recognize how diffusive systems operate in marine sediment. Hundreds of pore water profiles have been generated during scientific ocean drilling expeditions, including scores into CH_4 charged sediment sequences. These profiles almost universally show connectivity of pore water chemistry over hundreds of meters (**Figure 2**). This occurs because, given sufficient permeability and time, diffusive fluxes transport species from intervals of high concentration to intervals of low concentration. Hence, unless some impermeable layer exists in the sediment sequence, even CH_4 at depth impacts near seafloor concentrations. Indeed, ODP Leg 164 on the outer Blake Ridge wonderfully shows this phenomenon. The uppermost gas hydrate in sediment in this region probably lies at about 190 mbsf; nonetheless, its presence can be observed in shallow pore water profiles, because the flux of CH_4 from depth drives AOM near the seafloor (Borowski et al., 1999; Dickens, 2001). ~~Assuming that an impermeable layer does not exist in the upper few hundreds of meters of sediment on slopes of the ESM, the lack of gas hydrates and CH_4 suggests either insufficient POC to generate CH_4, or substantial loss of CH_4 over time.~~

For these reasons, bubble-mediated CH_4 transport from widespread gas hydrates occurring between transects is unlikely. No major physiographic provinces exist between transects (Fig. 1 and 2). All major sedimentary regions within the field area are included within the transects. All observed large-scale gas hydrate accumulations with bubble-mediated CH_4 transport also have significant CH_4 diffusion. This is because sediment sequences with gas hydrate have gas hydrate formation, gas hydrate dissociation, and gas hydrate dissolution all co-occurring (Dickens, 2003). The pore water gradients between the top of the gas hydrate stability zone and the seafloor occur due to steady-state formation and dissolution. Therefore, it is unlikely that widespread gas hydrate accumulations exist and are somehow only venting in small localized regions. Therefore, assuming that an impermeable layer does not exist in the upper few hundreds of meters of sediment on slopes of the CESS, the lack of gas hydrates and CH_4 suggests either insufficient POC to generate CH_4, or substantial loss of CH_4 over time.

The accumulation of POC on CESS slopes may be relatively low over the Plio-Pleistocene, an amount too small to drive methanogenesis. With low POC inputs, other microbial reactions can exhaust the organic matter needed for methanogenesis. This may, in fact, explain why the pore water chemistry suggests that metal-oxide reduction dominates the geochemical environment at most stations on the CESS. Additionally, Ba^{2+} concentrations do not provide evidence for bio-barite dissolution. Without further investigation, we can offer three possibilities as to why this might occur: (1) significant sea-ice concentrations, both at present-day and during past glacial intervals, greatly diminishes primary production within the water column, one may ask, however, why this process would hinder production above CESS sediments and not above other Arctic provinces with demonstrated gas hydrate accumulations; (2) the extremely broad continental shelf prevents large accumulations of terrestrial organic rich sediment from reaching the slope, the enormous continental shelf, is indeed, the primary dissimilarity to other Arctic margins; or (3) highly variable sediment accumulation, perhaps corresponding to glacial-interglacial oscillations, creates a situation where organic matter can be consumed during intervals of low deposition. In the latter case, large glaciers in the past may have physically removed sediment (and organic matter) from the slope (Jakobsson et al., 2014).~~The accumulation of POC on slopes of the ESM may be relatively low over the Plio-Pleistocene, an amount too small to drive methanogenesis. With low POC inputs, other microbial reactions can exhaust the organic matter needed for methanogenesis. This may, in fact, explain why the pore water chemistry suggests that metal-oxide reduction dominates the geochemical environment at most~~

~~stations on the ESM. Without further investigation, we can offer three possibilities as to why this might occur: (1) significant sea-ice concentrations, both at present-day and during past glacial intervals, greatly diminishes primary production within the water column, (2) the extremely broad continental shelf prevents large accumulations of terrestrial organic rich sediment from reaching the slope, or (3) highly variable sediment accumulation, perhaps corresponding to glacial-interglacial oscillations, creates a situation where organic matter can be consumed during intervals of low deposition. In the latter case, large glaciers in the past may have physically removed sediment (and organic matter) from the slope (Jakobsson et al., 2014)~~

There is also the issue of POC that likely accumulated in the Cretaceous through early Eocene (Sluijs et al., 2006; Backman et al., 2009). In theory, organic-rich sediment accumulated around the Arctic during this time, which should have generated CH_4. This CH_4 could either be too deeply buried to migrate into the modern GHSZ or have been lost in the intervening time.

6. Conclusions

Leg 2 of the SWERUS-C3 expedition recovered sediments and pore waters from numerous stations across the ESM continental slope. These stations extend from Wrangel Island to the New Siberian Islands, and give information from a climatically sensitive but highly inaccessible area.

In an effort to understand CH_4 cycling on the ESM continental slope, we generated detailed pore water profiles of multiple dissolved constituents at the stations. The pore water profiles are coherent and interpretable, and give a general view: most stations have low SO_4^{2-} and HCO_3^- fluxes (<9.2 and 6.8 mol/m^2-kyr respectively), a moderate decrease in δ^{13}C-DIC values with depth (-3.6‰/m average), no dissolved H_2S, moderate rise in HPO_4^{2-} and NH_4

concentrations, and slightly decreasing Ca^{2+}, Mg^{2+}, and Sr^{2+} concentrations. Except for one station on the Lomonosov Ridge, metal oxide reduction appears to be the dominant geochemical environment affecting shallow sediment, and there is no evidence for upward diffusing CH_4. These results strongly suggest that gas hydrates do not occur on slopes of the ~~ESM~~CESS. This directly conflicts with multiple publications, which have assumed large quantities of CH_4 and gas hydrate in the region. It is possible that CH_4 and gas hydrate occur where the Lomonosov Ridge intersects the ~~ESM~~CESS.

The contradiction between models for gas hydrate in the region and actual data may arise for two basic reasons. First, in relatively recent geological times, insufficient POC accumulates along the slope to form CH_4 and gas hydrates; second, CH_4 generated from POC deposited in older geological times is too deeply buried or has been lost.

Acknowledgments. The authors would like to thank the SWERUS-C3 Leg 2 crew as well as reviewers.

Table List

Table 1 - ~~Rhizon Efficacy~~

~~**Table 2** - Rhizon Flow Rates~~

~~**Table 3** -~~ QA/QC

Table ~~4~~2 - Published and Calculated Fluxes

a = Coffin et al., 2013; b = Personal Communication; c = Coffin et al., 2007; d = Coffin et al., 2006; e = Coffin et al., 2008; f = Hamdan et al., 2011 and Coffin et al., 2014; g = Dickens and Snyder, 2009; h= Snyder et al., 2007; i = Mountain et al., 1994; j = Lin et al., 2006; k = Berelson et al., 2005; l = Hensen et al., 2003; m = Dickens, 2001; n = Geprags et al., 2016; o = Claypool et al., 2006; p = Keigwin et al., 1998; q = Berg, 2008; r = Borowski et al., 2000; s = D'Hondt et al., 2002; t = D'Hondt et al., 2004; u = Torres et al., 2009; v = Burns, 1998; w = Kastner et al., 2008; x = Paull et al., 1996; y = Flood et al., 1995; z = Wefer et al., 1998; 1 = Prell et al., 1998; 2 = Takahashi et al., 2011; 3 = Riedel et al., 2006; 4 = Tamaki et al., 1990; 5 = Lyle et al., 1997; 6 = Moore et al., 2001; 7 = Kimura et al., 1997; 8 = Suess et al., 1988; 9 = D’Hondt et al., 2003. ‡ = Calculated from published material.

~~**Table S1** - All Results~~

Figure Captions

Figure 1. Generalized Arctic map with background from GeoMapApp (http://www.geomapapp.org; Ryan et al., 2009). Observed sulfate-methane transitions during the MITAS 1 expedition shown in black diamonds (Coffin et al., 2013) and Arctic Coring Expedition (ACEX) shown as red squares (Backman et al., 2009).~~Inserted gas hydrate models based on Max and Lowrie, 1993; Max and Johnson, 2012; and Soloviev, 2002.~~

Figure 2. Bathymetric map of Eurasian Arctic showing the overall cruise track of Leg 2 along with the four transects and coring locations. Multicores shown as yellow triangles, gravity and piston cores as white stars, and the ship trackline as gray line from Barrow, Alaska.

~~Idealized pore water concentration profiles for high and low upward methane flux. Discrete data points for sites 722 (Arabian Sea; Seifert and Michaelis, 1991; D'Hondt et al., 2002) and 1230 (offshore Peru; Donohue et al., 2006) are given as reference.~~

Figure 3. Idealized pore water concentration profiles for high and low upward methane flux. Discrete data points for sites 722 (Arabian Sea; Seifert and Michaelis, 1991; D'Hondt et al., 2002) and 1230 (offshore Peru; Donohue et al., 2006) are given as reference.~~Bathymetric map of the Eurasian Arctic showing the overall cruise track of Leg 2, along with the four transects and coring locations.~~

Figure 4. Transect 1. results. IAPSO standard seawater (black dotted line) shown for comparison.~~Rhizon sampling of S28 (a) overall core with Rhizon samples inserted and attached to syringes; (b) close-up showing pore water filling syringes.~~

Figure 5. Transect 2. results. IAPSO standard seawater (black dotted line) shown for comparison.~~Measured temperature and pH of Station 33 over 24 hours showing temperature increase and concomitant decrease in pH. Only three pH profiles were collected due to pH meter failure.~~

Figure 6. Transect 3. results. IAPSO standard seawater (black dotted line) shown for comparison.~~Transect 1 results. ACEX results (grey triangles; Backman et al., 2009) and IAPSO standard seawater (black dotted line) shown for comparison.~~

Figure 7. Transect 4. results. IAPSO standard seawater (black dotted line) shown for comparison.~~Transect 2 results. ACEX results (grey triangles; Backman et al., 2009) and IAPSO standard seawater (black dotted line) shown for comparison.~~

Figure 8. Lomonosov Ridge Station results. IAPSO standard seawater (black dotted line), and representative stations from the four transects shown for comparison.~~Transect 3 results. ACEX results (grey triangles; Backman et al., 2009) and IAPSO standard seawater (black dotted line) shown for comparison.~~

Figure 9. Relationship of (a) sulfate change (ΔSO_4^{2-}) and carbonate corrected alkalinity change ($\Delta Alk+Ca^{2+}+Mg^{2+}$) following 2:1 ratio; (b) the second order polynomial association of NH_4^+ to Alkalinity; and (c) decreasing δ^{13}C-DIC values with alkalinity increase. Methane charged sites (1230, 1426, and 1427; 1230, Shipboard Scientific Party, 2003; 1426 and 1427, Expedition Scientists, 2014) given for comparison.~~Transect 4 results. ACEX results (grey triangles; Backman et al., 2009) and IAPSO standard seawater (black dotted line) shown for comparison.~~

Figure 10. C:N:P ratio indirectly shown with $\Delta Alk/\Delta NH_4^+$ and $\Delta Alk/\Delta HPO_4^{2-}$. Several global sites, 994, 995, 997, 1059, 1225, 1230, 1426, 1427, and 1319 (994-997, 1059, Borowski et al., 2000; 1225 and 1230, Shipboard Scientific Party, 2003; 1426 and 1427, Expedition Scientists, 2014) given for comparison. Blue marginal distribution curves show global distribution while red gives CESS stations (this project). CESS pore waters have higher C:N and lower C:P than comparative sites.~~Lomonosov Ridge Station results. ACEX results (grey triangles; Backman et al., 2009), IAPSO standard seawater (black dotted line), and representative stations from the four transects shown for comparison.~~

Figure 11. Bicarbonate (HCO_3^-) and sulfate (SO_4^{2-}) flux exponential relationship with SMT depth for all sites listed in Table 2.~~Calcium "error" with sampling time. X-Axis equal to duration of time between core retrieval and rhizon pore water completion.~~

Figure 12. Ratio of carbonate corrected alkalinity change ($\Delta Alk+Ca^{2+}+Mg^{2+}$) and sulfate change ($\Delta SO_4^{2-}$) to the product of DIC and δ^{13}C-DIC value (AT13-2 and KC151, Kastner et al., 2008a; PC02-PC14, Coffin et al., 2008; 994-997, 1059, Borowski et al., 2000; Paull et al., 2000; 1326 and 1329, Torres and Kastner, 2009; GC233 and GB425, Hu et al., 2010; D-5 – D-8 and D-F, Hu et al., 2015; C9-C19, Luo et al., 2013; PC-07, Smith and Coffin, 2014; 1230, Shipboard Scientific Party, 2003; 1244 and 1247, Claypool et al., 2006; 1305 and 1306, Party, 2005) including global sites for comparison) showing the paucity of methane charged sites actually reaching 1:1 C:S ratio. Error bars are one sigma. CESS plotted pore waters substitute alkalinity for DIC. With the absence of sulfide, DIC and alkalinity should be roughly equivalent in these pore waters. CESS locations use the same symbols as previous figures.

~~Relationship of (a) porosity and (b) rhizon extraction rate revealing the (c) exponential correlation in flow rate with porosities commonly observed in piston, gravity, and multicores.~~

~~**Figure 13.** Relationship of (a) sulfate change (ΔSO_4^{2-}) and carbonate corrected alkalinity change (ΔAlk+Ca^{2+}+Mg^{2+}) following 2:1 ratio; (b) the second order polynomial association of NH_4^+ to Alkalinity; and (c) decreasing δ^{13}C-DIC values with alkalinity increase. Methane charged sites (1230, 1426, and 1427; 1230, Shipboard Scientific Party, 2003; 1426 and 1427, Expedition Scientists, 2014) given for comparison.~~

~~**Figure 14.** C:N:P ratio indirectly shown with ΔAlk/ΔNH_4^+ and ΔAlk/ΔHPO_4^{2-}. Several global sites, 994, 995, 997, 1059, 1225, 1230, 1426, 1427, and 1319 (994-997, 1059, Borowski et al., 2000; 1225 and 1230, Shipboard Scientific Party, 2003; 1426 and 1427, Expedition Scientists, 2014) given for comparison. Blue marginal distribution curves show global distribution while red gives ESM stations (this project). ESM pore waters have higher C:N and lower C:P than comparative sites.~~

~~**Figure 15.** Bicarbonate (HCO_3^-) and sulfate (SO_4^{2-}) flux exponential relationship with SMT depth for all sites listed in Table 4.~~

~~**Figure 16.** Ratio of carbonate corrected alkalinity change (ΔAlk+Ca^{2+}+Mg^{2+}) and sulfate change (ΔSO_4^{2-}) to the product of DIC and δ_{13}C-DIC value (AT13-2 and KC151, Kastner et al., 2008a; PC02-PC14, Coffin et al., 2008; 994-997, 1059, Borowski et al., 2000; Paull et al., 2000; 1326 and 1329, Torres and Kastner, 2009; GC233 and GB425, Hu et al., 2010; D-5 – D-8 and D-F, Hu et al., 2015; C9-C19, Luo et al., 2013; PC-07, Smith and Coffin, 2014; 1230, Shipboard Scientific Party, 2003; 1244 and 1247, Claypool et al., 2006; 1305 and 1306, Party, 2005) including global sites for comparison) showing the paucity of methane charged sites actually reaching 1:1 C:S ratio. Two simple models of OSR and OSR + AOM (following Chatterjee et al., 2011; and Malinverno and Pohlman, 2011); given as dotted lines. When an additional flux of HCO_3^- is added from below the SMT the C:S ratio is unlikely to reach 1:1.~~

~~Error bars are one sigma. ESM plotted pore waters substitute alkalinity for DIC. With the absence of sulfide, DIC and alkalinity should be roughly equivalent in these pore waters. ESM locations use the same symbols as previous figures.~~

References:

Aagaard, K., Coachman, L. K., and Carmack, E. C.: On the halocline of the Arctic Ocean, Deep Sea Res., 28, 529-545, 1981.

Aagaard, K. and Carmack, E. C.: The role of sea ice and other fresh water in the Arctic Circulation, J. Geophys. Res., 94, 14485–14498, 1989.

Aharon, P. and Fu, B.: Microbial sulfate reduction rates and sulfur and oxygen isotope fractionations at oil and gas seeps in deepwater Gulf of Mexico. Geochimica et Cosmochimica Acta, 64(2), pp.233-246, 2000.

Alekseev, M. N.: Paleogeography and geochronology in the Russian eastern arctic during the second half of the quaternary, Quatern. Int., 41/42, 11–15, 1997.

Alperin, M. J., Reeburgh, W. S., and Whiticar, M. J.: Carbon and hydrogen isotope fractionation resulting from anaerobic methane oxidation, Global Biogeochem. Cy., 2, 279-288, 1988.

Andreassen, K., Hogstad, K., and Berteussen, K. A.: Gas hydrate in the southern Barents Sea indicated by a shallow seismic anomaly, First Break, 8, 235–245, 1990.

Andreev, A. A., Grosse, G., Schirrmeister, L., Kuznetsova, T. V., Kuzmina, S. A., Bobrov, A. A., Tarasov, P. E., Novenko, E., Yu., Meyer, H., Derevyagin, A., Yu., Kienast, F., Bryantseva, A., and Kunitsky, V. V.: Weichselian and Holocene palaeoenvironmental history of the Bol'shoy Lyakhovsky Island, New Siberian Archipelago, Arctic Siberia. Boreas 38, 72–110, 2009.

Archer, D. E.: Methane hydrate stability and anthropogenic climate change, Biogeosciences, 4, 993-1057, 2007.

Archer, D.: A model of the methane cycle, permafrost, and hydrology of the Siberian continental margin, Biogeosciences, 12 (10), 2953–2974, 2015.

Augstein, E.: Die Expedition ARCTIC'96 mit FS" Polarstern"(ARK XII) mit der Arctic Climate System Study (ACSYS); The expedition ARCTIC'96 of RV" Polarstern"(ARK XII) with the Arctic Climate System Study (ACSYS). Berichte zur Polarforschung (Reports on Polar Research), 234, 1997.

Backman, J., and Moran, K.: Expanding the Cenozoic paleoceanographic record in the Central Arctic Ocean: IODP Expedition 302 Synthesis: Central European Journal of Geosciences, 1, 2, 157-175, 2009.

Bakhmutov, V., Whitledge, T., Wood, K. and Ostrovskiy, A.: Report on the execution of marine research in the Bering Strait, East Siberian and the Chukchi Sea by the Russian-American Expedition under the program of" RUSALCA" during the period from 23 August through 30 September, 2009.

Barnes, R. O. and Goldberg, E. D.: Methane production and consumption in anoxic marine sediments, Geol. 4, 297–300, 1976.

Beaudoin, Y. C., Waite, W., Boswell, R., and Dallimore, S. R.: Frozen Heat: A UNEP Global Outlook on Methane Gas Hydrates. Volume 1. UN. Environ. Programme, GRID-Arendal, 2014

Berelson, W. M., Prokopenko, M., Sansone, F. J., Graham, A. W., McManus, J. and Bernhard, J. M.: Anaerobic diagenesis of silica and carbon in continental margin sediments: discrete zones of TCO 2 production. Geochimica et cosmochimica acta, 69 (19), 4611-4629, 2005.

Berg, P., Risgaard-Petersen, N., and Rysgaard, S.: Interpretation of measured concentration profiles in sediment pore water, Limnol. Oceanogr., 43, 1500-1510, 1998.

Berg, R.D.: Diffusional methane fluxes within continental margin sediments and depositional constraints on formation factor estimates, ProQuest, 2008.

Berner, R. A.: Diagenetic models of dissolved species in the interstitial waters of compacting sediments, Am. J. Sci., 275, 88–96, 1975.

Berner, R. A.: Stoichiometric models for nutrient regeneration m anoxic sediment?, Limnology, 22, 781-786, 1977

Berner, R. A.: Early Diagenesis: A Theoretical Approach, Princeton University Press, Princeton, N. J., 1980.

Bhatnagar, G., Chatterjee, S., Chapman, W. G., Dugan, B., Dickens, G. R., and Hirasaki G. J.: Analytical theory relating the depth of the sulfate-methane transition to gas hydrate distribution and saturation, Geochem. Geophy. Geosy., 12, 1-21, 2011.

Biastoch, A., Treude, T., Ruepke, L. H., Riebesell, U., Roth, C., Burwicz, E. B., Park, W., Latif, M., Boening, C. W., Madec, G., and Wallmann, K.: Rising Arctic Ocean temperatures cause gas hydrate destabilization and ocean acidification, Geophys. Res. Lett., 38, 1-5, 2011.

Boetius, A., Ravenschlag, K., Schubert, C. J., Rickert, D., Widdel, F., Gieseke, A., Amann, R., Jørgensen, B. B., Witte, U. and Pfannkuche, O.: A marine microbial consortium apparently mediating anaerobic oxidation of methane, Nature, 407, 623-626, 2000.

Borowski, W. S., Paull, C. K., and Ussler III, W.: Marine porewater sulfate profiles indicate in situ methane flux from underlying gas hydrate, Geol. 24, 655– 658, 1996.

Borowski, W. S., Paull, C. K., and Ussler W. III: Global and local variations of interstitial sulfate gradients in deepwater, continental margin sediments: Sensitivity to underlying methane and gas hydrates, Mar. Geol., 159, 131–154, 1999.

Borowski, W. S., Hoehler, T. M., Alperin, M. J., Rodriguez, N. M. and Paull, C.K.: Significance of anaerobic methane oxidation in methane-rich sediments overlying the Blake Ridge gas hydrates. In Proceedings of the ocean drilling program, scientific results (Vol. 164, pp. 87-99, 2000).

Borowski, W. S., Cagatay, N., Ternois, Y., and Paull, C. K.: Data Report: carbon isotopic composition of dissolved CO2, CO2 gas, and methane, Blake –Bahama Ridge and Northeast Bermuda Rise, ODP Leg 172, In: Keigwin, L. D., Rio, D., Acton, G. D., Arnold, E. (Eds.), Proceedings of the ODP. Scientific Results (College Station, TX), vol. 172, 1–16, 2001.

Boudreau, B. P. and Westrich, J. T.: The dependence of bacterial sulfate reduction on sulfate concentration in marine sediments, Geochimica Cosmochimica Acta, 48, 2503–2516, 1984.

Buffett, B. and Archer, D.: Global inventory of methane clathrate: sensitivity to changes in the deep ocean, Earth Planet. Sc. Lett., 227, 185–199, 2004.

Burns, S.J.: Carbon isotopic evidence for coupled sulfate reduction-methane oxidation in Amazon Fan sediments. Geochimica et Cosmochimica Acta, 62(5), 797-804, 1998.

Carcione, J. M. and Tinivella, U.: Bottom-simulation reflectors: Seismic velocities and AVO effects, Geophysics, 65, 54–67, 2000.

Chatterjee, S., Dickens, G. R., Bhatnagar, G., Chapman, W. G., Dugan, B., Snyder, G. T., and Hirasaki, G. J.: Pore water sulfate, alkalinity, and carbon isotope profiles in shallow sediment above marine gas hydrate systems: A numerical modeling perspective, J. Geophys. Res-Sol. Ea., 116, 1-25, 2011.

Chand, S., Mienert, J., Andreassen, K., Knies, J., Plassen, L., and Fotland, B.: Gas hydrate stability zone modelling in areas of salt tectonics and pockmarks of the Barents Sea suggests an active hydrocarbon venting system, Mar. Petrol. Geol., 25, 625–636, 2008.

Clark, D. L.: Early history of the Arctic Ocean, Paleoceanography, 3, 539-550, 1988.

Claypool, G. E. and Kvenvolden, K. A.: Methane and other hydrocarbon gases in marine sediment, Annu. Rev. Earth Pl. Sc., 11, 299-327, 1983.

Claypool, G. E., Milkov, A. V., Lee, Y. J., Torres, M. E., Borowski, W.S., and Tomaru, H.: Microbial Methane Generation and Gas Transport in Shallow Sediments of an Accretionary Complex, Southern Hydrate Ridge (ODP Leg 204), Offshore Oregon USA, In: Trehu, A.M., Bohrmann, G., Torres, M.E., Colwell, F.S. (Eds.), In Proceedings of the ODP, Scientific Results. Ocean Drilling Program, College Station, Texas, 2006.

Cline, J. D.: Spectrophotometric determination of hydrogen sulfide in natural waters, Limnol. Oceanogr., 14, 454-458, 1969.

Coffin, R. B., Pohlman, J. W., Gardner, J., Downer, R., Wood, W., Hamdan, L., Walker, S., Plummer, R., Gettrust, J., and Diaz, J.: Methane hydrate exploration on the mid Chilean coast: a geochemical and geophysical survey, J. Petrol. Sci. Eng., 56, 32-41, 2007.

Coffin, R., Hamdan, L., Pohlman, J., Wood, W., Pecher, I., Henrys, S., Greinert, J., and Faure, K.: Geochemical characterization of concentrated gas hydrate deposits on the Hikurangi Margin, New Zealand. Preliminary Geochemical Cruise Report. NRL/MR/ 6110-07, 2007.

Coffin, R. B., Hamdan, L. J., Plummer, R., Smith, J., Gardner, J., Hagen, R., and Wood, W.: Analysis of Methane and Sulfate Flux in Methane-charged Sediments from the Mississippi Canyon, Gulf of Mexico, Mar. Petrol. Geol., 25, 977–987, 2008.

Coffin, R. B., Plummer, R. B., Yoza, B., Larsen, R. K., Millholland, L. C., and Montgomery, M. T.: Spatial variation in shallow sediment methane sources and cycling on the Alaskan Beaufort Sea Shelf/Slope, Mar. Petrol. Geol., 45, 186-197, 2013.

Coffin, R. B., Hamdan, L. J., Smith, J. P., Rose, P. S., Plummer, R. E., Yoza, B., Pecher, I. and Montgomery, M.T.: Contribution of vertical methane flux to shallow sediment carbon pools across Porangahau ridge, New Zealand. Energies, 7 (8), 5332-5356, 2014.

Collett, T.S.: Energy resource potential of natural gas hydrates, AAPG Bull., 86, 1971–1992, 2002.

Collett, T. S., Lee, M. W., Agena, W. F., Miller, J. J., Lewis, K. A., Zyrianova, M. V., Boswell, R., and Inks, T. L.: Permafrost associated natural gas hydrate occurrences on the Alaska North Slope, Mar. Petrol. Geol., 28, 279-294, 2010.

D'Hondt, S., Rutherford, S., and Spivack, A.J.: Metabolic activity of subsurface life in deep-sea sediments, Science, 295, 2067-2070, 2002.

D’Hondt, S. L., Jørgensen, B. B., Miller, D. J., and Shipboard Scientific Pary: Proceedings of the Ocean Drilling Program, Initial Reports Volume 201, 2003.

D'Hondt, S., Jørgensen, B. B., Miller, D. J., Batzke, A., Blake, R., Cragg, B. A., Cypionka, H., Dickens, G. R., Ferdelman, T., Hinrichs, K. U. and Holm, N.G.: Distributions of microbial activities in deep subseafloor sediments. Science, 306 (5705), 2216-2221, 2004.

Danyushevskaya, A., Yashin, D. S., and Kirillow, O. V.: Geochemical patterns of distribution of organic carbon in the bottom sediments of Arctic seas, Oceanology, 20, 183-188, 1980.

Darby, D. A., Naidu, A. S., Mowatt, T. C., and Jones, G.: Sediment composition and sedimentary processes in the Arctic Ocean. In: Y. Herman (Editor), The Arctic Seas:

Climatology, Oceanography, Geology and Biology, Van Nostrand Reinhold, New York, 657-720, 1989.

~~De Lange, G. J., Cranston, R. E., Hydes, D. H. and Boust, D.: Extraction of pore water from marine sediments: A review of possible artifacts with pertinent examples from the North Atlantic. Mar. Geol., 109, 53-76, 1992.~~

Dehairs, F., Chesselet, R., and Jedwab, J.: Discrete suspended particles of barite and the barium cycle in the ocean, Earth Planet. Sci. Lett., 49, 528–550, 1980.

Devol, A. H.: Are high rates of sulphate reduction associated with anaerobic oxidation of methane?, Nature, 291, 407-408, 1981.

Dickens, G. R., Paull, C. K. and Wallace, P.: Direct measurement of in situ methane quantities in a large gas hydrate reservoir. Nature, 385, 426-428, 1997.

Dickens, G. R.: Sulfate profiles and barium fronts in sediment on the Blake Ridge. Present and past methane fluxes through a large gas hydrate reservoir, Geochim. Cosmochim. Ac., 65, 529-543, 2001.

Dickens, G. R.: Rethinking the global carbon cycle with a large, dynamic and microbially mediated gas hydrate capacitor. EPSL, 213 (3), 169-183, 2003.

Dickens, G. R.: Rhizon sampling of pore waters on scientific drilling expeditions: an example from the IODP Expedition 302, Arctic Coring Expedition (ACEX). Sci. Drill 4, 22–25, 2007.

Dickens, G.R. and Snyder, G.T.: Interpreting upward methane flux from marine pore water profiles, In: Fire in the Ice, NETL Methane Hydrate Newsletter 9 (1), 7-10, 2009.

~~Domenico, P.A. and Schwartz, F.W.: Physical and chemical hydrogeology, (Vol. 44), New York: Wiley, 1998.~~

D'Hondt, S., Rutherford, S., and Spivack, A. J.: Metabolic activity of subsurface life in deep-sea sediments, Science, 295, 2067–2070, 2002.

Dmitrenko, I. A., Polyakov, I. V., Kirillov, S. A., Timokhov, L. A., Frolov, I. E., Sokolov, V. T., Simmons, H. L., Ivanov, V. V., and Walsh, D.: Toward a warmer Arctic Ocean: spreading of the early 21st century Atlantic Water warm anomaly along the Eurasian Basin margins, J. Geophys. Res-Oceans 113, 1-13, 2008.

Dmitrenko, I. A., Bauch, D., Kirillov, S. A., Koldunov, N., Minnett, P. J., Ivanov, V. V., Hölemann, J. A., and Timokhov, L. A.: Barents Sea upstream events impact the properties of Atlantic water inflow into the Arctic Ocean: Evidence from 2005 to 2006 downstream observations, Deep-Sea Research I, 56, 513–527, 2009

Donohue, C. M., Snyder, G. T., and Dickens, G. R.: Data report: major cation concentrations of interstitial waters collected from deep sediments of Eastern Equatorial Pacific and Peru Margin (ODP Leg 201), Proceedings of ODP, Scientific Results, 201, Ocean Drilling Program, College Station, TX, 2006.

Dymond, J., Suess, E., and Lyle, M.: Barium in deep-sea sediment: A geochemical proxy for paleoproductivity, Paleoceanography 7, 163–181, 1992.

Elliott, S., Maltrud, M., Reagan, M., Moridis, G., and Cameron-Smith P.: Marine methane cycle simulations for the period of early global warming, J. Geophys. Res-Biogeo., 116, 1-13, 2011.

Engen, Ø., Faleide, J. I., and Dyreng, T. K.: Opening of the Fram Strait gateway: A review of plate tectonic constraints: Tectonophysics, 450, 1-69, 2008.

Expedition 346 Scientists: Asian Monsoon: onset and evolution of millennial-scale variability of Asian monsoon and its possible relation with Himalaya and Tibetan Plateau uplift, IODP Preliminary Report, 346, 2014.

Eiken, O. and Hinz, K.: Contourites in the Fram Strait, Sediment Geol., 82, 15–32, 1993.

Ferré, B., Mienert, J., and Feseker, T.: Ocean temperature variability for the past 60 years on the Norwegian-Svalbard margin influences gas hydrate stability on human time scales, J. Geophys. Res., 117, 1-14, 2012.

Flood, R. D., Piper, D. J. W., Klaus, A., and Scientific Research Party: Proceedings of the Ocean Drilling Program, Initial Reports, 155: College Station, TX (Ocean Drilling Program), 1995.

Froelich, P., Klinkhammer, G. P., Bender, M. A. A., Luedtke, N. A., Heath, G. R., Cullen, D., Dauphin, P., Hammond, D., Hartman, B., and Maynard, V.: Early oxidation of organic matter in pelagic sediments of the eastern equatorial Atlantic: suboxic diagenesis, Geochim. Cosmochim. Ac., 43, 1075-1090, 1979.

Gao, H., Schreiber, F., Collins, G., Jensen, M. M., Kostka, J. E., Lavik, G., de Beer, D., Zhou, H. Y., and Kuypers, M. M.: Aerobic denitrification in permeable Wadden Sea sediments, The ISME J., 4, 417-426, 2010.

Geprägs, P., Torres, M. E., Mau, S., Kasten, S., Römer, M., and Bohrmann, G.: Carbon cycling fed by methane seepage at the shallow Cumberland Bay, South Georgia, sub-Antarctic, Geochem. Geophy. Geosy., 17, 1401-1418, 2016.

Gieskes, J. M. and Rogers, W. C.: Alkalinity determination in interstitial waters of marine sediments, J. Sediment. Res., 43(1), 272-277, 1973.

Gieskes J. M.: The alkalinity-total carbon dioxide system in seawater, In The Sea, vol. 5 (ed. E. D. Goldberg). John Wiley and Sons, New York, 123–151, 1974.

Gieskes, J. M., Gamo, T., and Brumsack, H.: Chemical methods for interstitial water analysis aboard JOIDES Resolution, 1991.

Gingele, F. and Dahmke, A.: Discrete barite particles and barium as tracers of paleoproductivity in South Atlantic sediments, Paleoceanography, 9, 151–168, 1994.

Giustiniani, M., Tinivella, U., Jakobosson, M., and Rebesco, M.: Arctic Ocean gas hydrate stability in a changing climate, J. Geol. Res., 1-10, 2013.

Goldhaber, M.: Kinetic Models of Sulfur Diagenesis in Recent Marine Sediments, In Transactions-AGU, 55, 696-697, 1974.

Grantz, A., Boucher, G., and Whitney, O. T.: Possible solid gas hydrate and natural gas deposits beneath the continental slope of the Beaufort Sea, U.S. Geological Survey Circulation Number 733, 1976.

Grantz, A., Mann, D. M., and May, S. D.: Tracklines of multichannel seismic-reflection data collected by the U.S. Geological Survey in the Beaufort and Chukchi Seas in 1977 for which profiles and stack tapes are available, U.S. Geological Survey Open-File Report 1982, 82-735, 1982.

Greinert, J., Bohrmann, G., and Suess, E.: Gas hydrate-associated carbonates and methane-venting at Hydrate Ridge: classification, distribution, and origin of authigenic lithologies, Natural gas hydrates: Occurrence, distribution, and detection, 99-113, 2001.

Gualtieri, L., Vartanyan, S., Brigham-Grette, J., and Anderson, P. M.: Evidence for an ice-free Wrangel Island, Northeast Siberia during the Last Glacial Maximum, Boreas 34, 264–273, 2005.

~~Gusev, E., Anikina, N., Andreeva, I., Bondarenko, S., Derevyanko, L., Iosifidi, A., Klyuvitkina, T., Litvinenko, I., Petrova, V., Polyakova, E., Popov, V., and Stepanova, A.: Stratigraphy of Late Cenozoic sediments of the western Chukchi Sea: New results of shallow drilling and seismic reflection profiling, Global Planet. Change, 68, 115–131, 2009.~~

Haacke, R. R., Westbrook, G. K., and Riley, M.: Controls on the formation and stability of gas hydrate-related bottom-simulating reflectors (BSRs): a case study from the west Svalbard continental slope, J. Geophys. Res., 113, 1-17, 2008.

Hamdan, L. J., Gillevet, P. M., Pohlman, J. W., Sikaroodi, M., Greinert, J., and Coffin, R.B.: Diversity and biogeochemical structuring of bacterial communities across the Porangahau ridge accretionary prism, New Zealand, FEMS Microbiol. Ecol., 77, 518-532, 2011.

Haraldsson, C., Anderson, L. G., Hassellöv, M., Hulth, S., and Olsson, K.: Rapid, high-precision potentiometric titration of alkalinity in ocean and sediment pore waters, Deep Sea Research Part I: Oceanographic Research Papers, 44, 2031-2044, 1997.

Hart, P. E., Pohlman, J. W., Lorenson, T. D., and Edwards, B. D.: Beaufort Sea Deep-water gas hydrate recovery from a seafloor mound in a region of widespread BSR occurence, in Proceedings of the 7th International Conference on Gas Hydrates (ICGH 2011), Edinburgh, Scotland, 2011.

Hensen, C., Zabel, M., Pfiefer, K., Schwenk, T., Kasten, S., Riedinger, N., Schulz, H. D., Boetius, A.: Control of sulfate porewater profiles by sedimentary events and the significance of anaerobic oxidation of methane for the burial of sulfur in marine sediments, Geochimica Cosmochimica Acta 67, 2631-2647, 2003.

Holbrook, W. S., Hoskins, H., Wood, W. T., Stephen, R. A., and Lizarralde, D.: Methane hydrate and free gas on the Blake ridge from vertical seismic profiling, Science, 273, 1840–1843, 1996.

Holmes, R. M., McClelland, J. W., Peterson, B. J., Shiklomanov, I. A., Shiklomanov, A. I., Zhulidov, A. V., Gordeev, V. V., and Bobrovitskaya, N. N.: A circumpolar perspective on fluvial sediment flux to the Arctic Ocean, Global Biogeochem. Cy., 16, 1-14, 2002.

Holler, T., Wegener, G., Knittel, K., Boetius, A., Brunner, B., Kuypers, M. M., and Widdel, F.: Substantial 13C/12C and D/H fractionation during anaerobic oxidation of methane by marine consortia enriched in vitro, Environ. Microbiol. Rep., 1, 370-376, 2009.

Hovland, M. and Svensen, H.: Submarine pingoes: Indicators of shallow gas hydrates in a pockmark at Nyegga, Norwegian Sea, Mar. Geol., 228, 15–23, 2006.

Hu, X., Cai, W. -J, Wang, Y., Luo, S., and Guo X.: Pore-water geochemistry of two contrasting brine-charged seep stations in the northern Gulf of Mexico continental slope, Mar. Geochem., 118, 99–107, 2010.

Hu, Y., Feng, D., Liang, Q., Xia, Z., Chen, L., and Chen, D.: Impact of anaerobic oxidation of methane on the geochemical cycle of redox-sensitive elements at cold-seep stations of the northern South China Sea. Deep Sea Research Part II: Topical Studies in Oceanography, 2015.

Hustoft, S., Bünz, S., Mienert, J., and Chand, S.: Gas hydrate reservoir and active methane-venting province in sediments on <20Ma young oceanic crust in the Fram Strait, offshore NW-Svalbard, Earth Planet. Sc. Lett., 284, 12-24, 2009.

Hyndman, R. D. and Dallimore, S. R.: Natural gas hydrates studies, Canada Recorder, 26, 11–20, 2001.

Jakobsson, M.: Hypsometry and volume of the Arctic Ocean and its constituent seas: Geochemistry, Geophysics, Geosystems, 3, 5, 1-18, 2002

Jakobsson, M., Grantz, A., Kristoffersen, Y., and Macnab, R.: Physiographic provinces of the Arctic Ocean seafloor, GSA Bull., 115, 1443-1455, 2003.

Jakobsson, M., Backman, J., Rudels, B., Nycander, J., Frank, M., Mayer, L., Jokat, W., Sangiorgi, F., O'Regan, M., Brinkhuis, H., King, J., and Moran, K.: The early Miocene Onset of a Ventilated Circulation Regime in the Arctic Ocean: Nature, 447, 21, 986-990, 2007.

Jakobsson, M., Polyak, L., Edwards, M., Kleman, J., and Coakley, B.: Glacial geomorphology of the Central Arctic Ocean: the Chukchi Borderland and the Lomonosov Ridge, Earth Surf. Proc. Land., 33, 526-545, 2008.

Jakobsson, M., Andreassen, K., Bjarnadóttir, L. R., Dove, D., Dowdeswell, J. A., England, J. H., Funder, S., Hogan, K., Ingólfsson, Ó., Jennings, A., Krog-Larsen, N., Kirchner, N., Landvik, J. Y., Mayer, L., Möller, P., Niessen, F., Nilsson, J., O'Regan, M., Polyak, L., Nørgaard-Pedersen, N., and Stein, R.: Arctic Ocean glacial history, Quaternary Sci. Rev., 92, 40-67, 2014.

Jakobsson, M., Nilsson, J., Anderson, L., Backman, J., Björk, G., Cronin, T.M., Kirchner, N., Koshurnikov, A., Mayer, L., Noormets, R. and O'Regan, M.: Evidence for an ice shelf covering the central Arctic Ocean during the penultimate glaciation. Nature communications, 7, 2016.

Jørgensen, B. B., Bang, M., and Blackburn, T. H.: Anaerobic mineralization in marine sediments from the Baltic Sea-North Sea transition, Mar. Ecol. Progress Series, 59, 39-54, 1990.

Jørgensen, B. B., Weber, A. and Zopfi, J.: Sulfate reduction and anaerobic methane oxidation in Black Sea sediments. Deep Sea Research Part I: Oceanographic Research Papers, 48 (9), 2097-2120, 2001.

Jørgensen, B. B., Böttcher, M. E., Lüschen, H., Neretin, L. N., and Volkov, I. I.: Anaerobic methane oxidation and the deep H2S sink generate isotopically heavy sulfides in Black Sea sediments, Geochim. Cosmochim. Ac., 68, 2095–2118, 2004.

Jørgensen, B. B. and Parkes, R. J.: Role of sulfate reduction and methane production by organic carbon degradation in eutrophic fjord sediments (Limfjorden, Denmark), Limnol. Oceanogr, 55, 1338-1352, 2010.

Jokat, W.: The expedition of the Research Vessel" Polarstern" to the Arctic in 2009 (ARK-XXIV/3). Berichte zur Polar-und Meeresforschung (Reports on Polar and Marine Research), 615, 2010.

Jokat, W. and Ickrath, M.: Structure of ridges and basins off East Siberia along 81° N, Arctic Ocean, Mar. Petrol. Geol., 64, 222-232, 2015.

Joye, S. B., Boetius, A., Orcutt, B. N., Montoya, J. P., Schulz, H. N., Erickson, M. J. and Lugo, S.K.: The anaerobic oxidation of methane and sulfate reduction in sediments from Gulf of Mexico cold seeps. Chemical Geology, 205 (3), 219-238, 2004.

Jenkyns, H. C., Forster, A., Schouten, S., and Sinninghe Damsté, J. S.: High temperatures in the Late Cretaceous Arctic Ocean, Nature, 432, 888–892, 2004.

Judge, A. S.: Natural gas hydrates in Canada, In: M.H. French (Editor), Proceedings of the Fourth Canadian Permafrost Conference 1981, Roger J.E. Brown Memorial Volume, National Research Council of Canada, Ottawa, Ont., 320-328, 1982.

Kastner, M., Claypool, G., and Robertson, G.: Geochemical constraints on the origin of the pore fluids and gas hydrate distribution at Atwater Valley and Keathley Canyon, northern Gulf of Mexico, Mar. Petr. Geol., 25, 860–872, 2008a.

Kastner, M., Torres, M., Solomon, E., and Spivack, A. J.: Marine pore fluid profiles of dissolved sulfate; do they reflect in situ methane fluxes?, In: Fire in the Ice, NETL Methane Hydrate Newsletter, Summer, 2008b.

Keigwin, L. D., Rio, D., Acton, G. D., and Shipboard Scientific Party: Proceedings of the Ocean Drilling Program, Initial Reports, 172: College Station, TX (Ocean Drilling Program), 1998.

Kimura, G., Silver, E. A., Blum, P., Shipboard Scientific Party: Proceedings of the Ocean Drilling Program, Initial Reports, Vol. 170, 1997.

Klauda, J. B. and Sandler, S. I.: Global distribution of methane hydrate in ocean sediment, Energy Fuel, 19, 469–78, 2005.

Klump, J. V. and Martens, C. S.: Biogeochemical cycling in an organic rich coastal marine basin—II. Nutrient sediment-water exchange processes, Geochim. Cosmochim. Ac., 45, 101-121, 1981.

Kvenvolden, K. A., and Grantz, A.: Gas hydrates in the Arctic Ocean region, in The Arctic Ocean Region, Geology of North America, Geol. Soc. of Am., Boulder, Colo., 539-549, 1990.

Kvenvolden, K. A.: Gas hydrates: Geological perspective and global change, Rev. Geophys., 31, 173–187, 1993.

Kvenvolden, K. A. and Lorenson, T. D.: The global occurrence of natural gas hydrate. In: Paull, C. K., Dillon, W. P. (Eds.), Natural Gas Hydrates: Occurrence, Distribution, and Detection, AGU Geophy. Monograph Ser., 124, 3–18, 2001.

Laberg, J. S. and Andreassen, K.: Gas hydrate and free gas indications within the Cenozoic succession of the Bojornya Basin, western Barents Sea, Mar. Petrol. Geol., 13, 921-940, 1996.

Laberg, J. S., Andreassen, K., and Knutsen, S. M.: Inferred gas hydrate on the Barents Sea shelf a model for its formation and a volume estimate, Geo-Mar. Lett., 18, 26–33, 1998.

Lerman, A.: Migrational processes and chemical reactions in Sulfate profiles and barium fronts in sediment 539 interstitial waters, In The Sea, Volume VI (ed. E. D. Goldberg), Wiley, New York, 695-738, 1977.

Li, Y-H. and Gregory, S.: Diffusion of ions in sea sediments. Geochim. Cosmochim. Ac., 38, 703-714, 1974.

Lin, S., Hsieh, W. C., Lim, Y. C., Yang, T. F., Liu, C. S., and Wang, Y.: Methane migration and its influence on sulfate reduction in the Good Weather Ridge region, South China Sea continental margin sediments, Terr. Atmos. Ocean. Sci., 17, 883-902, 2006.

Lorenson, T. D. and Kvenvolden, K. A.: Methane in coastal seawater, sea ice, and bottom sediments, Beaufort Sea, Alaska, USGS Open-File Report 95–70, 1995.

Løvø, V., Elverhøi, A., Antonsen, P., Solheim, A., Butenko, G., Gregersen, O., and Liestøl O.: Submarine permafrost and gas hydrates in the northern Barents Sea, Norsk Polarinstitutt Rapportserie, 56, 1-171, 1990.

Luff, R. and Wallmann, K.: Fluid flow, methane fluxes, carbonate precipitation and biogeochemical turnover in gas hydrate-bearing sediments at hydrate ridge, Cascadia margin: numerical modeling and mass balances, Geochim. Cosmochim. Ac., 67, 3403–3421, 2003.

Luo, M., Chen, L., Wang, S., Yan, W., Wang, H., and Chen, D.: Pockmark activity inferred from pore water geochemistry in shallow sediments of the pockmark field in southwestern Xisha Uplift, northwestern South China Sea, Mar. Pet. Geol., 2013, 48, 247–259, 2013.

Lyle, M., Koizumi, I., Richter, C., and Shipboard Scientific Party: Proceedings of the Ocean Drilling Program, Initial Reports, Vol. 167, 1997.

MacKay, M. E., Jarrard, R. D., Westbrook, G. K., Hyndman, R. D., and Shipboard Scientific Party: Origin of bottom-simulating reflectors: geophysical evidence from the Cascadia accretionary prism, Geol., 22, 459–462, 1994.

Majorowicz, J. A. and Osadetz, K. G.: Gas hydrate distribution and volume in Canada. AAPG bulletin, 85 (7), 1211-1230, 2001.

Makogon, Y. F.: Natural gas hydrates–A promising source of energy, J. Nat. Gas Sc. Eng., 2, 49-59, 2010.

Malinverno, A. and Pohlman, J. W.: Modeling sulfate reduction in methane hydrate-bearing continental margin sediments: does a sulfate-methane transition require anaerobic oxidation of methane, Geochem. Geophy. Geosy., 12, 1-18, 2011.

März, C., Stratmann, A., Matthiessen, J., Meinhardt, A. K., Eckert, S., Schnetger, B., Vogt, C., Stein, R. and Brumsack, H. J.: Manganese-rich brown layers in Arctic Ocean sediments: composition, formation mechanisms, and diagenetic overprint. Geochimica et Cosmochimica Acta, 75 (23), 7668-7687, 2011.

Max, M. D. and Lowrie, A.: Natural gas hydrates: Arctic and Nordic Sea potential. Arctic geology and petroleum potential, proceedings of the Norwegian Petroleum Society conference, 15-17 August 1990, Tromsø, Norway. No. 2. Elsevier Science Ltd., 1993.

Max, M. D. and Johnson, A. H.: Natural Gas Hydrate (NGH) Arctic Ocean potential prospects and resource base, OTC Arctic Technology Conference, 27-53, 2012.

McGuire, A. D., Anderson, L. G., Christensen, T. R., Dallimore, S., Guo, L. D., Hayes, D. J., Heimann, M., Lorenson, D. D., MacDonald, R. W., and Roulet, N.: Sensitivity of the carbon cycle in the Arctic to climate change, Ecol. Monogr., 79, 523–555, 2009.

Miles, P. R.: Potential distribution of methane hydrate beneath the European continental margins, Geophys. Res. Lett., 22, 3179-3182, 1995.

Miller, M. D., Adkins, J. F., and Hodell, D. A.: Rhizon sampler alteration of deep ocean sediment interstitial water samples, as indicated by chloride concentration and oxygen and hydrogen isotopes, Geochem. Geophy. Geosy., 15, 2401-2413, 2014.

Miller, C., Little, D., Bhasin, A., Gardner, N. and Herbert, B., 2012. Surface energy characteristics and impact of natural minerals on aggregate-bitumen bond strengths and asphalt mixture durability. Transportation Research Record: Journal of the Transportation Research Board, (2267), 45-55, 2012.

Miller, M. D., Adkins, J. F., and Hodell, D. A.: Rhizon sampler alteration of deep ocean sediment interstitial water samples, as indicated by chloride concentration and oxygen and hydrogen isotopes, Geochem. Geophy. Geosy., 15, 2401-2413, 2014.

Moore, G. F., Taira, A., and Klaus, A., and Shipboard Scientific Party: Proceedings of the Ocean Drilling Program, Initial Reports Volume 190, 2001.

Moran, K., Backman, J., Brinkhuis, H., Clemens, S. C., Cronin, T., Dickens, G. R., Eynaud, F., Gattacceca, J., Jakobsson, M., Jordan, R.W., and Kaminski, M.: The Cenozoic palaeoenvironment of the arctic ocean, Nature, 441, 601-605, 2006.

Mountain, G. S., Miller, K. G., Blum, P., and Shipboard Scientific Party: Proc. ODP, Initial Reports, 150: College Station, TX (Ocean Drilling Program), 1994.

Murray, R. W., Miller, D. J., and Kryc, K. A.: Analysis of major and trace elements in rocks, sediments, and interstitial waters by inductively coupled plasma–atomic emission spectrometry (ICP-AES), ODP Technical Note 29, 2000.

Naidu, A. S., Cooper, L. W., Finney, B. P., Macdonald, R. W., Alexander, C., and Semiletov, I. P.: Organic carbon isotope ratios (δ13C) of Arctic Amerasian continental shelf sediments, Int. J. Earth Sci., 89, 522–532, 2000.

Niessen, F., Hong, J. K., Hegewald, A., Matthiessen, J., Stein, R., Kim, H., Kim, S., Jensen, L., Jokat, W., Nam, S.-I., and Kang, S.-H.: Repeated Pleistocene glaciation of the East Siberian Continental Margin, Nat. Geosci., 6, 842-846, 2013.

Niewohner, C., Hensen, C., Kasten, S., Zabel, M., and Schulz, H. D.: Deep sulfate reduction completely mediated by anaerobic methane oxidation in sediments of the upwelling area off Namibia, Geochim. Cosmochim. Ac., 62, 455–464, 1998.

Nöthen, K. and Kasten, S.: Reconstructing changes in seep activity by means of pore water and solid phase Sr/Ca and Mg/Ca ratios in pockmark sediments of the Northern Congo Fan, Mar. Geol., 287, 1-13, 2011.

O'Regan, M., Williams, C. J., Frey, K. E., Jakobsson, M.: A synthesis of the long-term paleoclimatic evolution of the Arctic. Oceanography 24(3), 66–80, 2011

O'Regan, M., Preto, P., Stranne, C., Jakobsson, M., and Koshurnikov, A.: Surface heat flow measurements from the East Siberian continental slope and southern Lomonosov Ridge, Arctic Ocean, Geochem. Geophy. Geosy., 17, 1-15, 2016.

Ostanin, I., Anka, Z., di Primio, R. and Bernal, A.: Hydrocarbon plumbing systems above the Snøhvit gas field: structural control and implications for thermogenic methane leakage in the Hammerfest Basin, SW Barents Sea. Marine and Petroleum Geology, 43, 127-146, 2013.

Party, S. S.: Integrated Ocean Drilling Program Expedition 303 Preliminary Report North Atlantic Climate Ice sheet–ocean atmosphere interactions on millennial timescales during the late Neogene-Quaternary using a paleointensity-assisted chronology for the North Atlantic, 1-51, 2005.

Paull, C. K., Ussler, W. III, and Dillon, W. P.: Is the extent of glaciation limited by marine gas-hydrates?, Geophys. Res. Lett., 18 432–434, 1991.

Paull, C. K., Matsumoto, R., Wallace, P. J., and Shipboard Scientific Party: Proceedings of the IODP, Initial Reports. Volume 164: College Station, TX, USA, 1996.

Paull, C. K, Lorenson, T. D., Borowski, W. S., Ussler, III W., Olsen, K., and Rodriguez, N. M.: Isotopic composition of CH_4, CO_2 species, and sedimentary organic matter within samples from the Blake Ridge: gas source implications, In: Paull C. K., Matsumoto, R, Wallace, P. J., and Dillon, W. P., (Eds) Proceedings of the ODP, Sci. Res., Vol. 164 67–78, (ODP), 2000.

Pecher, I. A., Kukowski, N., Huebscher, C., Greinert, J., and Bialas, J.: The link between bottom-simulating reflections and methane flux into the gas hydrate stability zone - new evidence from Lima Basin, Peru Margin, Earth Planet. Sc. Lett., 185, 343-354, 2001.

Peterson, B. J., Holmes, R. M., McClelland, J. W., Vorosmarty, C. J., Lammers, R. B., Shiklomanov, A. I., Shiklomanov, I. A., and Rahmstorf, S.: Increasing river discharge to the Arctic Ocean, Science, 298, 2171–2173, 2002.

Petersen, C. J., Bünz, S., Hustoft, S., Mienert, J., and Klaeschen, D.: High-resolution P-Cable 3D seismic imaging of gas chimney structures in gas hydrated sediments of an Arctic sediment drift, Mar. Petrol. Geol., 1–14, 2010.

Phrampus, B. J., Hornbach, M. J., Ruppel, C. D., and Hart P. E.: Widespread gas hydrate instability on the upper US Beaufort margin, J. Geophys. Res-Sol. Ea., 119, 8594–8609, 2014

Piñero, E., Marquardt, M., Hensen, C., Haeckel, M., and Wallmann K.: Estimation of the global inventory of methane hydrates in marine sediments using transfer functions, Biogeosciences 10, 959–975, 2013.

Pohlman, J. W., Riedel, M., Waite, W., Rose, K., and Lapham, L.: Application of Rhizon samplers to obtain high-resolution pore-fluid records during geo-chemical investigations of gas hydrate systems, Fire in the Ice: Methane Hydrate Newsletter, US Department of Energy/National Energy Technology Laboratory, Fall, 2008.

Posewang, J. and Mienert, J.: High-resolution seismic studies of gas hydrates west of Svalbard, Geo-Mar. Lett., 19, 150–156, 1999.

Prell, W. L., Niitsuma, N., and Shipboard Scientific Party: Proceedings of the Ocean Drilling Program, Initial Reports, 117: College Station, TX (Ocean Drilling Program), 1998.

Rachor, E.: The expedition ARK-XI/1 of RV" Polarstern" in 1995: [ARK XI/1, Bremerhaven-Tromsø-, 07.07. 1995-20.09. 1995]. Berichte zur Polarforschung (Reports on Polar Research), 226, 1995.

Reagan, M. T. and Moridis, G. J.: Dynamic response of oceanic hydrate deposits to ocean temperature change, J. Geophys. Res., 113, 1-21, 2008.

Reagan, M. T. and Moridis, G. J.: Large-scale simulation of methane hydrate dissociation along the West Spitsbergen margin, Geophys. Res. Lett., 36, 1-5, 2009.

Redfield, A. C.: The biological control of chemical factors in the environment, Am. Sci., 46, 221-230, 1958.

Regnier, P., Dale, A. W., Arndt, S., LaRowe, D. E., Mogollón, J., and Van Cappellen, P.: Quantitative analysis of anaerobic oxidation of methane (AOM) in marine sediments: a modeling perspective, Earth-Sci. Rev., 106, 105-130, 2011.

Reeburgh, W. S.: Methane consumption in Cariaco Trench waters and sediments, Earth Planet Sci. Lett., 28, 337–344, 1976.

Riedel, M., Collett, T.S., Malone, M.J., and the Expedition 311 Scientists Proceedings of the Integrated Ocean Drilling Program, Volume 311, 2006.

Riedinger, N., Kasten, S., Gröger, J., Franke, C. and Pfeifer, K.: Active and buried authigenic barite fronts in sediments from the Eastern Cape Basin, Earth Planet. Sc. Lett., 241, 876-887, 2006.

Riedinger, N., Formolo, M. J., Lyons, T. W., Henkel, S., Beck, A., and Kasten, S.: An inorganic geochemical argument for coupled anaerobic oxidation of methane and iron reduction in marine sediments, Geobiology, 12, 172-181, 2014.

Rudels, B., Muench, R. D., Gunn, J., Schauer, U., and Friedrich, H. J.: Evolution of the Arctic Ocean boundary current north of the Siberian shelves, Journal of Marine Systems, 25, 1, 77-99, 2000.

Ryan, W. B. F., Carbotte, S. M., Coplan, J. O., O'Hara, S., Melkonian, A., Arko, R., Weissel, R. A., Ferrini, V., Goodwillie, A., Nitsche, F., Bonczkowski, J., and Zemsky, R.: Global Multi-Resolution Topography synthesis, Geochem. Geophys. Geosyst., 10, 1-9, 2009.

~~Sander, B. C. and Kalff, J.: Factors controlling bacterial production in marine and freshwater sediments, Microb. Ecol., 26, 79-99, 1993.~~

~~Sauvage, J.: Dissolved Inorganic Carbon and Alkalinity in Marine Sedimentary Interstitial Water, Master Thesis, University of Rhode Island, 2013.~~

Schrum, H. S., Murray, R. S., and Gribsholt B.: Comparison of rhizon sampling and whole round squeezing for marine sediment porewater, Sci. Drill., 13, 47–50, 2012.

Schulz, H. D.: Quantification of early diagenesis: dissolved constituents in marine pore water, In Mar. Geochem., Springer Berlin Heidelberg, 85-128, 2000.

Seeberg-Elverfeldt, J., Schlüter, M., Feseker, T., and Kölling, M.: Rhizon sampling of pore waters near the sediment/water interface of aquatic systems, Limnol. Oceanogr. Methods, 3, 361-371, 2005.

Seifert, R. and Michaelis, W.: Organic compounds in sediments and pore waters of Sites 723 and 724, In Prell, W.L., Niitsuma, N., et al., Proc. ODP, Sci. Results, 117: College Station, TX (ODP), 529–545, 1991.

Serreze, M. C., Walsh, J. E., Chapin, III F. S., Osterkamp, T., Dyurgerov, M., Romanovsky, V., Oechel, W. C., Morison, J., Zhang T., and Barry, R. B.: Observational evidence of recent change in the northern high-latitude environment, Climatic Change, 46, 159–207, 2000.

Semiletov, I., Makshtas, O. A., Akasofu, S.I., and Andreas, E. L.: Atmospheric CO2 balance: the role of Arctic sea ice, Geophys. Res. Lett., 31, 1-4, 2004.

Shakhova, N, Semiletov, I, Salyuk, A, Yusupov, V, Kosmach, D, and Gustafsson, Ö.: Extensive Methane venting to the atmosphere from sediments of the East Siberian arctic shelf, Science, 327, 1246–1250, 2010a.

Shakhova, N., Semiletov, I., Leifer, I., Rekant, P., Salyuk, A., and Kosmach, D.: Geochemical and geophysical evidence of methane release from the inner East Siberian Shelf, J. Geophys. Res., 115, 1-14, 2010b.

Sher, A. V., Kuzmina, S. A., Kuznetsova, T. V., and Sulerzhitsky, L. D.: New insights into the Weichselian environment and climate of the East Siberian Arctic, derived from fossil insects, plants, and mammals, Quaternary Sci. Rev., 24, 533 – 569, 2005.

Shipboard Scientific Party: Leg 201 summary, In D'Hondt, S.L., Jørgensen, B.B., Miller, D.J., et al., Proc. ODP, Init. Repts., 201: College Station TX (Ocean Drilling Program), 1–81, 2003.

Sluijs, A., Schouten, S., Pagani, M., Woltering, M., Brinkhuis, H., Damsté, J.S.S., Dickens, G.R., Huber, M., Reichart, G.J., Stein, R. and Matthiessen, J.,: Subtropical Arctic Ocean temperatures during the Palaeocene/Eocene thermal maximum. Nature, 441 (7093), 610-613, 2006.

Smith, J. P. and Coffin, R. B.: Methane Flux and Authigenic Carbonate in Shallow Sediments Overlying Methane Hydrate Bearing Strata in Alaminos Canyon, Gulf of Mexico, Energies, 7, 6118-6141, 2014.

Snyder, G. T., Hiruta, A., Matsumoto, R., Dickens, G. R., Tomaru, H., Takeuchi, R., Komatsubara, J., Ishida, Y., and Yu, H.: Porewater profiles and authigenic mineralization in shallow marine sediments above the methane-charged system on Umitaka Spur, Japan Sea. Deep-Sea Research II 54, 1216–1239, 2007.

Soloviev, V. A.: Gas-hydrate-prone areas of the ocean and gas-hydrate accumulations, Journal of the Conference Abstracts, 6, 158, 2002.

Spielhagen, R. F., Werner, K., Sorensen, S. A., Zamelczyk, K., Kandiano, E., Budeus, G., Husum, K., Marchitto, T. M., and Hald, M.: Enhanced modern heat transfer to the Arctic by warm Atlantic water, Science 331, 450-453, 2011.

Stein, R., Boucsein, B., and Meyer, H.: Anoxia and high primary production in the Paleogene central Arctic Ocean: First detailed records from Lomonosov Ridge, Geophys. Res. Lett., 33, 1-6, 2006.

Stein, R.: Arctic Ocean sediments: processes, proxies, and paleoenvironment, Developments in Mar. Geol., 2. Elsevier, Amsterdam. 592 pp., 2008.

Stranne, C., O'Regan, M., Dickens, G. R., Crill, P., Miller, C., Preto, P., and Jakobsson, M.: Dynamic simulations of potential methane release from East Siberian continental slope sediments, Geochem. Geophy. Geosy., 17, 872-886, 2016.

Stroeve, J. C., Serreze, M. C., Holland, M. M., Kay, J. E., Malanik, J., and Barrett, A. P.: The Arctic’s rapidly shrinking sea ice cover: a research synthesis, Climatic Change, 110, 1005-1027, 2012.

Suess, E., von Huene, R., and Shipboard Scientific Party: Proceedings of the Ocean Drilling Program, Initial Reports, 112: College Station, TX (Ocean Drilling Program), 1988.

Takahashi, T. Broecker, V. S., and Langer, S.: Redfield ratio based on chemical data from isopycnal surfaces, J. Geophys. Res-Oceans, 90, 6907-6924, 1985.

Takahashi, K., Ravelo, A.C., Alvarez Zarikian, C.A., and the Expedition 323 Scientists Proceedings of the Integrated Ocean Drilling Program, Volume 323, 2011.

Tamaki, K., Pisciotto, K., Allan, J., and Shipboard Scientific Party: Proceedings of the Ocean Drilling Program, Initial Reports, Vol. 127, 1990.

Thatcher, K. E., Westbrook, G. K., Sarkar, S., and Minshull, T. A.: Methane release from warming-induced hydrate dissociation in the West Svalbard continental margin: Timing, rates, and geological controls, J. Geophys. Res-Sol. Ea., 118, 22–38, 2013.

Tian, H., Chen, G., Zhang, C., Melillo, J.M. and Hall, C.A.: Pattern and variation of C: N: P ratios in China's soils: a synthesis of observational data. Biogeochemistry, 98(1-3), pp.139-151, 2010.

Timokhov L. A.: Regional characteristics of the Laptev and the East Siberian seas: climate, topography, ice phases, thermohaline regime, and circulation, In: Russian-German cooperation in the Siberian Shelf seas: geo-system Laptev Sea, H. Kassens, H. W. Hubberten, S. Priamikov and R. Stein, editors. Berichte zur Polarforschung, 144, 15-31, 1994.

Torres, M. E., Kastner, M., Wortmann, U. G., Colwell, F., and Kim, J.: Estimates of methane production rates based on δ13C of the residual DIC in pore fluids from the Cascadia margin, EOS, 8(52), Fall Meet. Suppl., Abstract GC14A04, 2007.

Torres, M. E. and Kastner M.: Data report: Clues about carbon cycling in methane-bearing sediments using stable isotopes of the dissolved inorganic carbon, IODP Expedition 311, Proceedings of the IODP, 311, 2009.

Treude, T., Krause, S., Maltby, J., Dale, A.W., Coffin, R. and Hamdan, L.J.: Sulfate reduction and methane oxidation activity below the sulfate-methane transition zone in Alaskan Beaufort Sea continental margin sediments: Implications for deep sulfur cycling. Geochimica et Cosmochimica Acta, 144, 217-237, 2014

Troup, B. N., Bricker, O. P., and Bray, J. T.: Oxidation effect on the analysis of iron in the interstitial water of recent anoxic sediments, Nature 249, 237-239, 1974.

Ussler, W. and Paull, C.K.: Rates of anaerobic oxidation of methane and authigenic carbonate mineralization in methane-rich deep-sea sediments inferred from models and geochemical profiles. Earth and Planetary Science Letters, 266(3), 271-287, 2008.

Vanneste, M., Guidard, S., and Mienert, J.: Bottom-simulating reflections and geothermal gradients across the western Svalbard margin, Terra Nova, 17, 510–516, 2005.

Wallmann, K., Pinero, E., Burwicz, E., Haeckel, M., Hensen, C., Dale, A. W., and Ruepke, L.: The global inventory of methane hydrate in marine sediments: A theoretical approach, Energies, 5, 2449–2498, 2012.

~~Wang, G., Spivack, A. J., and D'Hondt, S.: Gibbs energies of reaction and microbial mutualism in anaerobic deep subseafloor sediments of ODP Site 1226, Geochim. Cosmochim. Ac., 74, 3938-3947, 2010.~~

Weaver, J. S. and Stewart, J. M.: In-situ hydrates under the Beaufort Sea Shelf, In: M.H. French (Editor), Proceedings of the Fourth Canadian Permafrost Conference 1981, Roger J. E. Brown Memorial Volume, Nat. Res. Council Can., Ottawa, Ont., 312-319, 1982.

Wefer, G., Berger, W. H., Richter, C., and Shipboard Scientific Party: Proceedings of the Ocean Drilling Program, Initial Reports, 175: College Station, TX (Ocean Drilling Program), 1998.

Woodgate R. A., Aaagard, K., Muench, R. D., Gunn, J., Björk, G., Rudels, B., Roach, A. T., and Schauer, U.: The Arctic Ocean boundary current along the Eurasian slope and the adjacent Lomonosov Ridge: Water mass properties, transports and transformation from moored instruments, Deep Sea Research, 48, 1757-1792, 2001.

Yamamoto, K. and Dallimore, S.: Aurora-JOGMEC-NRCan Mallik 2006–2008 Gas Hydrate Research Project progress. In: Fire in the Ice, NETL Methane Hydrate Newsletter, Summer 2008, 1–5, 2008.

Ye, H., Yang, T., Zhu, G., Jiang, S., and Wu, L.: Pore water geochemistry in shallow sediments from the northeastern continental slope of the South China Sea, Mar. Petrol. Geol., 75, 68-82, 2016.

Yoshinaga, M. Y., Holler, T., Goldhammer, T., Wegener, G., Pohlman, J. W., Brunner, B., Kuypers, M. M., Hinrichs, K. U. and Elvert, M.: Carbon isotope equilibration during sulphate-limited anaerobic oxidation of methane. Nature Geoscience, 7(3), 190-194, 2014.

Figures

Figure 1.

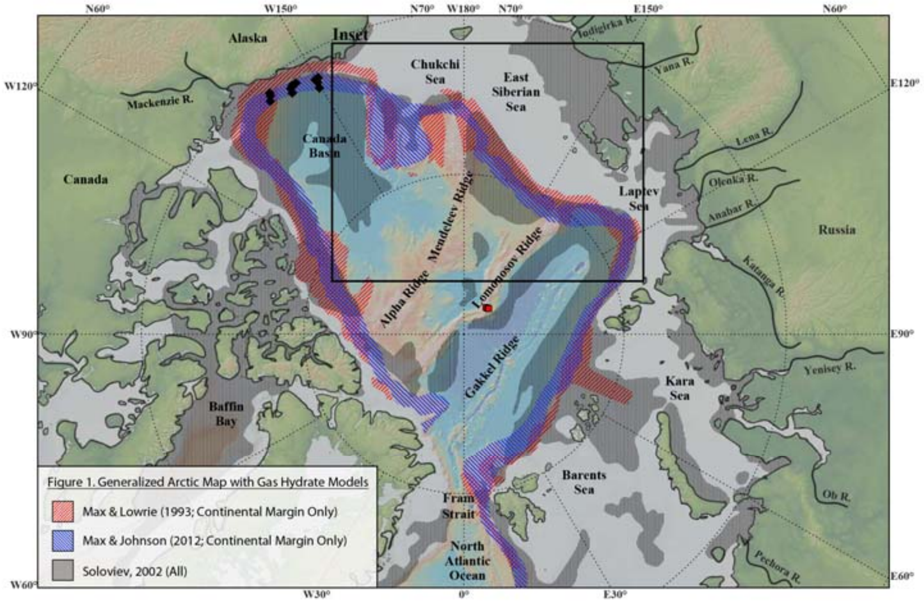
Figure 1. Generalized Arctic Map with Gas Hydrate Models
🟥 Max & Lowrie (1993; Continental Margin Only)
🟦 Max & Johnson (2012; Continental Margin Only)
⬛ Soloviev, 2002 (All)
Inset
N60°
W150°
N70°
W180°
N70°
E150°
N60°
W120°
E120°
W90°
E90°
W60°
W30°
0°
E30°
E60°
Alaska
Mackenzie R.
Canada
Canada Basin
Chukchi Sea
East Siberian Sea
Indigirka R.
Yana R.
Lena R.
Olenka R.
Anabar R.
Laptev Sea
Russia
Katanga R.
Mendeleev Ridge
Alpha Ridge
Lomonosov Ridge
Gakkel Ridge
Yenisey R.
Kara Sea
Baffin Bay
Barents Sea
Fram Strait
North Atlantic Ocean
Ob R.
Pechora R.

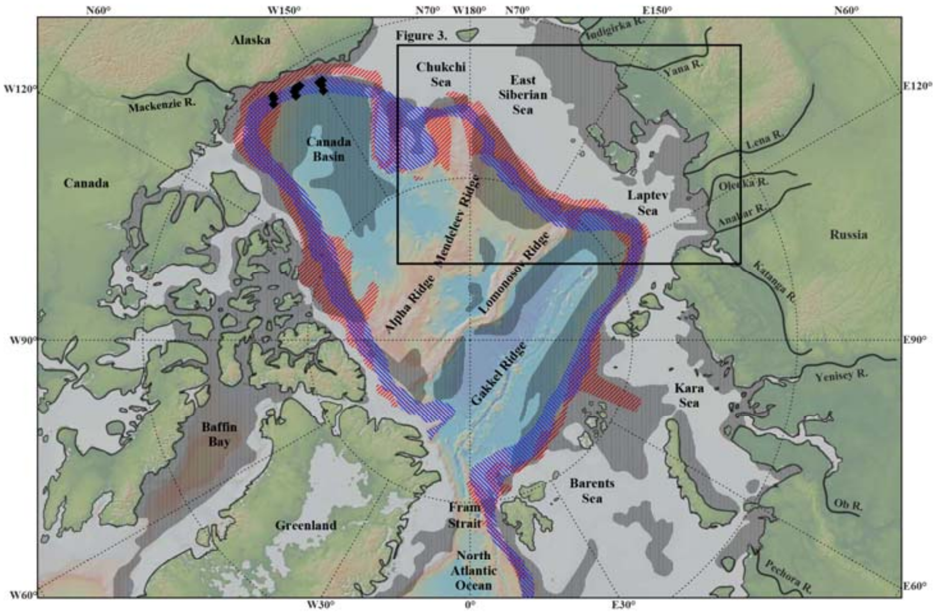

Gas hydrate models: ▨ Max & Lowrie, 1993 (Continental Margin); ▨ Max & Johnson, 2012 (Continental Margin);

& ▨ Soloviev, 2002. Observed SMT (◆ ; Coffin, et al., 2013) locations.

Figure 2.

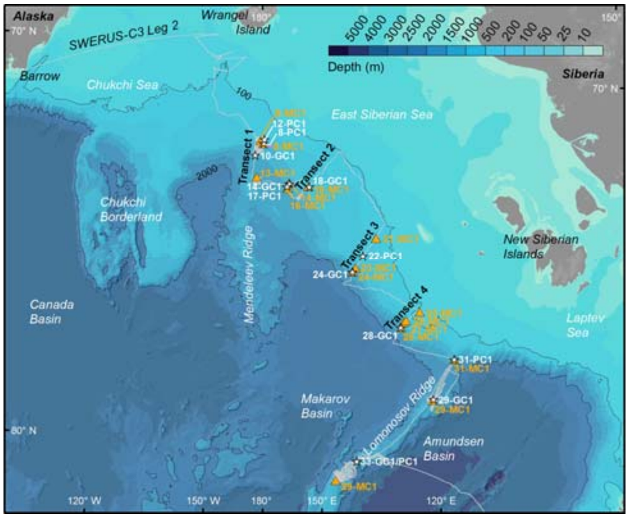
Alaska
70° N
Wrangel Island
180°
SWERUS-C3 Leg 2
5000
4000
3000
2500
2000
1500
1000
500
200
100
50
25
10
Depth (m)
150°
Siberia
70° N
Barrow
Chukchi Sea
100
East Siberian Sea
12-PC1
8-PC1
10-GC1
Transect 1
Transect 2
2000
14-GC1
17-PC1
18-GC1
16-MC1
Chukchi Borderland
Mendeleev Ridge
Transect 3
22-PC1
24-GC1
24-MC1
New Siberian Islands
Canada Basin
Transect 4
28-GC1
Laptev Sea
31-PC1
31-MC1
Makarov Basin
Lomonosov Ridge
29-GC1
29-MC1
80° N
Amundsen Basin
33-GC1/PC1
120° W
150° W
180°
150° E
120° E

Figure 3.

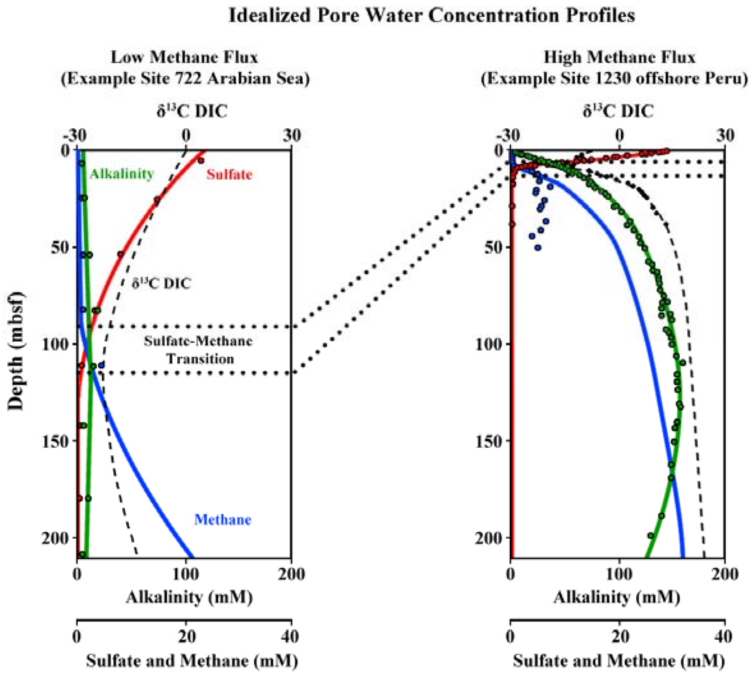
Idealized Pore Water Concentration Profiles
Low Methane Flux
(Example Site 722 Arabian Sea)
High Methane Flux
(Example Site 1230 offshore Peru)
δ13C DIC
-30
0
30
Alkalinity
Sulfate
δ13C DIC
Sulfate-Methane
Transition
Methane
Depth (mbsf)
0
50
100
150
200
Alkalinity (mM)
0
100
200
Sulfate and Methane (mM)
0
20
40

~~**Figure 3.**~~

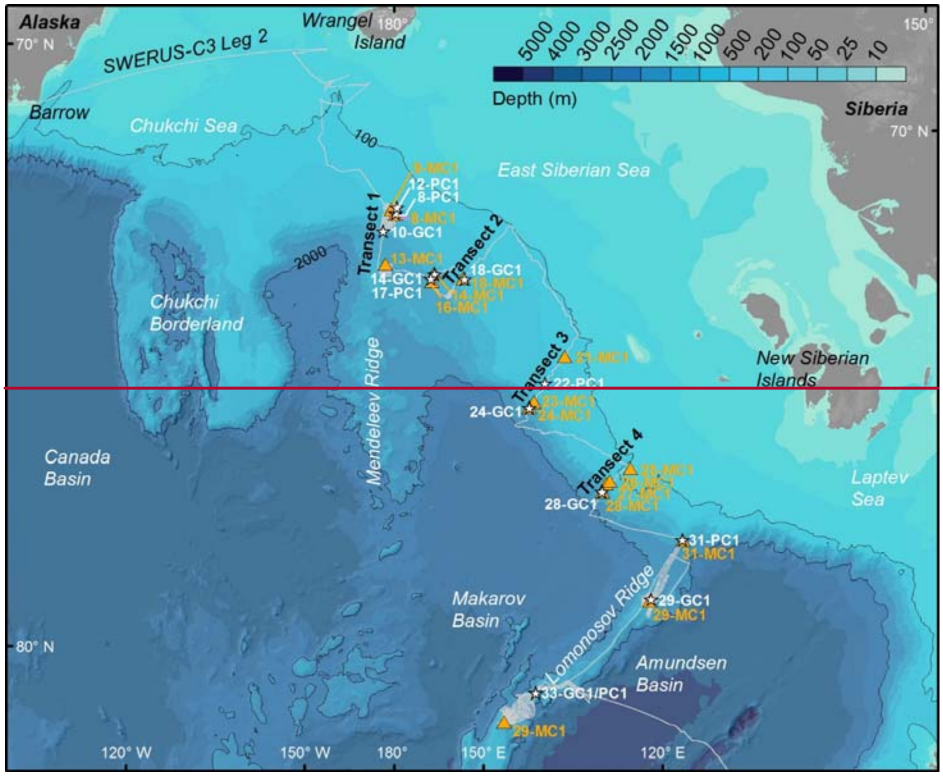
Alaska
70° N
SWERUS-C3 Leg 2
Wrangel Island
180°
150°
5000
4000
3000
2500
2000
1500
1000
500
200
100
50
25
10
Depth (m)
Siberia
70° N
Barrow
Chukchi Sea
100
East Siberian Sea
9-MC1
12-PC1
8-PC1
8-MC1
10-GC1
Transect 1
Transect 2
2000
13-MC1
14-GC1
17-PC1
18-GC1
18-MC1
14-MC1
16-MC1
Chukchi Borderland
Mendeleev Ridge
Transect 3
21-MC1
22-PC1
23-MC1
24-GC1
24-MC1
New Siberian Islands
Canada Basin
Transect 4
25-MC1
26-MC1
27-MC1
28-GC1
28-MC1
Laptev Sea
31-PC1
31-MC1
Makarov Basin
Lomonosov Ridge
29-GC1
29-MC1
80° N
Amundsen Basin
33-GC1/PC1
29-MC1
120° W
150° W
180°
150° E
120° E

Figure 4.

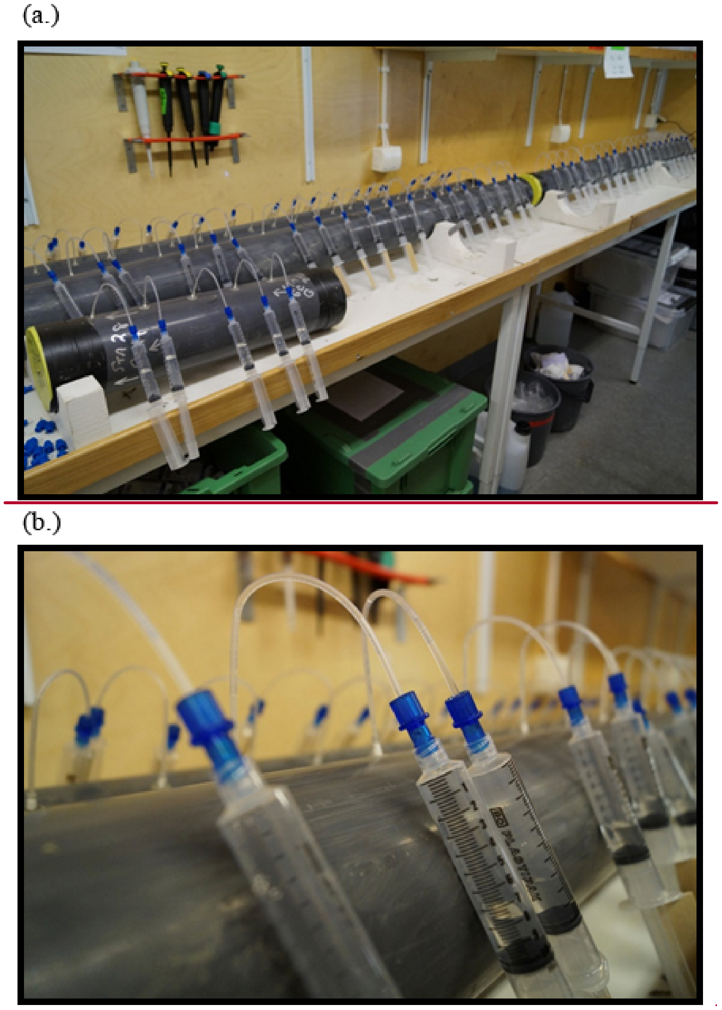

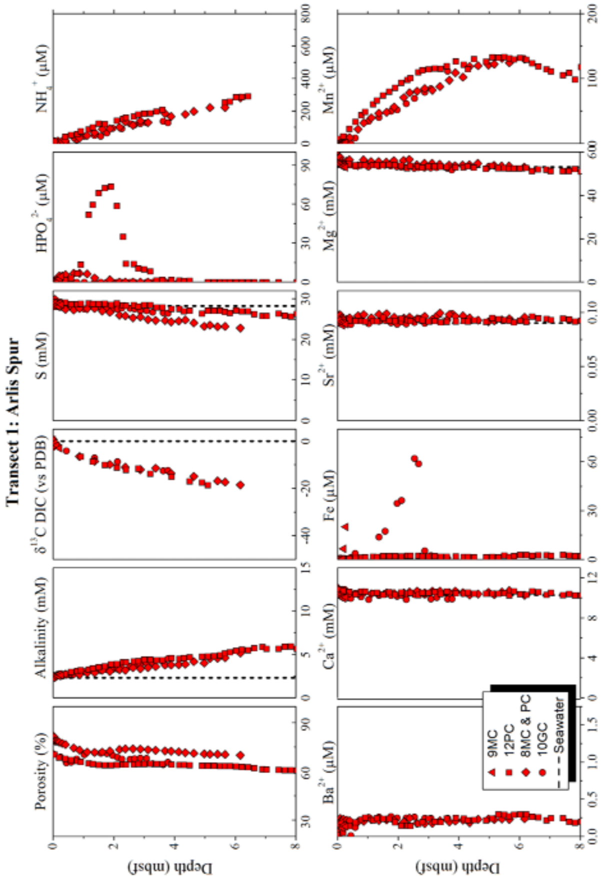
Transect 1: Arlis Spur
Porosity (%)
Alkalinity (mM)
δ13C DIC (vs PDB)
S (mM)
HPO4 2- (μM)
NH4 + (μM)
Ba2+ (μM)
Ca2+ (mM)
Fe (μM)
Sr2+ (mM)
Mg2+ (mM)
Mn2+ (μM)
Depth (mbsf)
9MC
12PC
8MC & PC
10GC
Seawater

Figure 5.

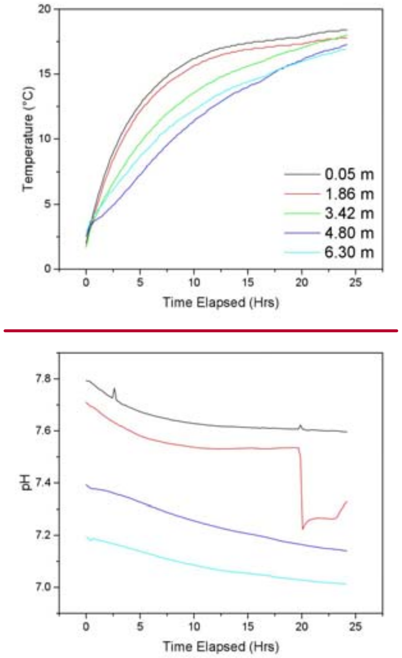
20
15
10
5
0
Temperature (°C)
0
5
10
15
20
25
Time Elapsed (Hrs)
0.05 m
1.86 m
3.42 m
4.80 m
6.30 m
7.8
7.6
7.4
7.2
7.0
pH
0
5
10
15
20
25
Time Elapsed (Hrs)

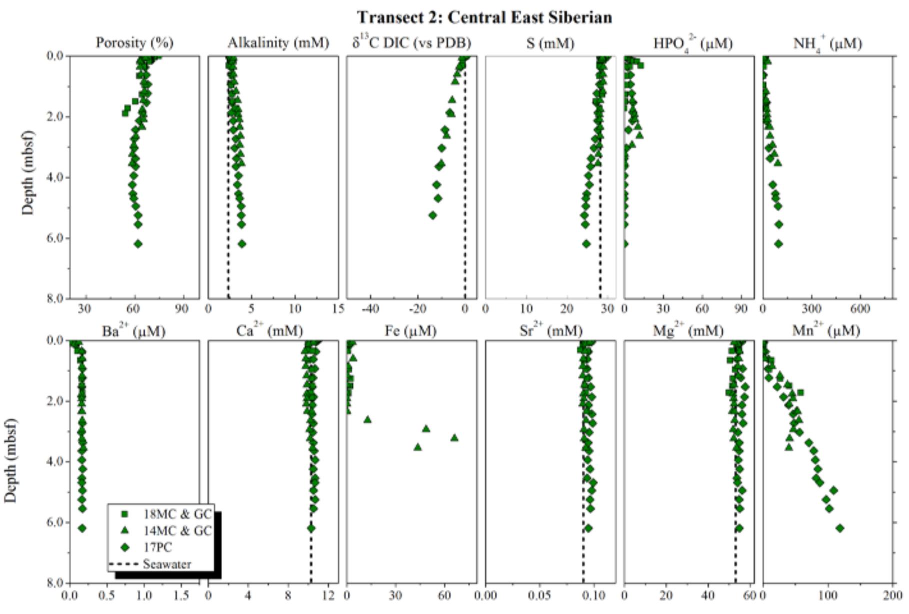
Transect 2: Central East Siberian
Porosity (%)
Alkalinity (mM)
δ^{13}C DIC (vs PDB)
S (mM)
HPO$_4^{2-}$ (μM)
NH$_4^+$ (μM)
Ba^{2+} (μM)
Ca^{2+} (mM)
Fe (μM)
Sr^{2+} (mM)
Mg^{2+} (mM)
Mn^{2+} (μM)
Depth (mbsf)
0.0
2.0
4.0
6.0
8.0
30
60
90
0
5
10
15
-40
-20
0
10
20
30
300
600
0.5
1.0
1.5
4
8
12
0.00
0.05
0.10
40
100
200
18MC & GC
14MC & GC
17PC
Seawater

Figure 6.

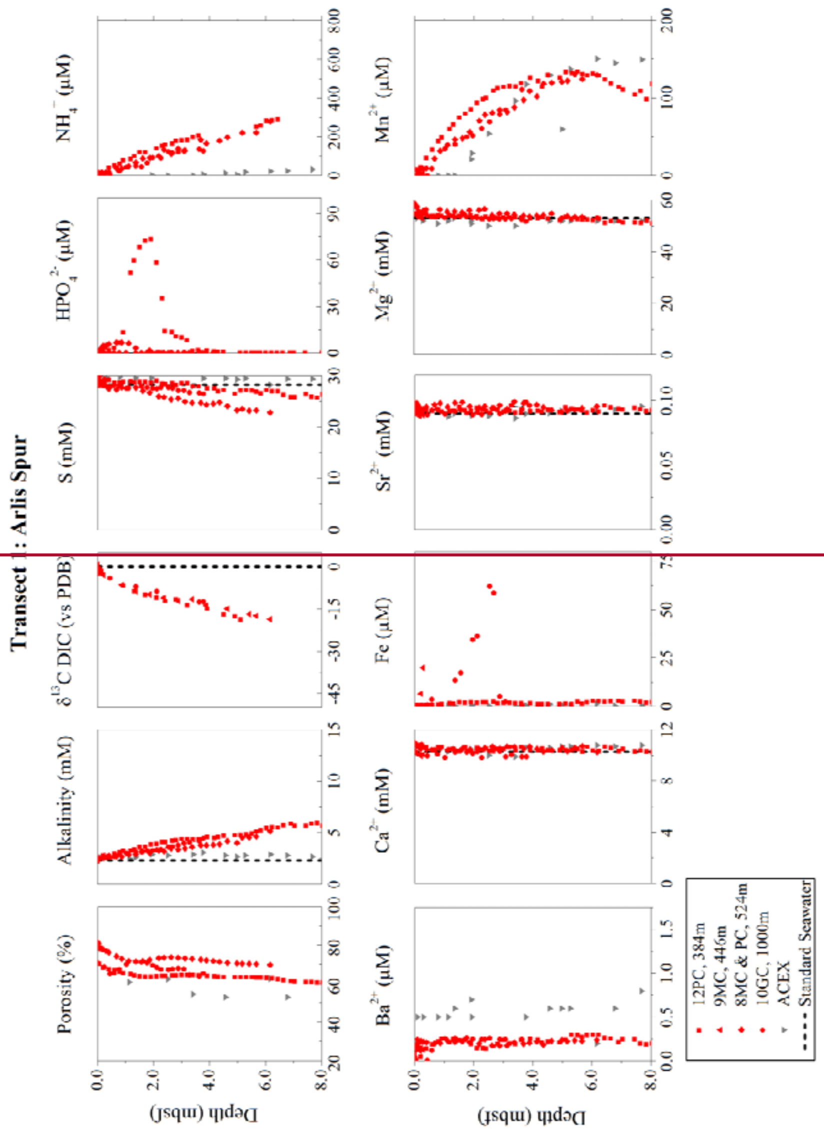
Transect 1: Arlis Spur
Porosity (%)
20 40 60 80 100
Alkalinity (mM)
0 5 10 15
δ13C DIC (vs PDB)
-45 -30 -15 0
S (mM)
0 10 20 30
HPO4 2- (μM)
0 30 60 90
NH4 + (μM)
0 200 400 600 800
Depth (mbsf)
0.0 2.0 4.0 6.0 8.0
Ba2+ (μM)
0.0 0.5 1.0 1.5
Ca2+ (mM)
0 4 8 12
Fe (μM)
0 25 50 75
Sr2+ (mM)
0.00 0.05 0.10
Mg2+ (mM)
0 20 40 60
Mn2+ (μM)
0 100 200
12PC, 384m
9MC, 446m
8MC & PC, 524m
10GC, 1000m
ACEX
Standard Seawater

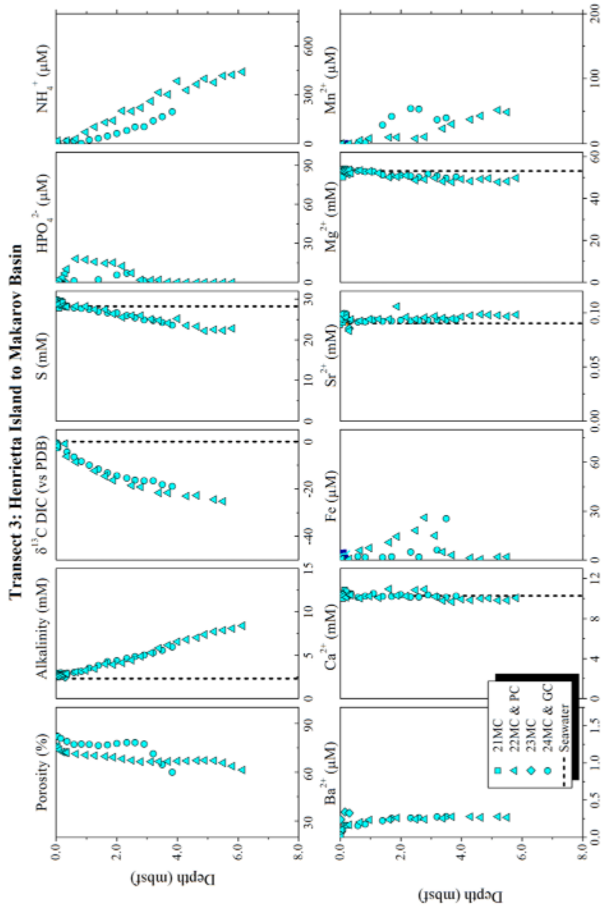
Transect 3: Henrietta Island to Makarov Basin
Porosity (%)
Alkalinity (mM)
δ13C DIC (vs PDB)
S (mM)
HPO4 2- (μM)
NH4 + (μM)
Ba2+ (μM)
Ca2+ (mM)
Fe (μM)
Sr2+ (mM)
Mg2+ (mM)
Mn2+ (μM)
Depth (mbsf)
21MC
22MC & PC
23MC
24MC & GC
Seawater

Figure 7.

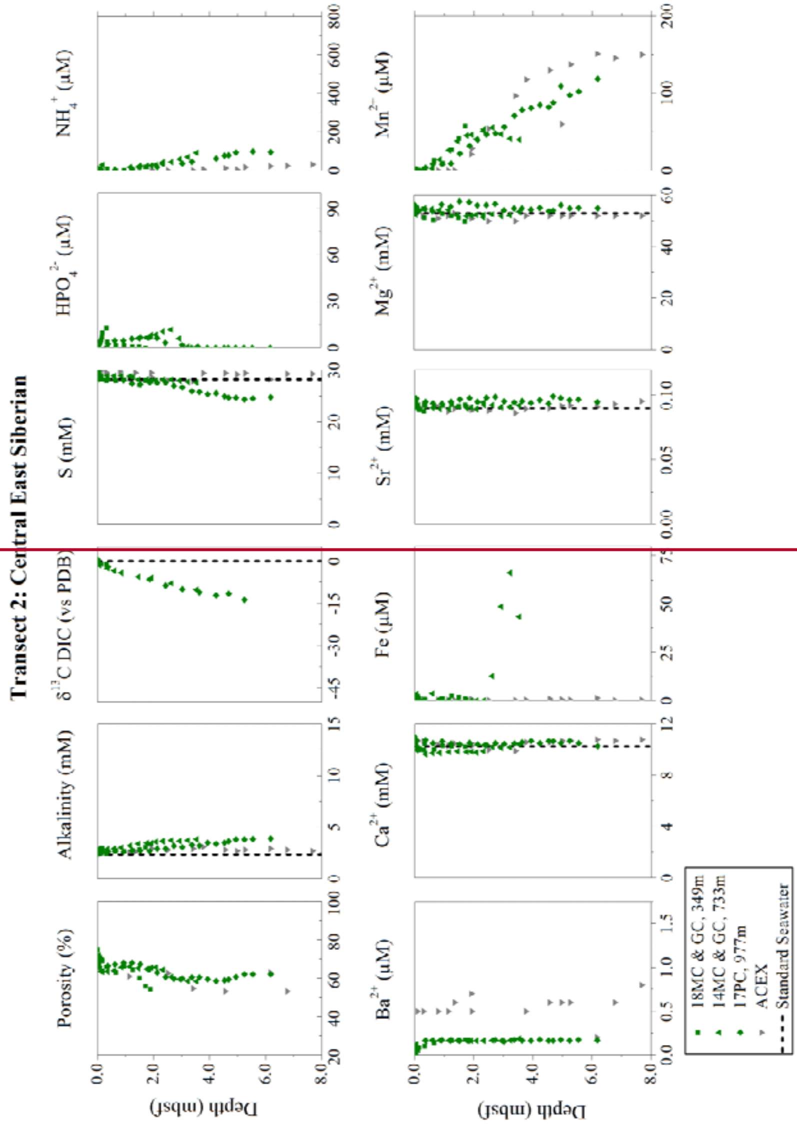
Transect 2: Central East Siberian
Porosity (%)
Alkalinity (mM)
δ13C DIC (vs PDB)
S (mM)
HPO4 2- (µM)
NH4 + (µM)
Ba2+ (µM)
Ca2+ (mM)
Fe (µM)
Sr2+ (mM)
Mg2+ (mM)
Mn2+ (µM)
Depth (mbsf)
Depth (mbsf)
0.0
2.0
4.0
6.0
8.0
20 40 60 80 100
0 5 10 15
-45 -30 -15 0
0 10 20 30
0 30 60 90
0 200 400 600 800
0.0 0.5 1.0 1.5
0 4 8 12
0 25 50 75
0.00 0.05 0.10
0 20 40 60
0 100 200
18MC & GC, 349m
14MC & GC, 733m
17PC, 977m
ACEX
Standard Seawater

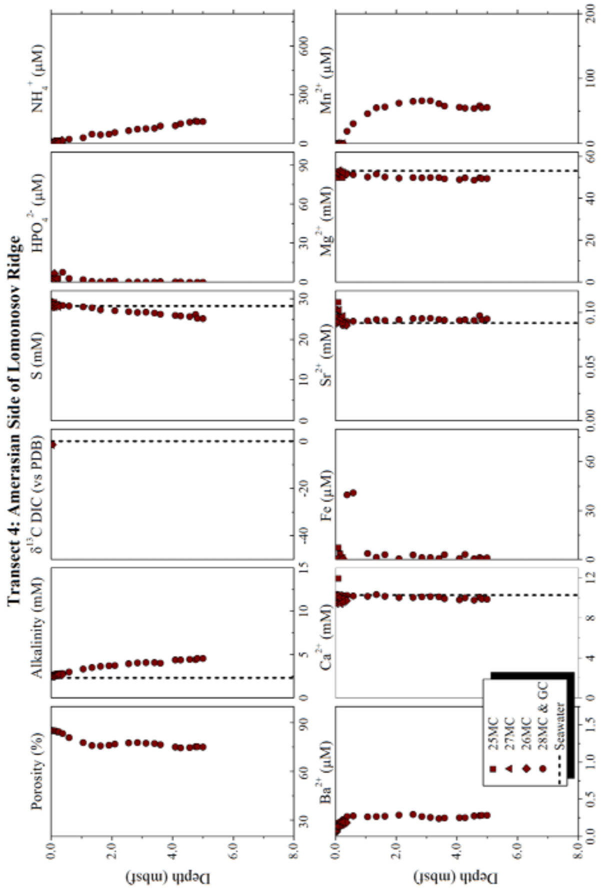
Transect 4: Amerasian Side of Lomonosov Ridge

Figure 8.

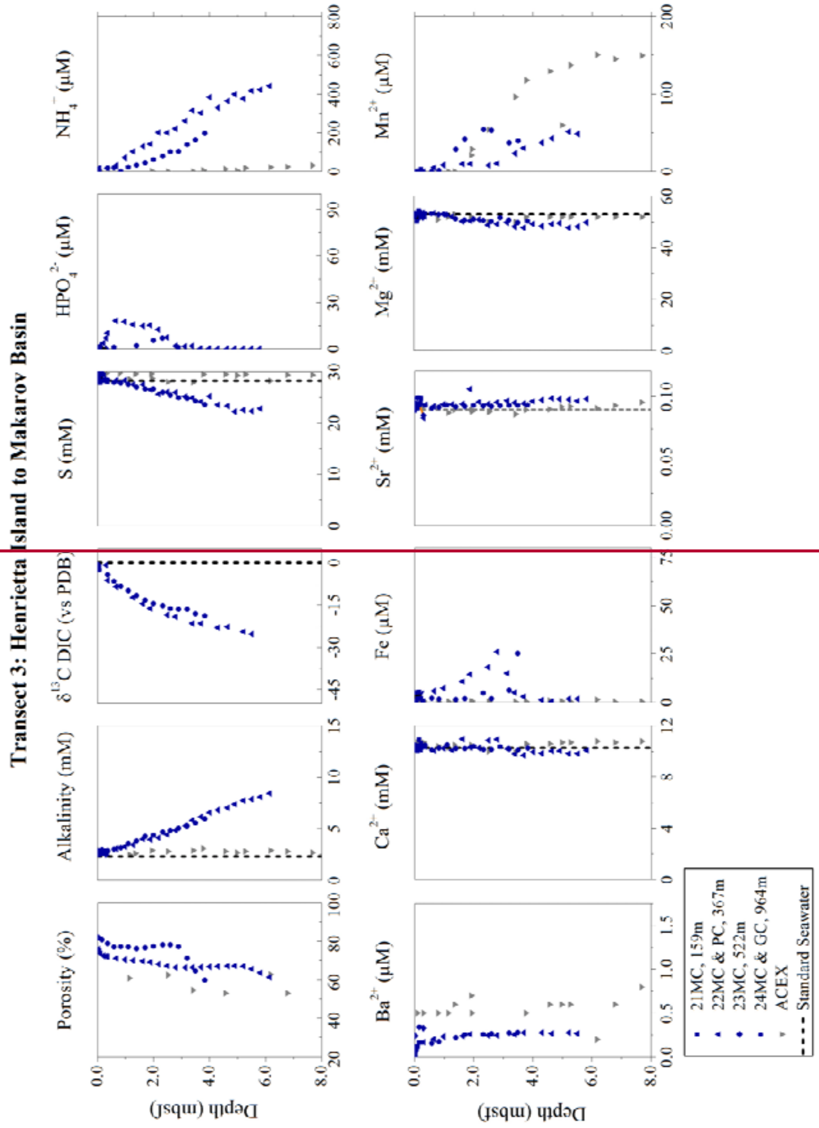
Transect 3: Henrietta Island to Makarov Basin
Porosity (%)
Alkalinity (mM)
δ13C DIC (vs PDB)
S (mM)
HPO4 2- (μM)
NH4 + (μM)
Ba2+ (μM)
Ca2+ (mM)
Fe (μM)
Sr2+ (mM)
Mg2+ (mM)
Mn2+ (μM)
Depth (mbsf)
21MC, 159m
22MC & PC, 367m
23MC, 522m
24MC & GC, 964m
ACEX
Standard Seawater

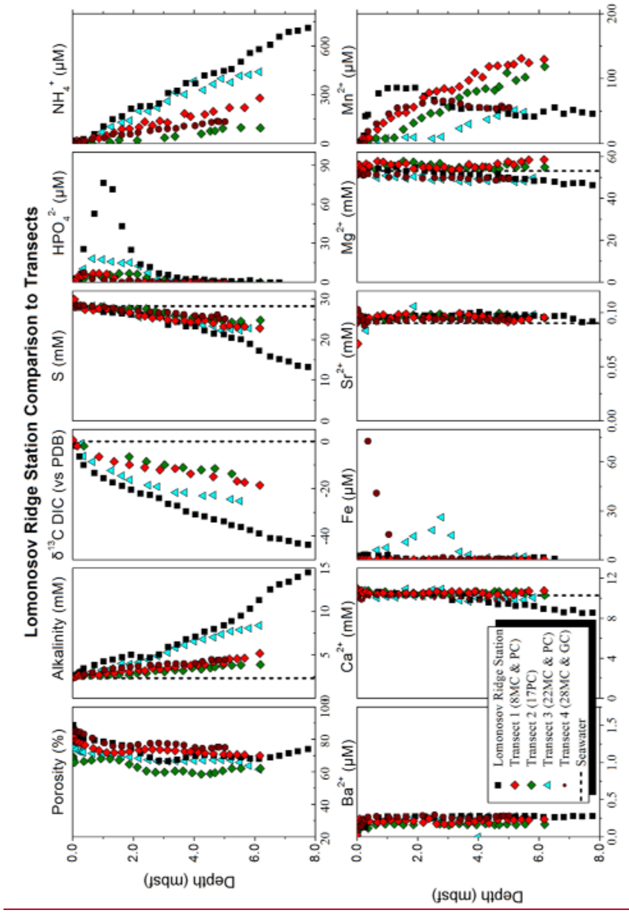
Lomonosov Ridge Station Comparison to Transects
Porosity (%)
Alkalinity (mM)
δ13C DIC (vs PDB)
S (mM)
HPO4 2- (µM)
NH4 + (µM)
Ba2+ (µM)
Ca2+ (mM)
Fe (µM)
Sr2+ (mM)
Mg2+ (mM)
Mn2+ (µM)
Depth (mbsf)
Lomonosov Ridge Station
Transect 1 (8MC & PC)
Transect 2 (17PC)
Transect 3 (22MC & PC)
Transect 4 (28MC & GC)
Seawater

Figure 9.

Transect 4: Amerasian Side of Lomonosov Ridge

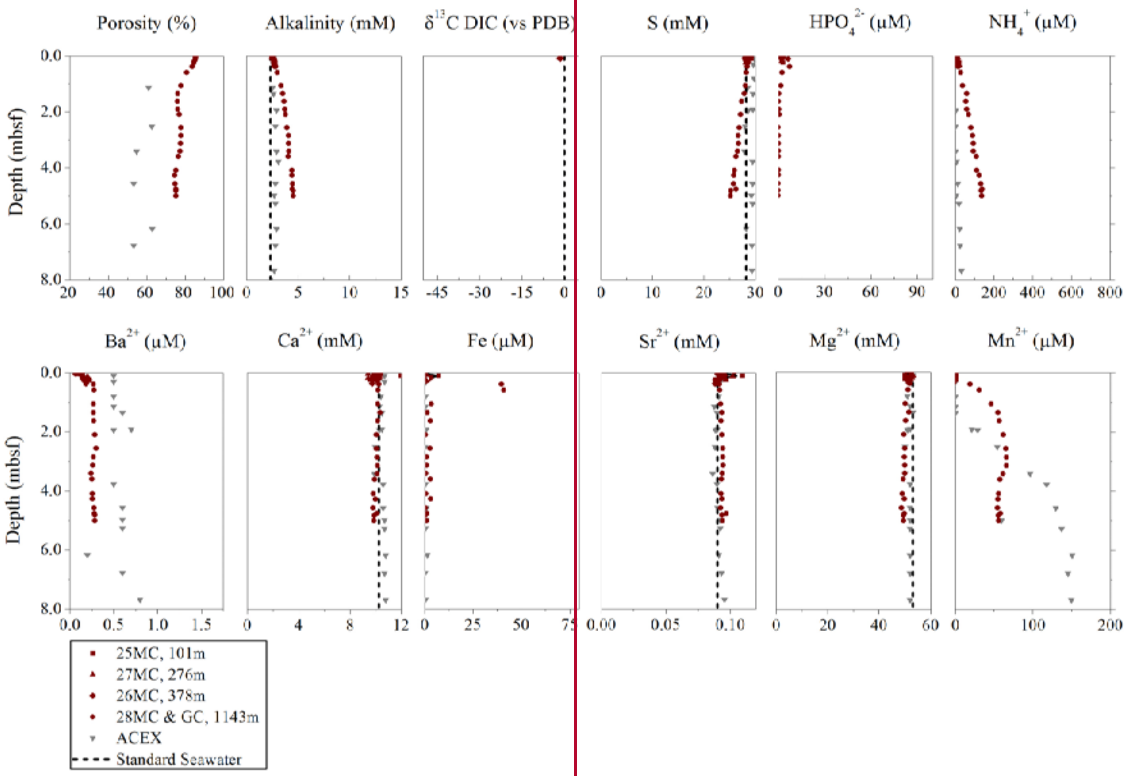

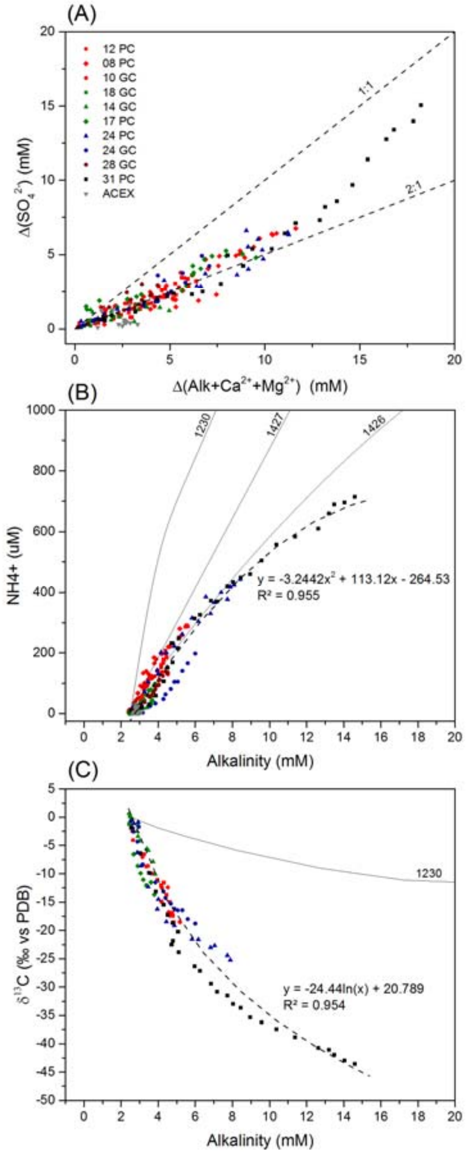
(A)
12 PC
08 PC
10 GC
18 GC
14 GC
17 PC
24 PC
24 GC
28 GC
31 PC
ACEX
1:1
2:1
Δ(SO$_4^{2-}$) (mM)
Δ(Alk+Ca^{2+}+Mg^{2+}) (mM)
(B)
1230
1427
1426
NH4+ (uM)
y = -3.2442x^2 + 113.12x - 264.53
R² = 0.955
Alkalinity (mM)
(C)
1230
δ^{13}C (‰ vs PDB)
y = -24.44ln(x) + 20.789
R² = 0.954
Alkalinity (mM)

Figure 10.

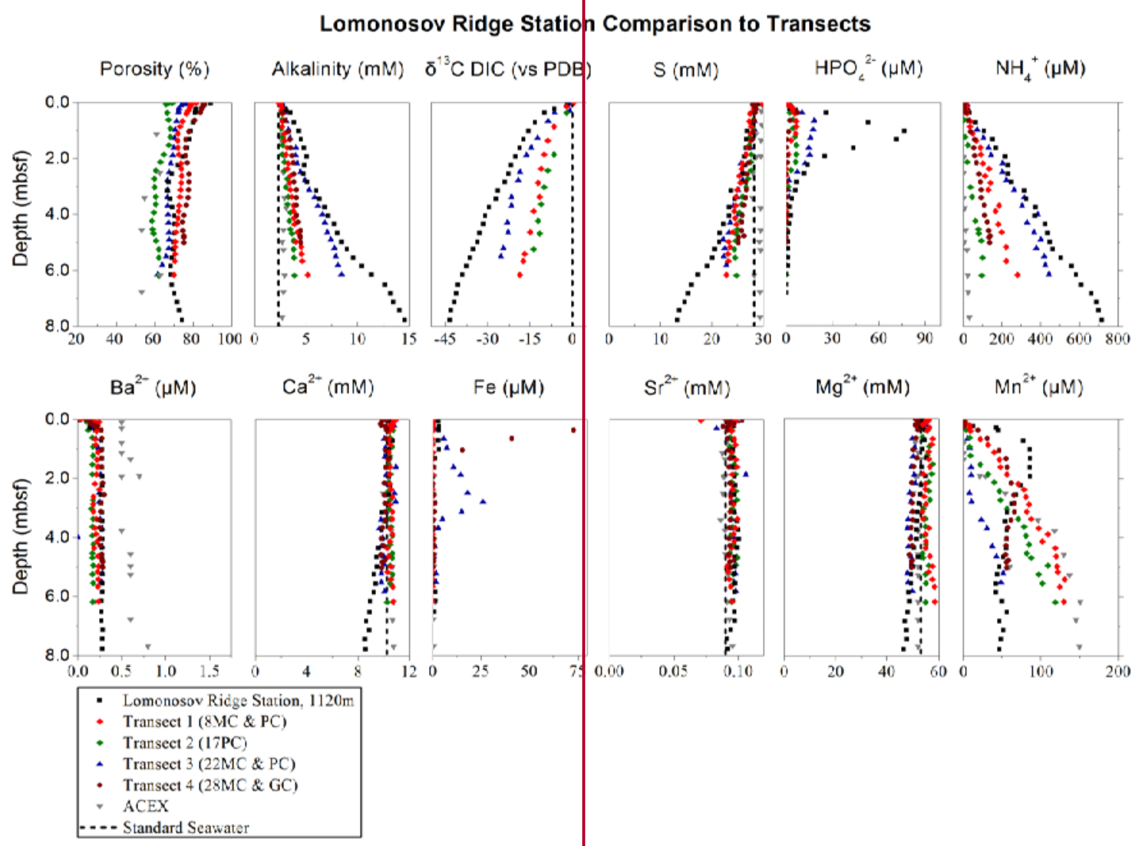
Lomonosov Ridge Station Comparison to Transects
Porosity (%)
Alkalinity (mM)
δ13C DIC (vs PDB)
S (mM)
HPO42- (μM)
NH4+ (μM)
Ba2- (μM)
Ca2+ (mM)
Fe (μM)
Sr2- (mM)
Mg2+ (mM)
Mn2+ (μM)
Depth (mbsf)
0.0
2.0
4.0
6.0
8.0
20 40 60 80 100
0 5 10 15
-45 -30 -15 0
0 10 20 30
0 30 60 90
0 200 400 600 800
0.0 0.5 1.0 1.5
0 4 8 12
0 25 50 75
0.00 0.05 0.10
0 20 40 60
0 100 200
Lomonosov Ridge Station, 1120m
Transect 1 (8MC & PC)
Transect 2 (17PC)
Transect 3 (22MC & PC)
Transect 4 (28MC & GC)
ACEX
Standard Seawater

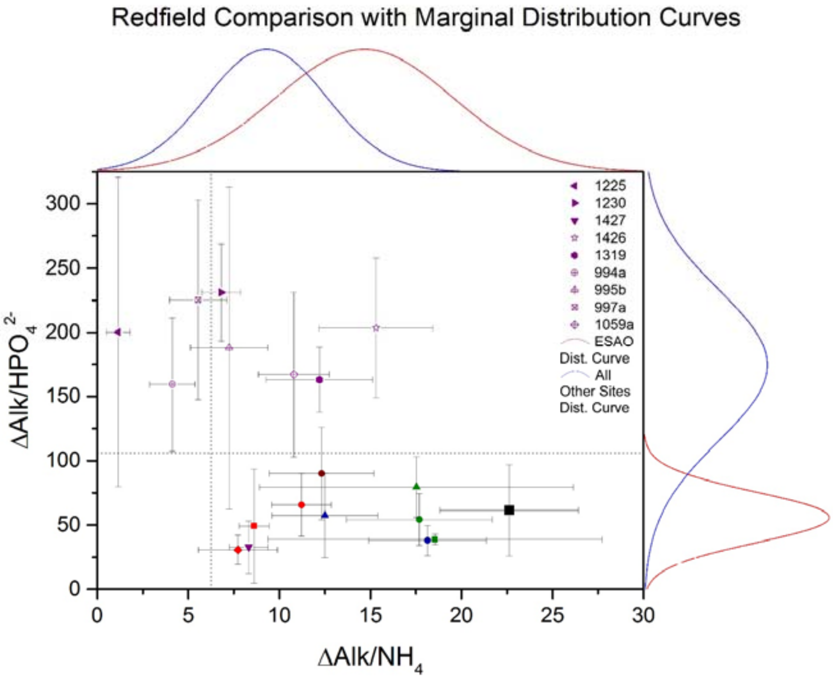
Redfield Comparison with Marginal Distribution Curves
ΔAlk/HPO$_4^{2-}$
ΔAlk/NH$_4$
0
50
100
150
200
250
300
0
5
10
15
20
25
30
1225
1230
1427
1426
1319
994a
995b
997a
1059a
ESAO Dist. Curve
All Other Sites Dist. Curve

Figure 11.

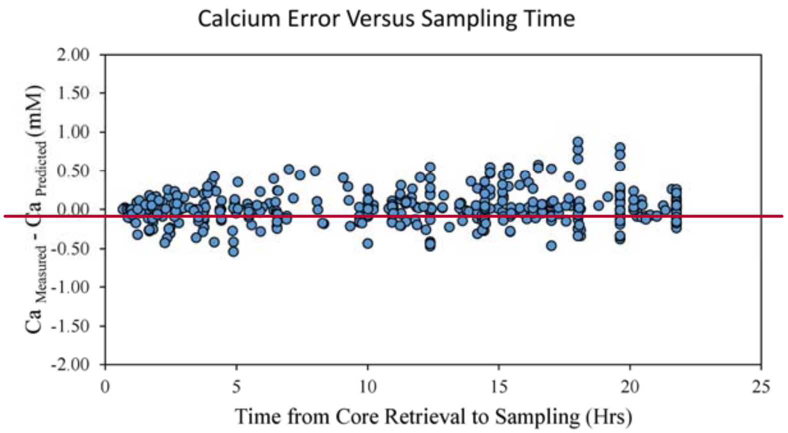
Calcium Error Versus Sampling Time
2.00
1.50
1.00
0.50
0.00
-0.50
-1.00
-1.50
-2.00
Ca Measured - Ca Predicted (mM)
0
5
10
15
20
25
Time from Core Retrieval to Sampling (Hrs)

~~Figure 12.~~

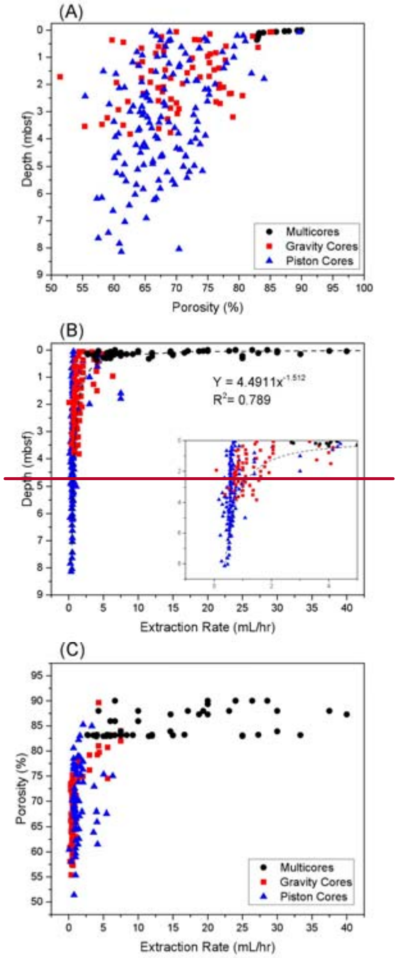
(A)
Depth (mbsf)
0
1
2
3
4
5
6
7
8
9
50
55
60
65
70
75
80
85
90
95
100
Porosity (%)
● Multicores
■ Gravity Cores
▲ Piston Cores
(B)
Depth (mbsf)
Y = 4.4911x^-1.512
R²= 0.789
0
5
10
15
20
25
30
35
40
Extraction Rate (mL/hr)
(C)
Porosity (%)
95
90
85
80
75
70
65
60
55
50
Extraction Rate (mL/hr)
● Multicores
■ Gravity Cores
▲ Piston Cores

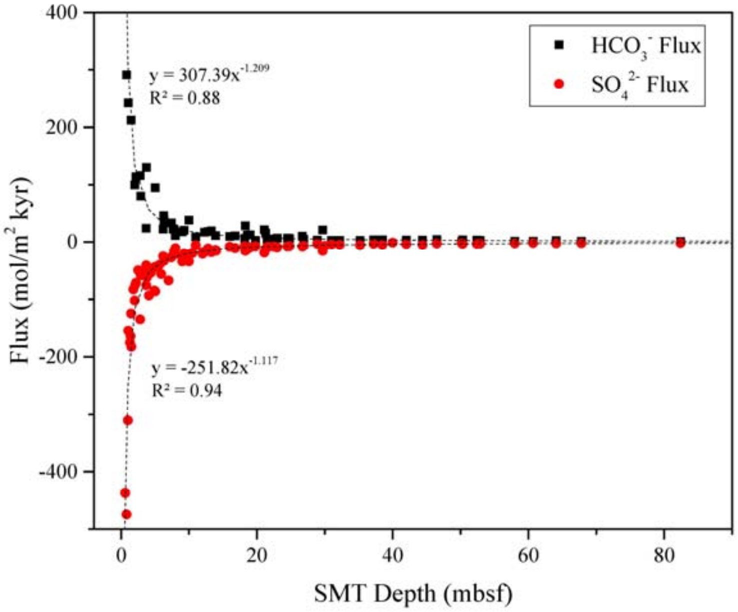
400
200
0
-200
-400
Flux (mol/m^2 kyr)
0
20
40
60
80
SMT Depth (mbsf)
HCO_3^- Flux
SO_4^{2-} Flux
y = 307.39x$^{-1.209}$
R² = 0.88
y = -251.82x$^{-1.117}$
R² = 0.94

~~Figure 13.~~

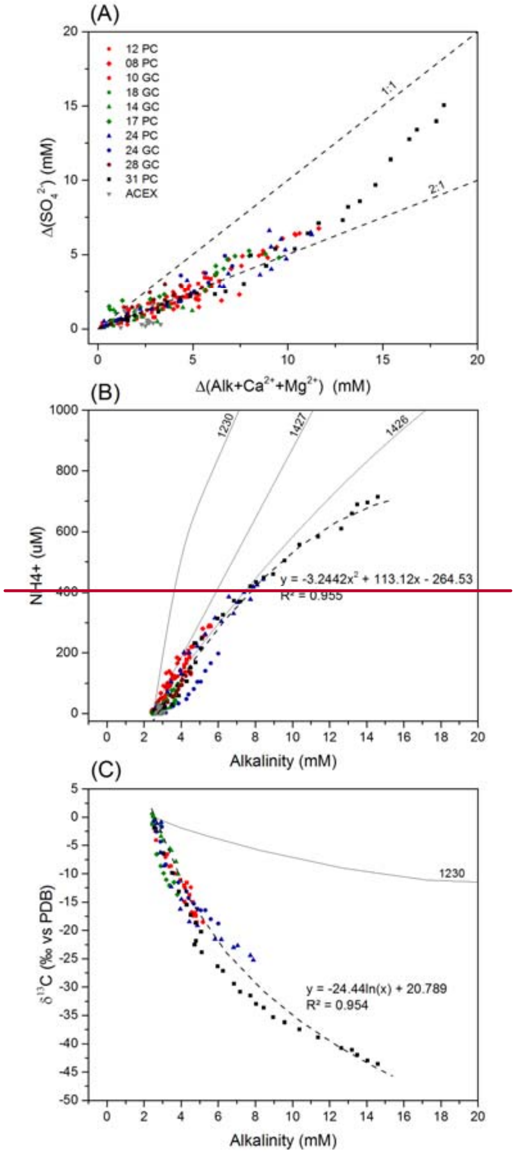
(A)
12 PC
08 PC
10 GC
18 GC
14 GC
17 PC
24 PC
24 GC
28 GC
31 PC
ACEX
1:1
2:1
$\Delta(SO_4^{2-})$ (mM)
$\Delta(Alk+Ca^{2+}+Mg^{2+})$ (mM)
0
5
10
15
20
(B)
1230
1427
1426
$y = -3.2442x^2 + 113.12x - 264.53$
$R^2 = 0.955$
NH4+ (uM)
Alkalinity (mM)
0
200
400
600
800
1000
(C)
1230
$y = -24.44\ln(x) + 20.789$
$R^2 = 0.954$
$\delta^{13}C$ (‰ vs PDB)
Alkalinity (mM)
5
0
-5
-10
-15
-20
-25
-30
-35
-40
-45
-50
2
4
6
8
12
14
16
18

~~**Figure 14.**~~

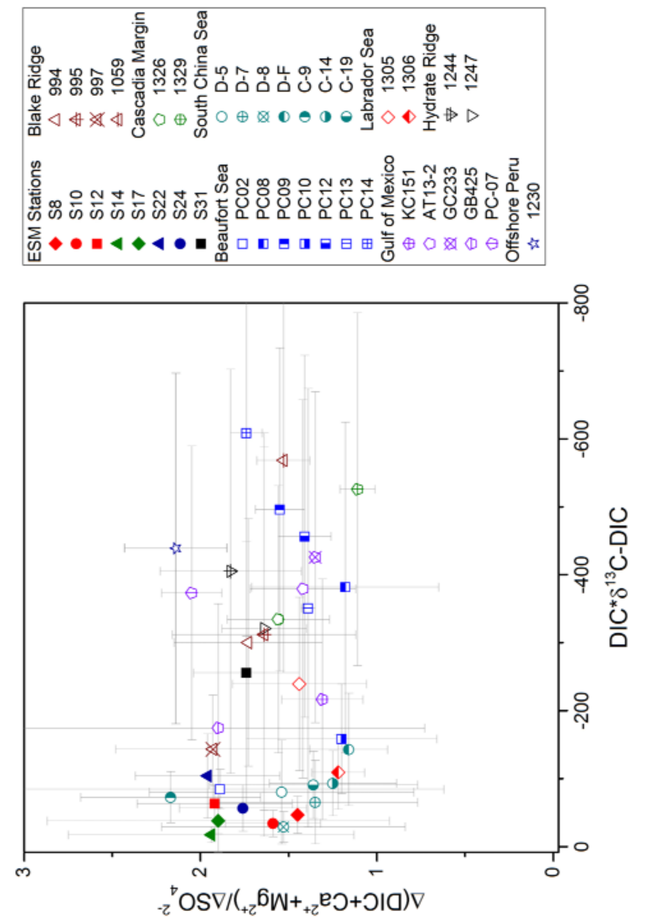
Δ(DIC+Ca2++Mg2+)/ΔSO42-
3
2
1
0
DIC*δ13C-DIC
0
-200
-400
-600
-800
ESM Stations
◆ S8
● S10
■ S12
▲ S14
◆ S17
▲ S22
● S24
■ S31
Beaufort Sea
□ PC02
◧ PC08
⬒ PC09
◧ PC10
⬓ PC12
⊟ PC13
⊞ PC14
Gulf of Mexico
⊕ KC151
⬡ AT13-2
⊠ GC233
⬡ GB425
⬡ PC-07
Offshore Peru
☆ 1230
Blake Ridge
△ 994
△ 995
⊠ 997
△ 1059
Cascadia Margin
⬡ 1326
⊕ 1329
South China Sea
○ D-5
⊕ D-7
⊗ D-8
◐ D-F
◒ C-9
◑ C-14
◓ C-19
Labrador Sea
◇ 1305
◆ 1306
Hydrate Ridge
▽ 1244
▽ 1247

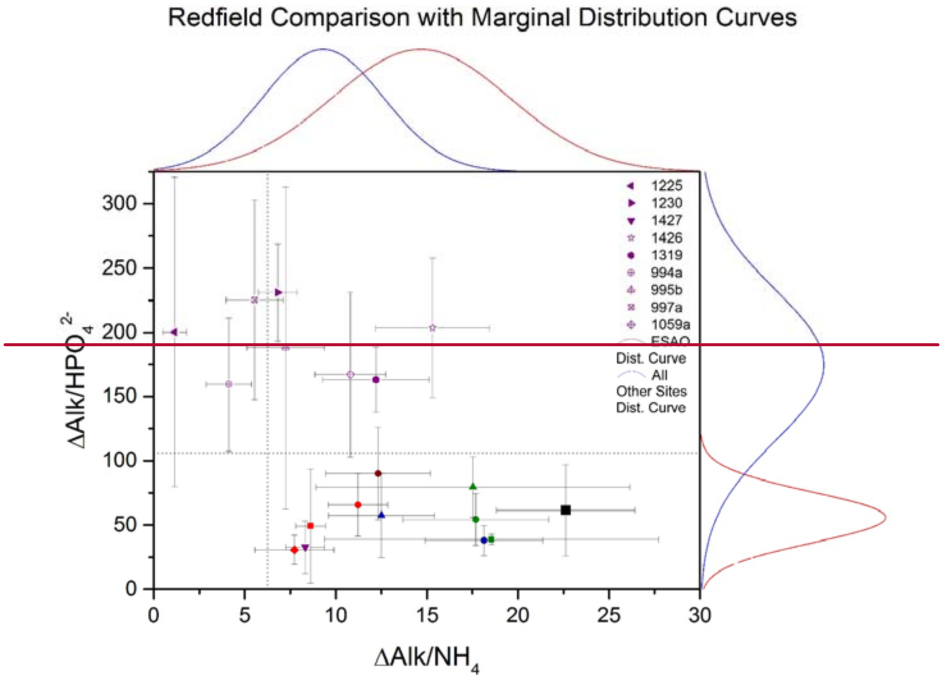
Redfield Comparison with Marginal Distribution Curves
1225
1230
1427
1426
1319
994a
995b
997a
1059a
ESAO Dist. Curve
All Other Sites Dist. Curve
ΔAlk/HPO$_4^{2-}$
0
50
100
150
200
250
300
ΔAlk/NH$_4$
0
5
10
15
20
25
30

~~Figure 15.~~

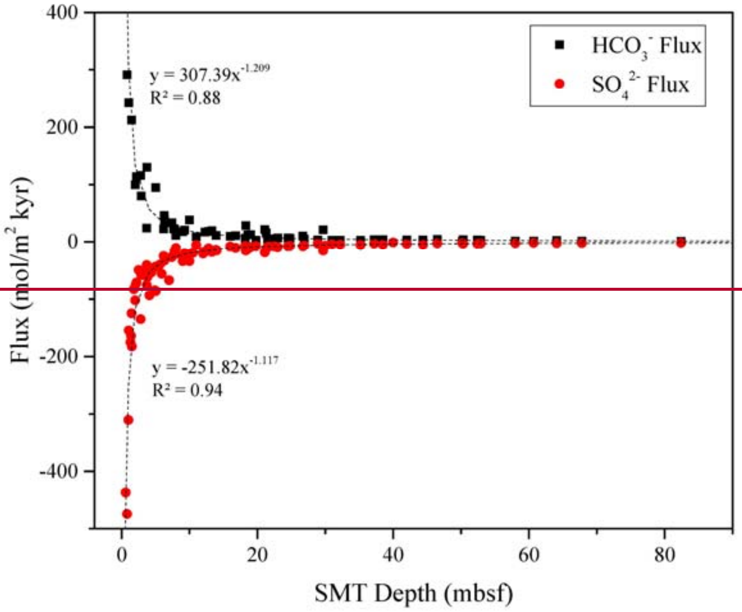

400
200
0
-200
-400
Flux (mol/m² kyr)
0
20
40
60
80
SMT Depth (mbsf)
HCO3- Flux
SO4 2- Flux
y = 307.39x-1.209
R² = 0.88
y = -251.82x-1.117
R² = 0.94

~~**Figure 16.**~~

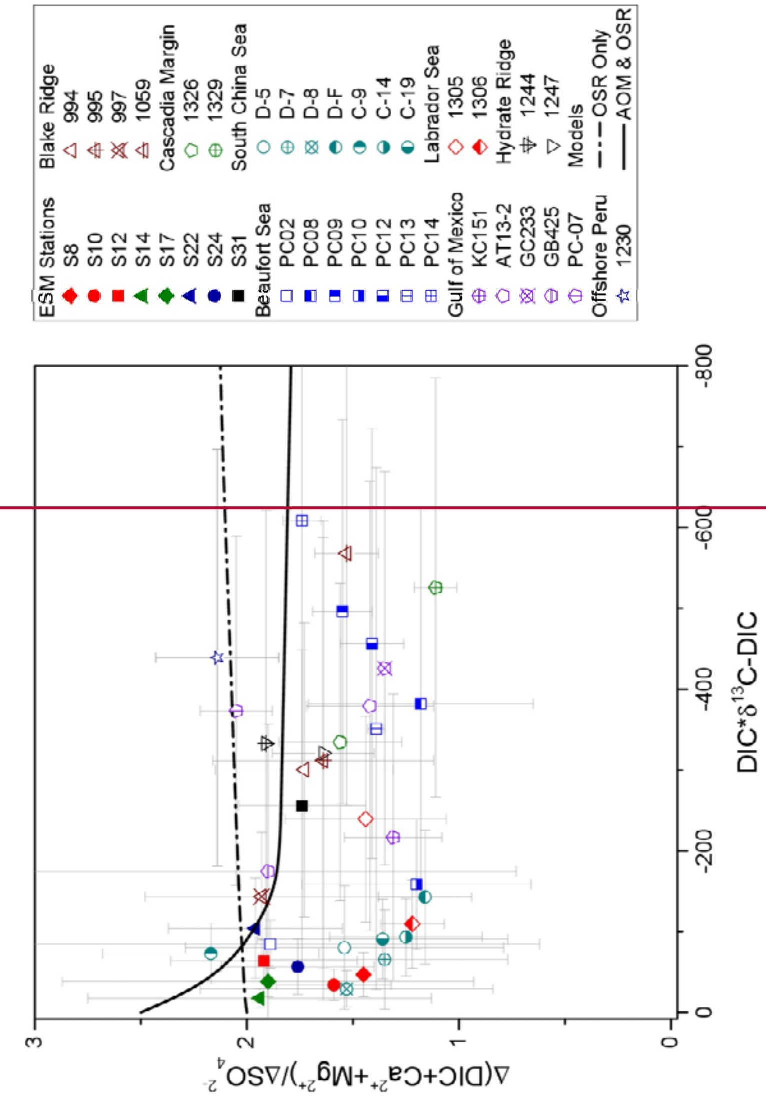

Δ(DIC+Ca^{2+}+Mg^{2+})/ΔSO$_4^{2-}$
DIC*δ^{13}C-DIC
0
1
2
3
0
-200
-400
-600
-800
ESM Stations
S8
S10
S12
S14
S17
S22
S24
S31
Beaufort Sea
PC02
PC08
PC09
PC10
PC12
PC13
PC14
Gulf of Mexico
KC151
AT13-2
GC233
GB425
PC-07
Offshore Peru
1230
Blake Ridge
994
995
997
1059
Cascadia Margin
1326
1329
South China Sea
D-5
D-7
D-8
D-F
C-9
C-14
C-19
Labrador Sea
1305
1306
Hydrate Ridge
1244
1247
Models
OSR Only
AOM & OSR

Table 1 Rhizon Efficacy

Station	Location		Water Depth	Core Type	Core Length	Total Time from Coring to Sampling		Rhizon Extraction Time	
	Lattitude	Longitude	(m)		(m)	Average (hrs)	Range (hrs)	Average (hrs)	Range (hrs)
8	75° 09' 11.4912" N	179° 52' 23.0952" E	524	MC	0.16	0.92	(0.57 - 1.15)	0.47	(0.08 - 1.21)
9	75° 03' 24.2166" N	179° 49' 13.497" W	446	MC	0.29	1.13	(0.87 - 1.26)	0.91	(0.19 - 1.47)
13	76° 11' 10.7772" N	179° 16' 42.102" W	1118	MC	0.17	1.40	(1.20 - 1.68)	0.40	(0.20 - 0.68)
14	76° 21' 10.3926" N	176° 27' 39.9954" E	733	MC	0.20	2.51	(0.83 - 4.42)	1.76	(0.08 - 3.67)
16	76° 30' 43.2540" N	176° 37' 55.1670" E	1023	MC	0.21	2.81	(1.87 - 3.70)	1.44	(0.51 - 2.33)
18	76° 24' 32.8680" N	173° 52' 44.9178" E	349	MC	0.33	2.11	(1.32 - 2.68)	1.21	(0.42 - 1.78)
21	77° 34' 56.4918" N	163° 17' 36.7326" E	159	MC	0.24	4.02	(3.45 - 4.37)	0.73	(0.17 - 1.08)
22	78° 13' 25.9572" N	164° 25' 36.3612" E	367	MC	0.32	0.73	(0.68 - 0.75)	0.38	(0.33 - 0.41)
23	78° 39' 51.7206" N	165° 01' 57.8352" E	522	MC	0.32	1.48	(0.67 - 1.93)	1.24	(0.35 - 1.85)
24	78° 48' 00.1080" N	165° 22' 55.8552" E	982	MC	0.32	1.79	(0.85 - 2.18)	1.34	(0.52 - 1.67)
25	79° 13' 34.6362" N	152° 40' 32.2284" E	101	MC	0.25	0.97	(0.83 - 1.17)	0.63	(0.51 - 0.83)
26	79° 44' 31.6782" N	154° 23' 20.3244" E	378	MC	0.37	1.83	(0.80 - 2.80)	1.53	(0.50 - 2.51)
27	79° 39' 52.6824" N	154° 07' 34.5324" E	276	MC	0.26	1.65	(1.35 - 2.18)	1.30	(1.01 - 1.83)
28	79° 55' 10.3584" N	154° 21' 12.7578" E	1145	MC	0.27	1.53	(0.85 - 2.27)	1.10	(0.42 - 1.83)
29	81° 20' 33.9750" N	141° 46' 31.6668" E	899	MC	0.23	1.55	(1.05 - 2.05)	1.17	(0.67 - 1.67)
31	79° 55' 13.4070" N	143° 09' 53.0994" E	1157	MC	0.39	2.38	(1.80 - 3.38)	2.08	(1.50 - 3.08)
32	85° 08' 28.2582" N	151° 35' 24.5220" E	837	MC	0.33	4.38	(2.38 - 5.05)	3.33	(1.33 - 4.01)
Multicore Average and Range					0.27	1.95	(0.57 - 5.05)	1.24	(0.08 - 4.01)
8	75° 08' 06.3342" N	179° 51' 05.9004" E	515	PC	6.42	18.56	(4.81 - 20.85)	15.22	(1.78 - 17.5)
10	75° 30' 12.6462" N	179° 05' 59.265" W	1000	GC	3.99	11.01	(3.38 - 12.38)	10.31	(1.83 - 11.83)
12	75° 00' 57.3114" N	179° 45' 09.9900" E	384	PC	8.43	21.44	(20.27 - 21.77)	17.95	(16.42 - 19.15)
14	76° 22' 04.9146" N	176° 25' 56.9670" E	737	GC	2.75	14.58	(6.55 - 17.11)	9.00	(5.22 - 10.01)
17	76° 27' 52.6248" N	176° 43' 25.7628" E	977	PC	6.37	19.62	(18.12 - 19.62)	16.58	(15.08 - 16.58)
18	76° 24' 41.7240" N	173° 47' 17.6454" E	351	GC	1.95	7.72	(3.02 - 14.37)	6.40	(1.73 - 12.92)
22	78° 13' 22.5336" N	164° 27' 42.6306" E	364	PC	6.45	19.79	(13.5 - 25.17)	17.71	(11.42 - 23.08)
24	78° 47' 48.9186" N	165° 21' 59.5080" E	964	GC	4.05	12.25	(10.94 - 14.19)	5.89	(4.83 - 7.42)
28	79° 55' 28.0302" N	154° 23' 44.7180" E	1143	GC	5.23	12.78	(3.33 - 14.33)	6.98	(5.58 - 16.63)
29	81° 17' 57.6816" N	141° 46' 57.1794" E	824	GC	4.66	17.43	(9.25 - 18.02)	13.38	(4.72 - 14.12)
31	79° 54' 53.4270" N	143° 14' 00.4488" E	1120	PC	8.07	11.95	(3.90 - 18.07)	9.25	(1.33 - 15.50)
33	84° 16' 29.5422" N	148° 44' 07.1484" E	886	GC	3.59	12.20	(9.57 - 19.07)	8.55	(5.92 - 15.42)
33	84° 16' 55.3368" N	148° 38' 48.3102" E	888	PC	6.24	11.06	(7.55 - 17.88)	9.48	(5.82 - 16.25)
Gravity/Piston Core Average and Range					5.25	14.65	(3.02 - 25.17)	11.28	(1.33 - 23.08)

Table 2 Rhizon Flow Rates

Station	Flow Rate (mL/hr)			Flow Rate Decrease per meter
	Average	Min	Max	(mL/hr/m)
8	25.28	8.33	37.50	243.06
9	11.36	5.16	26.82	59.21
13	23.68	14.63	33.33	70.36
14	8.31	0.55	24.00	130.30
16	8.31	0.55	24.00	79.37
18	10.77	3.93	26.40	70.23
21	13.00	2.77	40.00	201.71
22	26.82	25.00	30.00	18.52
23	13.52	5.41	28.57	77.22
24	9.51	6.00	19.35	49.46
25	16.24	12.00	20.00	36.36
26	8.85	4.00	20.00	49.23
27	8.09	5.45	10.00	21.65
28	11.80	5.45	24.00	74.18
29	10.36	6.00	16.50	58.33
31	5.16	3.24	6.67	10.07
32	5.21	3.75	11.25	23.44
Multicore Average	12.72	6.60	23.43	74.86
8	1.13	0.29	5.61	0.84
10	1.35	0.38	5.45	1.33
12	0.53	0.17	0.67	0.04
14	1.19	1.00	1.92	0.14
17	0.61	0.36	0.73	0.02
18	2.76	0.08	6.35	2.83
22	0.59	0.22	0.88	0.11
24	1.71	1.25	2.07	0.20
28	1.74	0.70	3.00	0.70
29	0.80	0.64	2.12	0.35
31	2.03	0.65	7.50	0.19
33	1.26	0.65	1.69	0.14
33	1.11	0.62	1.69	0.13
Gravity/Piston Core Average	1.29	0.54	3.05	0.54

Table 3 QA/QC Results

Analysis	Sample Type	Number	Result
Alkalinity	Spiked	15	PE = 1.53%
Alkalinity	Duplicate	8	PD = 1.30%
δ^{13}C-DIC	Seawater Standard	2	0.23‰ and 0.32‰
δ^{13}C-DIC	Blind Field Duplicate	4	PD = 22.98%
δ^{13}C-DIC	Field Blank	1	No Result
δ^{13}C-DIC	Duplicate	10	PD = 14.70%
Metals	Spiked	51	RSD = 2.55% (Ba), 2.17% (Ca), 1.53% (Fe), 0.77% (Mg), 1.73% (Mn), 1.88% (S), and 1.42% (Sr)
Metals	Blind Field Duplicate	11	PD = 2.56% (Ba), 3.77% (Ca), 5.81% (Fe), 2.68% (Mg), 3.07% (Mn), 0.71% (S), and 3.79% (Sr)
Metals	Field Blank	2	BDL
Phosphate	VKI Standard	2	PE = 1.28% and 2.69%
Ammonia	VKI Standard	2	PE = 2.40% and 6.25%

Notes:
PE = Percent Error
PD = Percent Difference
RSD = Relative Standard Deviation
BDL = Below Detection Limit

Table 1 QA/QC Results

Analysis	Sample Type	Number	Result
Alkalinity	Spiked	15	PE = 1.53%
Alkalinity	Duplicate	8	PD = 1.30%
δ^{13}C-DIC	Seawater Standard	2	0.23‰ and 0.32‰
δ^{13}C-DIC	Blind Field Duplicate	4	PD = 22.98%
δ^{13}C-DIC	Field Blank	1	No Result
δ^{13}C-DIC	Duplicate	10	PD = 14.70%
Metals	Spiked	51	RSD = 2.55% (Ba), 2.17% (Ca), 1.53% (Fe), 0.77% (Mg), 1.73% (Mn), 1.88% (S), and 1.42% (Sr)
Metals	Blind Field Duplicate	11	PD = 2.56% (Ba), 3.77% (Ca), 5.81% (Fe), 2.68% (Mg), 3.07% (Mn), 0.71% (S), and 3.79% (Sr)
Metals	Field Blank	2	BDL
Phosphate	VKI Standard	2	PE = 1.28% and 2.69%
Ammonia	VKI Standard	2	PE = 2.40% and 6.25%

Notes: PE = Percent Error
PD = Percent Difference
RSD = Relative Standard Deviation
BDL = Below Detection Limit

~~Table 4 - Reported and Calculated Fluxes~~

Formatted Table

~~Ocean~~	~~Location~~	~~Water Depth (m)~~	~~SMT Depth (mbsf)~~	~~SO_4^{2-} Flux (mol/m^{2}kyr)~~	~~Alkalinity Flux (mol/m^{2}kyr)~~	~~δ^{13}C at SMT (‰)~~
~~Arctic~~	~~Beaufort Sea – Cape Halkett[a,b]~~	~~280~~	~~1.06~~	~~-154.8~~	~~242.6~~	~~-21.5~~
~~Arctic~~	~~Beaufort Sea – Cape Halkett[a,b]~~	~~342~~	~~1.47~~	~~-124.7~~	~~212.3~~	~~-20.2~~
~~Arctic~~	~~Beaufort Sea – Cape Halkett[a,b]~~	~~1005~~	~~3.73~~	~~-44.2~~	~~130.3~~	~~-18.2~~
~~Arctic~~	~~Beaufort Sea – Cape Halkett[a,b]~~	~~1458~~	~~6.29~~	~~-27.4~~	~~46.3~~	~~-19.7~~
~~Arctic~~	~~East Siberian Slope~~	~~349~~	~~61~~	~~-1.8~~	~~1.7~~	~~–~~
~~Arctic~~	~~East Siberian Slope~~	~~367~~	~~25~~	~~-6.9~~	~~6.3~~	~~–~~
~~Arctic~~	~~East Siberian Slope~~	~~384~~	~~64~~	~~-2.4~~	~~2.3~~	~~–~~
~~Arctic~~	~~East Siberian Slope~~	~~524~~	~~35~~	~~-5.6~~	~~2.8~~	~~–~~
~~Arctic~~	~~East Siberian Slope~~	~~733~~	~~58~~	~~-2.1~~	~~1.5~~	~~–~~
~~Arctic~~	~~East Siberian Slope~~	~~977~~	~~58~~	~~-2.1~~	~~1.6~~	~~–~~
~~Arctic~~	~~East Siberian Slope~~	~~964~~	~~23~~	~~-9.2~~	~~6.8~~	~~–~~
~~Arctic~~	~~East Siberian Slope~~	~~1000~~	~~52~~	~~-3.3~~	~~3.3~~	~~–~~
~~Arctic~~	~~East Siberian Slope~~	~~1143~~	~~44~~	~~-5.1~~	~~3.5~~	~~–~~
~~Arctic~~	~~East Siberian Slope~~	~~1120~~	~~14~~	~~-13.9~~	~~11.3~~	~~–~~
~~Atlantic~~	~~New Jersey Continental Slope[q,i]~~	~~912~~	~~28.9~~	~~-3.3~~	~~3.6‡~~	~~–~~
~~Atlantic~~	~~Blake Ridge[q,p]~~	~~1293~~	~~50.3~~	~~-3.4~~	~~3.8‡~~	~~–~~
~~Atlantic~~	~~Blake Ridge[q,p]~~	~~1798~~	~~26.9~~	~~-6.6~~	~~4.9‡~~	~~–~~
~~Atlantic~~	~~Blake Ridge[q,x]~~	~~2567~~	~~42.0~~	~~-3.8~~	~~3.5‡~~	~~–~~
~~Atlantic~~	~~Blake Ridge[q,x]~~	~~2641~~	~~24.5~~	~~-7.6~~	~~6.9‡~~	~~–~~
~~Atlantic~~	~~Blake Ridge[q,x]~~	~~2777~~	~~21.7~~	~~-8.3~~	~~5.4‡~~	~~–~~
~~Atlantic~~	~~Blake Ridge[q,x]~~	~~2770~~	~~22.5~~	~~-7.8~~	~~4.7‡~~	~~–~~
~~Atlantic~~	~~Blake Ridge[q,x]~~	~~2798~~	~~21.5~~	~~-8.7~~	~~4.4‡~~	~~–~~
~~Atlantic~~	~~Blake Ridge[q,p]~~	~~2985~~	~~9.3~~	~~-20.0~~	~~20.4‡~~	~~–~~
~~Atlantic~~	~~Blake Ridge[q,p]~~	~~3481~~	~~12.3~~	~~-17.1~~	~~17.0‡~~	~~–~~
~~Atlantic~~	~~Blake Ridge[q,p]~~	~~4040~~	~~16.8~~	~~-10.5~~	~~10.8‡~~	~~–~~
~~Atlantic~~	~~Gulf of Mexico – Keathley Canyon[w]~~	~~1300~~	~~9~~	~~-33‡~~	~~17‡~~	~~-49.6~~
~~Atlantic~~	~~Gulf of Mexico – Atwater Valley[w]~~	~~1300~~	~~0.1~~	~~-2901~~	~~–~~	~~–~~
~~Atlantic~~	~~Gulf of Mexico – Atwater Valley[w]~~	~~1300~~	~~0.1~~	~~-2901~~	~~–~~	~~–~~
~~Atlantic~~	~~Gulf of Mexico – Atwater Valley[w]~~	~~1300~~	~~0.6~~	~~-437~~	~~–~~	~~–~~
~~Atlantic~~	~~Gulf of Mexico – Atwater Valley[w]~~	~~1300~~	~~7~~	~~-67~~	~~–~~	~~-46.3~~
~~Atlantic~~	~~Amazon Fan[q,v,y]~~	~~3191~~	~~37.2~~	~~-3.2~~	~~4.1‡~~	~~-39.8~~
~~Atlantic~~	~~Amazon Fan[q,v,y]~~	~~3474~~	~~6.2~~	~~-24.6~~	~~22.7‡~~	~~-47.5~~
~~Atlantic~~	~~Amazon Fan[q,v,y]~~	~~3704~~	~~3.7~~	~~-40.3~~	~~24.3‡~~	~~-49.6~~
~~Atlantic~~	~~Western Africa[q,z]~~	~~426~~	~~12.8~~	~~-12.5~~	~~18.2‡~~	~~–~~
~~Atlantic~~	~~Western Africa[q,z]~~	~~738~~	~~52.9~~	~~-3.1~~	~~2.9‡~~	~~–~~
~~Atlantic~~	~~Western Africa[q,z]~~	~~1280~~	~~21.3~~	~~-12.0~~	~~15.6‡~~	~~-19.8~~
~~Atlantic~~	~~Western Africa[q,z]~~	~~1402~~	~~18.3~~	~~-14.9~~	~~28.3‡~~	~~–~~
~~Atlantic~~	~~Western Africa[q,z]~~	~~1713~~	~~38.5~~	~~-5.1~~	~~4.1‡~~	~~–~~

~~Atlantic~~	~~Western Africa[q,z]~~	~~2179~~	~~26.7~~	~~-7.8~~	~~10.4[‡]~~	~~–~~
~~Atlantic~~	~~Western Africa[q,z]~~	~~2382~~	~~21.1~~	~~-18.1~~	~~21.8[‡]~~	~~–~~
~~Atlantic~~	~~Western Africa[q,z]~~	~~2995~~	~~29.7~~	~~-14.9~~	~~20.9[‡]~~	~~–~~
~~Atlantic~~	~~Argentine Basin[l]~~	~~1228~~	~~10.5~~	~~-19.1~~	~~–~~	~~–~~
~~Atlantic~~	~~Argentine Basin[l]~~	~~1492~~	~~12~~	~~-20.2~~	~~–~~	~~–~~
~~Atlantic~~	~~Argentine Basin[l]~~	~~1568~~	~~4.9~~	~~-84.6~~	~~–~~	~~–~~
~~Atlantic~~	~~Argentine Basin[l]~~	~~1789~~	~~5.9~~	~~-55.6~~	~~–~~	~~–~~
~~Atlantic~~	~~Argentine Basin[l]~~	~~3247~~	~~10~~	~~-21.8~~	~~–~~	~~–~~
~~Atlantic~~	~~Argentine Basin[l]~~	~~3167~~	~~14~~	~~-14.7~~	~~–~~	~~–~~
~~Atlantic~~	~~Argentine Basin[l]~~	~~3542~~	~~3.7~~	~~-75.4~~	~~–~~	~~–~~
~~Atlantic~~	~~Argentine Basin[l]~~	~~3551~~	~~5.6~~	~~-39.9~~	~~–~~	~~–~~
~~Atlantic~~	~~Argentine Basin[l]~~	~~3551~~	~~4.1~~	~~-93.3~~	~~–~~	~~–~~
~~Atlantic~~	~~Argentine Basin[l]~~	~~3623~~	~~5~~	~~-43.1~~	~~–~~	~~–~~
~~Atlantic~~	~~Argentine Basin[l]~~	~~4280~~	~~5.1~~	~~-43.5~~	~~–~~	~~–~~
~~Atlantic~~	~~Argentine Basin[l]~~	~~4799~~	~~12~~	~~-17.9~~	~~–~~	~~–~~
~~Indian~~	~~Oman[q,1]~~	~~591~~	~~50.2~~	~~-2.2~~	~~1.1[‡]~~	~~–~~
~~Indian~~	~~Oman[q,1]~~	~~804~~	~~46.5~~	~~-2.8~~	~~4.4[‡]~~	~~–~~
~~Indian~~	~~Oman[q,1]~~	~~1423~~	~~82.4~~	~~-1.8~~	~~0.8[‡]~~	~~–~~
~~Pacific~~	~~Bering Sea[p,2]~~	~~1008~~	~~6.3~~	~~-32.8~~	~~37.8~~	~~-25.1~~
~~Pacific~~	~~Cascadia[q,u,2]~~	~~959~~	~~9.0~~	~~-23.6~~	~~–~~	~~-23.8~~
~~Pacific~~	~~Cascadia[q,u,2]~~	~~1322~~	~~7.9~~	~~-21.3~~	~~–~~	~~-30.8~~
~~Pacific~~	~~Cascadia[q,u,2]~~	~~1828~~	~~2.5~~	~~-49.0~~	~~–~~	~~-33.9~~
~~Pacific~~	~~Cascadia - Hydrate Ridge[o]~~	~~834~~	~~8~~	~~-10.9~~	~~11.3~~	~~-19.6~~
~~Pacific~~	~~Cascadia - Hydrate Ridge[o]~~	~~850~~	~~7.65~~	~~-22.3~~	~~23.2~~	~~-30.2~~
~~Pacific~~	~~Cascadia - Hydrate Ridge[o]~~	~~871~~	~~7.4~~	~~-26.6~~	~~33.4~~	~~-24.9~~
~~Pacific~~	~~Cascadia - Hydrate Ridge[g]~~	~~896~~	~~7.8~~	~~-16~~	~~22~~	~~-22.5~~
~~Pacific~~	~~Umitaka Spur[h]~~	~~900~~	~~2.2~~	~~-71~~	~~114~~	~~–~~
~~Pacific~~	~~Umitaka Spur[h]~~	~~947~~	~~2.9~~	~~-58~~	~~80~~	~~–~~
~~Pacific~~	~~Umitaka Spur[h]~~	~~1034~~	~~2.0~~	~~-102~~	~~100~~	~~–~~
~~Pacific~~	~~Japan Sea[s,4]~~	~~901~~	~~10~~	~~-33.6~~	~~38.4[‡]~~	~~–~~
~~Pacific~~	~~California Margin[q,5]~~	~~955~~	~~13.3~~	~~-17.3~~	~~19.6[‡]~~	~~–~~
~~Pacific~~	~~California Margin[q,5]~~	~~1564~~	~~19.0~~	~~-9.3~~	~~12.8[‡]~~	~~–~~
~~Pacific~~	~~California Margin[q,5]~~	~~1926~~	~~31.0~~	~~-4.3~~	~~3.1[‡]~~	~~–~~
~~Pacific~~	~~Nankai Trough[q,6]~~	~~1741~~	~~32.2~~	~~-4.9~~	~~3[‡]~~	~~–~~
~~Pacific~~	~~Nankai Trough[s,6]~~	~~2997~~	~~11.0~~	~~-5.6~~	~~8.7[‡]~~	~~–~~
~~Pacific~~	~~Nankai Trough[q,6]~~	~~3020~~	~~18.2~~	~~-7.0~~	~~6.4[‡]~~	~~–~~
~~Pacific~~	~~Santa Barbara[k]~~	~~587~~	~~1.3~~	~~-175.2~~	~~–~~	~~–~~
~~Pacific~~	~~Soledad[k]~~	~~542~~	~~1~~	~~-310.3~~	~~–~~	~~–~~
~~Pacific~~	~~Pescadero[k]~~	~~408~~	~~1.4~~	~~-164.3~~	~~–~~	~~–~~

~~Pacific~~	~~Magdalena~~[k]	~~600~~	~~1.5~~	~~-182.5~~	~~–~~	~~–~~
~~Pacific~~	~~Alfonso~~[k]	~~713~~	~~0.8~~	~~-474.5~~	~~–~~	~~–~~
~~Pacific~~	~~Costa Rica Margin~~[q,7]	~~3306~~	~~16.0~~	~~-8.1~~	~~9.6~~[‡]	~~–~~
~~Pacific~~	~~Costa Rica Margin~~[q,7]	~~4177~~	~~19.8~~	~~-7.5~~	~~3.1~~[‡]	~~–~~
~~Pacific~~	~~Costa Rica Margin~~[q,7]	~~4311~~	~~18.6~~	~~-12.3~~	~~12.4~~[‡]	~~–~~
~~Pacific~~	~~Peru Margin~~[s,8]	~~161~~	~~30~~	~~-6.9~~	~~–~~	~~–~~
~~Pacific~~	~~Peru Margin~~[t,9]	~~427~~	~~40~~	~~-1.2~~	~~–~~	~~-25.4~~
~~Pacific~~	~~Peru Margin~~[t,9]	~~5086~~	~~9~~	~~-25.0~~	~~–~~	~~-13.2~~
~~Pacific~~	~~Chilean Coast~~[e]	~~586~~	~~5.55~~	~~-22.9~~	~~–~~	~~–~~
~~Pacific~~	~~Chilean Coast~~[e]	~~723~~	~~0.33~~	~~-362.0~~	~~–~~	~~–~~
~~Pacific~~	~~Chilean Coast~~[e]	~~980~~	~~2.92~~	~~-45.3~~	~~–~~	~~–~~
~~Pacific~~	~~Chilean Coast~~[e]	~~768~~	~~10.11~~	~~-13.3~~	~~–~~	~~–~~
~~Pacific~~	~~New Zealand - Porangahau Ridge~~[f]	~~1900-2150~~	~~12.8~~	~~-11.4~~	~~–~~	~~-31.4~~
~~Pacific~~	~~New Zealand - Porangahau Ridge~~[f]	~~1900-2150~~	~~4.4~~	~~-53.3~~	~~–~~	~~-31.6~~
~~Pacific~~	~~New Zealand - Porangahau Ridge~~[f]	~~1900-2150~~	~~3.6~~	~~-50.5~~	~~–~~	~~-31.4~~
~~Pacific~~	~~New Zealand - Porangahau Ridge~~[f]	~~1900-2150~~	~~2.1~~	~~-74.2~~	~~–~~	~~-33.4~~
~~Pacific~~	~~New Zealand - Porangahau Ridge~~[f]	~~1900-2150~~	~~3.8~~	~~-61.5~~	~~–~~	~~-35.0~~
~~Pacific~~	~~New Zealand - Porangahau Ridge~~[f]	~~1900-2150~~	~~1.8~~	~~-82.6~~	~~–~~	~~-48.8~~
~~Pacific~~	~~New Zealand - Hikurangi~~[b,d]	~~350~~	~~39.5~~	~~5~~[‡]	~~7.3~~[‡]	~~–~~
~~Pacific~~	~~New Zealand - Hikurangi~~[b,d]	~~332~~	~~12.9~~	~~19.3~~[‡]	~~13.6~~[‡]	~~–~~
~~Pacific~~	~~New Zealand - Hikurangi~~[b,d]	~~98~~	~~0.87~~	~~192.1~~[‡]	~~160.9~~[‡]	~~–~~
~~Pacific~~	~~New Zealand - Hikurangi~~[b,d]	~~285~~	~~3.64~~	~~65.2~~[‡]	~~59.6~~[‡]	~~–~~
~~Southern Ocean~~	~~Antarctic - Cumberland Bay~~[n]	~~237~~	~~5.03~~	~~-86~~	~~95~~	~~-25.4~~
~~Southern Ocean~~	~~Antarctic - Cumberland Bay~~[n]	~~260~~	~~0.80~~	~~-539~~	~~291~~	~~-23.5~~
~~Southern Ocean~~	~~Antarctic - Cumberland Bay~~[n]	~~275~~	~~2.80~~	~~-135~~	~~116~~	~~-15.5~~

~~Appendix 1.~~

~~These models follow Chatterjee et al., (2011) and Malinverno and Pohlman, (2011). The first model assumes the only sulfate reduction taking place is through OSR. Carbon fractionation through OSR is set at α = 1.01 from zero at the seafloor. Sulfate is completely consumed at 10m with a constant porosity of 70%. Diffusion is calculated by Equation 1 where the diffusivity in sediment is (Iverson and Jørgensen, 1993)~~

~~$D_S = \frac{D_O}{(1 + n(1 - \varphi))}$~~ ~~(9)~~

~~Diffusion in seawater (D_o) for sulfate is 0.56*10^{-5} cm^2/s (Iverson and Jørgensen, 1993) and 0.60*10^{-5} cm^2/s for bicarbonate (Li and Gregory, 1974). The saturation factor (*n*) was assumed to be 3 for clay/silt sediments, and the sedimentation rate was set at an arbitrary 25 cm/kyr. The conceptual framework for the second model is set to include both OSR and AOM. A SMT is set at five meters below the seafloor while sulfate reduction takes place at the surface. Carbon fractionation through AOM is set at α = 1.0175. Both downward diffusing sulfate and upward methane fluxes are set at 120 mol/m^2 kyr. The δ^{13}C-CH_4 of the upward diffusing methane is set at -70‰, but an additional flux of DIC set at 20‰ is added from below the SMT.~~